Journal Pre-proof

Galloyl esters of *trans*-stilbenes are inhibitors of FASN with anticancer activity on non-small cell lung cancer cells

Yu-Jia Tan, Azhar Ali, Sheng-Yang Tee, Jun-Ting Teo, Xi Yu, Mei-Lin Go, Yulin Lam

PII: S0223-5234(19)30731-7

DOI: https://doi.org/10.1016/j.ejmech.2019.111597

Reference: EJMECH 111597

To appear in: *European Journal of Medicinal Chemistry*

Received Date: 4 June 2019

Revised Date: 17 July 2019

Accepted Date: 5 August 2019

Please cite this article as: Y.-J. Tan, A. Ali, S.-Y. Tee, J.-T. Teo, X. Yu, M.-L. Go, Y. Lam, Galloyl esters of *trans*-stilbenes are inhibitors of FASN with anticancer activity on non-small cell lung cancer cells, *European Journal of Medicinal Chemistry* (2019), doi: https://doi.org/10.1016/j.ejmech.2019.111597.

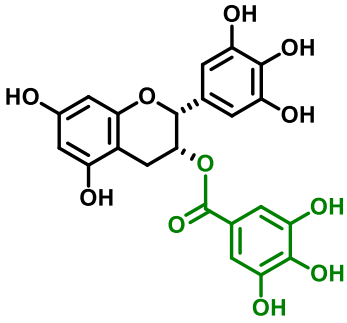

(-)-EGCG

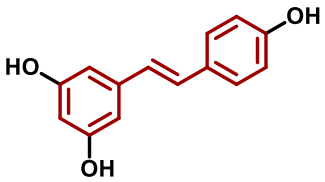

Resveratrol

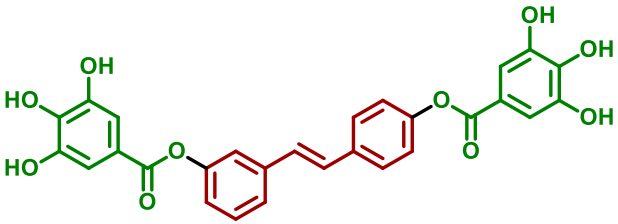

EC1

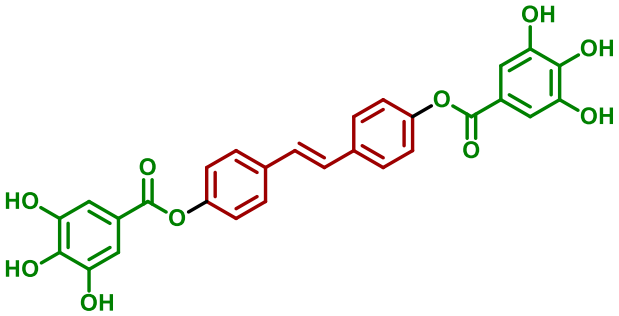

EC5

Growth inhibitory IC_{50} on NSCLC cell lines

EC1	IC_{50} H1703	1.28 μM
	IC_{50} PC-9	5.0 μM
EC5	IC_{50} H1703	1.0 μM
	IC_{50} PC-9	2.3 μM

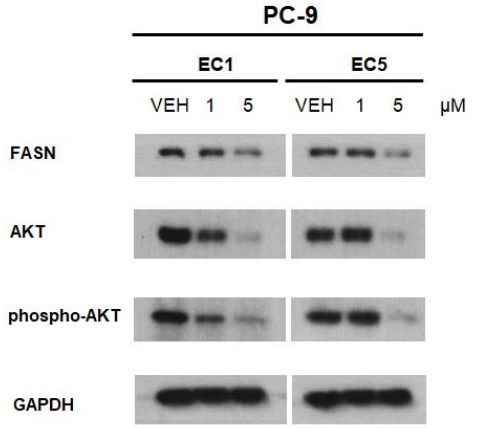

Galloyl esters of *trans*-stilbenes are inhibitors of FASN with anticancer activity on non-small cell lung cancer cells

Yu-Jia Tan [a #], Azhar Ali [b #], Sheng-Yang Tee [a], Jun-Ting Teo [b], Xi Yu [c], Mei-Lin Go [c *], Yulin Lam [a *]

[a] Department of Chemistry, National University of Singapore, 3 Science Drive 3, 117543, Singapore. [b] Cancer Science Institute of Singapore, Yong Loo Lin School of Medicine, 14 Medical Drive, 117599, Singapore; [c] Department of Pharmacy, National University of Singapore, 18 Science Drive 4, 117543, Singapore.

Co-First Authors; * Co-Corresponding authors.

Abstract

Fatty acid synthase (FASN) is a lipogenic enzyme that is selectively upregulated in malignant cells. There is growing consensus on the oncogenicity of FASN driven lipogenesis and the potential of FASN as a druggable target in cancer. Here, we report the synthesis and FASN inhibitory activities of two novel galloyl esters of *trans*-stilbene **EC1** and **EC5**. Inhibition of FASN was accompanied by a loss in AKT activation and profound apoptosis in several non-small cell lung cancer (NSCLC) cells at the growth inhibitory concentrations of **EC1** and **EC5**. Both FASN and phospho-AKT levels were concurrently downregulated. However, addition of a lipid concentrate to the treated cells reinstated cell viability and reversed the loss of FASN and AKT protein levels, thus recapitulating the causal relationship between FASN inhibition and the loss in cell viability.

Keywords FASN inhibitors, anticancer, galloyl esters of *trans*-stilbenes, Non-small cell lung cancer, EGCG

1. Introduction

The multifunctional enzyme fatty acid synthase (FASN) catalyzes the final steps in the *de novo* synthesis of fatty acids starting from acetyl-CoA, malonyl-CoA and NADPH [1–3]. The main product of this process is the 16-C fatty acid palmitate which is a major component of cell membranes, a precursor in the synthesis of structural lipids, a substrate in post-translational palmitoylation of membrane proteins and an important energy source when incorporated into triglycerides [4]. Healthy cells have low levels of FASN because their fatty acid requirements are largely met by dietary sources and not by *de novo* lipogenesis [5]. In contrast, malignant cells exhibit unusually high levels of FASN activity, even when dietary lipids are present in abundance [6,7]. Upregulated FASN activity is an early and pervasive hallmark of malignancies

that is inextricably linked to disease progression and poor prognosis [8–10]. Elevated FASN levels confer growth and survival benefits to cancer cells. Ostensibly, FASN signaling is correlated to the expression and activation of oncogenic proteins that direct malignant transformations [11–13]. Overexpression of the FASN gene has been shown to activate HER1/HER2 tyrosine kinase receptors in human breast epithelial cells, underscoring a *bona fide* oncogenic role for FASN [14]. Furthermore, RNA interference silencing of the FASN gene induced apoptosis in prostate cancer cells [15], synergistically enhanced the cytotoxicity of paclitaxel on breast cancer cells [16] and led to stable reversion of the malignant phenotype [17]. Collectively, these findings recapitulate a compelling role for FASN as a viable therapeutic target for cancer drug discovery [18,19].

First generation FASN inhibitors comprised several natural products such as cerulenin, thiolactomycin and (-)-epigallocatechin 3-gallate (EGCG) [20–22]. The green tea flavonoid EGCG is a gallate ester of epigallocatechin. Structurally it is a diastereomeric hydroxylated chroman with polyphenolic side chains at positions 2 (trihydroxyphenyl) and 3 (galloyloxy) (Figure 1A). EGCG is associated with a diversity of pharmacological properties which include neuroprotective, anticancer, cardiovascular and antimicrobial activities [23–26]. The pleiotropic profile of EGCG may be linked to the abundance of phenolic groups in its structure [27]. Ortho-disubstituted phenolic hydroxyl (OH) groups in EGCG are efficient redox cyclers and have dual functions as pro-oxidants and antioxidants [28,29]. In addition, polyphenolic groups impart amphiphilicity to the molecule, predisposing it to non-specific perturbation of membrane bilayers and consequential changes to membrane protein function [30]. Chemical reactivity also resides in the ester linkage of EGCG which may react with nucleophilic serine/threonine OH groups in enzymes to bring about inhibition. Notwithstanding, the inhibition of FASN by EGCG alludes to a specific interaction that is characterized by well-defined binding parameters [31]. The reaction kinetics pointed to an initial rapid and reversible binding to the ketoacyl reductase enzyme in the FASN complex, followed by slow irreversible inactivation [31]. EGCG was however a weak FASN inhibitor with an IC_{50} of 52 µM [31] and this has prompted attempts at understanding the structure activity requirements of the EGCG template with the aim of enhancing FASN inhibition [32,33]. To date, the most successful analogs were derived by replacing the chroman scaffold of EGCG with other ring systems [34]. Turrado and coworkers tested five scaffolds (cyclohexyl, phenyl, naphthalenyl, tetrahydronaphthalenyl, biphenyl) and found significant FASN inhibitory activity in only two - biphenyl and naphthalenyl – as exemplified by compounds **1** and **2** (Figure 1B) [34]. These findings hint at untapped opportunities for enhancing inhibitory potency through scaffold replacement in the EGCG template. Here, we confirmed the suitability of *trans*-stilbene

as an incipient scaffold with FASN inhibitory properties. Inhibition by the most promising analogs disrupted the FASN-AKT signaling axis to bring about apoptotic cell death in non-small cell lung cancer (NSCLC) cells.

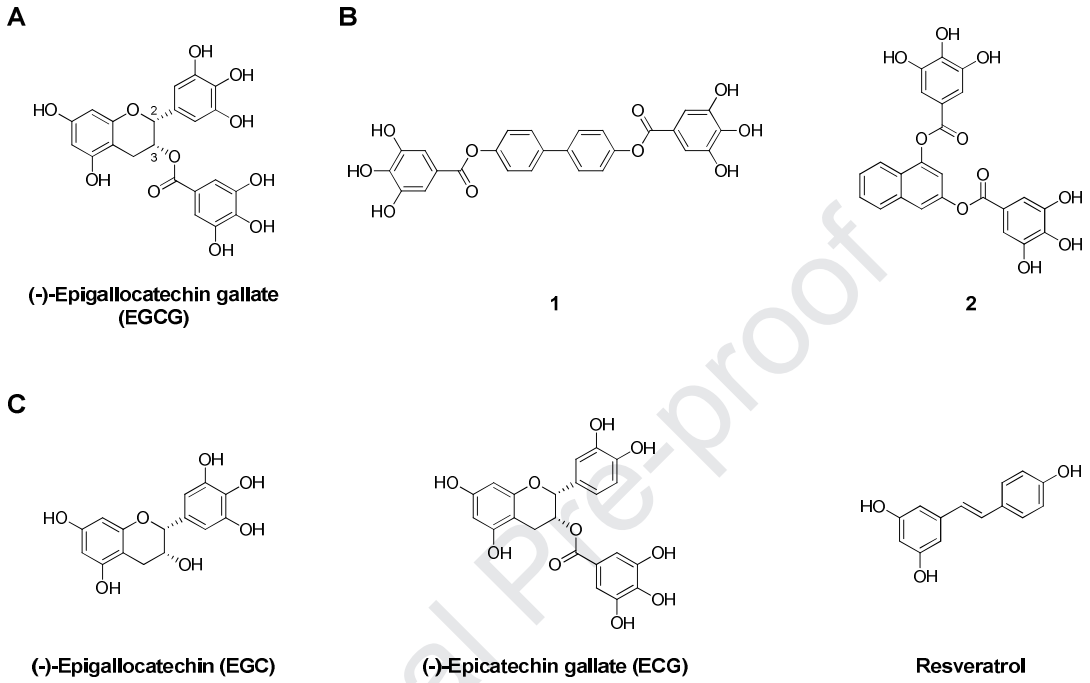

Figure 1. Chemical structures of (A) EGCG; (B) FASN inhibitors biphenyl **1** and naphthalenyl **2** [30]; (C) EGC, ECG and resveratrol.

2. Chemistry

Of the three identifiable structural features in EGCG (galloyloxy, trihydroxyphenyl, hydroxylated chroman), only the galloyloxy side chain is essential for inhibition. Thus, epigallocatechin (EGC, Figure 1C) which lacks this entity was a significantly weaker inhibitor than EGCG [35]. The role of the trihydroxyphenyl ring is less well-defined. Epicatechin gallate (ECG, Figure 1C) has one less hydroxyl (OH) group on the phenyl ring than EGCG but is comparable in terms of inhibitory activity [35]. As for the chroman ring, it acts primarily as a scaffold for positioning the other two entities at a specific distance from each other and to keep them in a near planar arrangement [33]. In our efforts to identify other scaffolds that could serve as superior substitutes to chroman, we selected *trans*-stilbene as a viable alternative, prompted mainly by its presence in the polyphenol resveratrol (Figure 1C) which has FASN inhibitory activity exceeding that of several naturally occurring flavones [33]. Accordingly, we designed stilbene analogs **EC1**-**EC5**, **EC10**-**12** bearing the galloyloxy side chains found in EGCG (Figure 2). Modifications in these analogs

centered on (i) varying the number of phenolic OH groups on these side chains from three in **EC1** to two (**EC2**) and one (**EC3**); (ii) positioning the galloyloxy side chains at the meta-para (3/4') positions in **EC1** and para-para (4/4') in **EC5**; (iii) reducing the number of galloyloxy side chains from two (**EC1**, **EC5**) to one (**EC10**, **EC11**) and (iv) undertaking phenolic OH to methoxy conversions in **EC4**, **EC7** and **EC12**. We also modified the previously reported "active" biphenyl scaffold of **1** by inserting a methylene residue between the phenyl rings to give the conformationally more flexible diphenylmethyl scaffold which is found in **EC6**-**EC8** (Figure 2). In the same way, we replaced the rigid naphthalene in **2** with the more flexible tetrahydronaphthalenyl ring in **EC9.** We also explored a 1-phenylnaphthalene analog **EC13** which was substituted with only one galloyloxy side chain. The structures of **EC9** and **EC13** are shown in Figure 2.

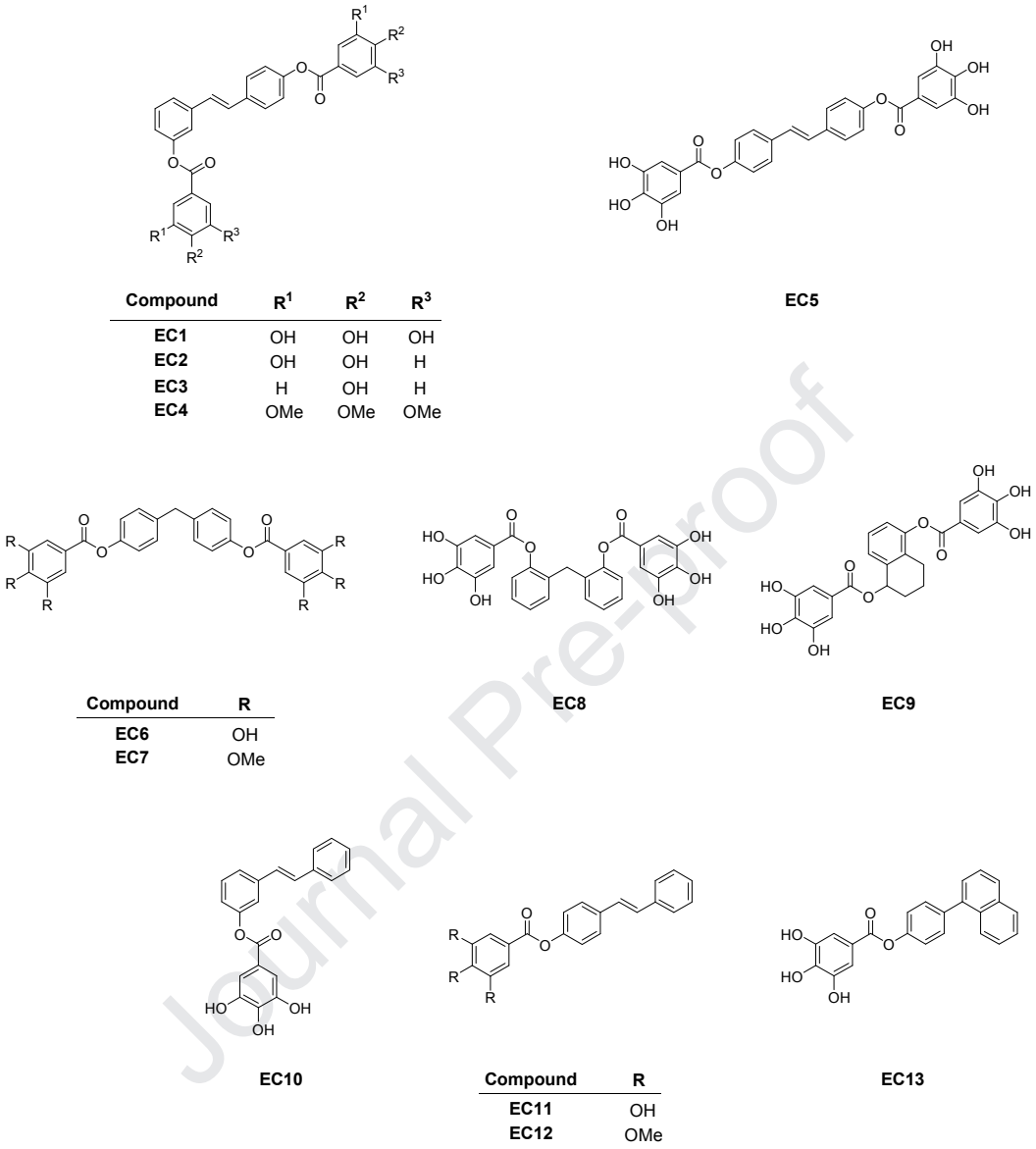

Figure 2. Chemical structures of EC analogs **EC1 - EC13**.

The synthesis of the EC analogs was achieved by a convergent approach in which the two main fragments (OH-bearing scaffolds, substituted benzoic acids) were separately synthesized and condensed. Except for the OH-bearing diphenylmethanes **13**, **14** and tetrahydronaphthalene **15** (found in **EC6**-**EC8** and **EC9** respectively) which were commercially available, the hydroxylated ring structures of the remaining compounds were obtained by synthesis.

The *trans*-stilbene scaffold was obtained by Heck coupling of a substituted styrene and substituted iodobenzene in the presence of catalytic palladium (II) acetate. The synthesis of *trans*-3,4-dihydroxystilbene **5a** is shown in Scheme 1. Briefly, 3-hydroxybenzaldehyde was

reacted with methyltriphenylphosphonium bromide and *n*-butyllithium in a Wittig reaction to give 3-hydroxystyene **3**. The OH groups in **3** and 4-iodophenol were acetylated to give **4a** and **5a** respectively, followed by Heck coupling of **4a** and **5a** to give the diacetoxystilbene **6a**. The protecting acetyl groups in **6a** were then removed by alkaline hydrolysis to give 3,4'-dihydroxystilbene **7a** which is the core scaffold in **EC1**-**EC4**. The same reaction sequence was followed to give 3-hydroxystilbene **7b** (from **4a** and **5b**) and 4-hydroxystilbene **7c** (from **4b** and **5a**) which are the scaffolds in **EC10** and **EC11**, **EC12** respectively. 4,4'-Dihydroxystilbene **8** which is found in **EC5** was prepared by Perkin condensation of 4-hydroxybenzaldehyde and 4-hydroxyphenylacetic acid in a microwave-assisted reaction (Scheme 2). To obtain the 1-(4-hydroxyphenyl)naphthalene scaffold of **EC13**, 1-naphthaleneboronic acid and 4-bromoanisole were subjected to Suzuki coupling to give 1-(4-methoxyphenyl)naphthalene **9** which on demethylation yielded the desired phenolic analog **10** (Scheme 3).

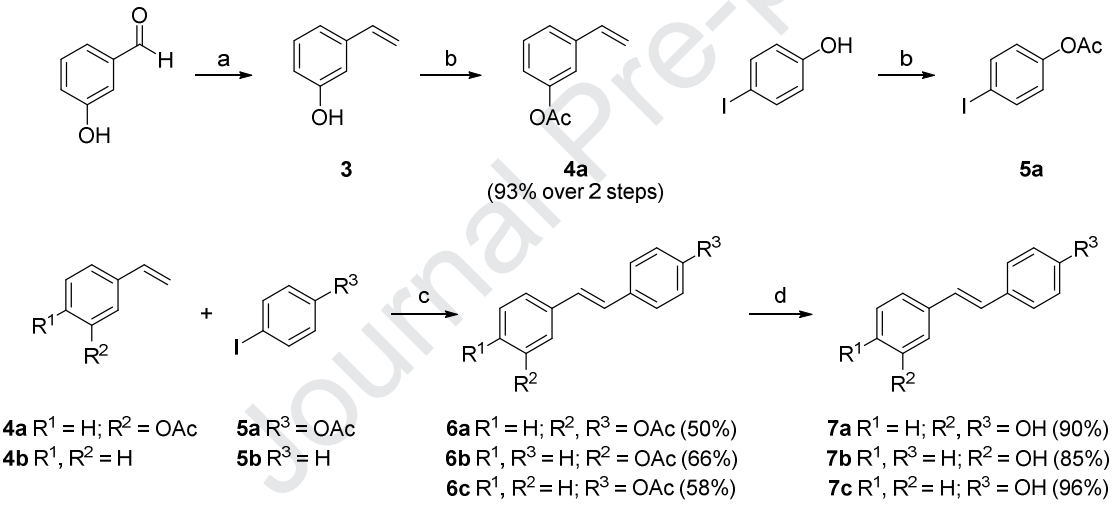

Scheme 1. Reagents and conditions: (a) CH_3PPh_3Br, *n*-BuLi, THF, 0 °C to r.t., 4 h (b) Ac_2O, DMAP, Et_3N, CH_2Cl_2, r.t., 1.5 h (c) $Pd(OAc)_2$, PPh_3, Et_3N, DMF, 75 °C, 18 h, 50-66% (d) LiOH, THF, 100 °C, 4 h, 85-96%.

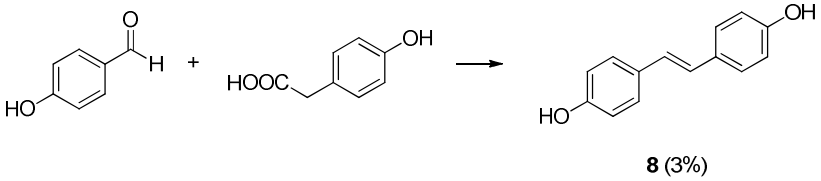

Scheme 2. Reagents and conditions: Piperidine, 1-methylimidazole, PEG 4600, MW, 160 °C, 25 min, 3%.

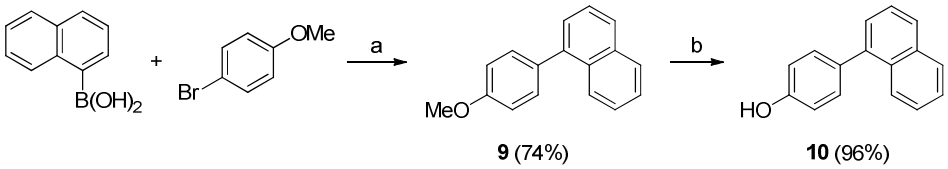

9 (74%) **10** (96%)

Scheme 3. Reagents and conditions: (a) $Pd(OAc)_2$, $Ba(OH)_2$, 95% aq. EtOH, r.t., 17 h, 74% (b) BBr_3, CH_2Cl_2, 0 °C to r.t., 12 h, 96%.

To minimize side reactions in the final esterification step, the phenolic OH groups in **11a-c** were reacted with *tert*-butyldimethylsilyl chloride (TBSCl) to give the corresponding silyloxy analogs **12a**-**c** (Scheme 4).

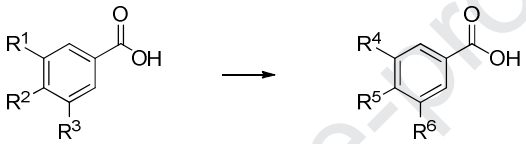

11a R^1, R^2, R^3 = OH
11b R^1, R^2 = OH, R^3 = H
11c R^2= OH, R^1, R^3 = H

12a R^4, R^5, R^6 = OTBS
12b R^4, R^5 = OTBS, R^6 = H
12c R^5= OTBS, R^4, R^6 = H

Scheme 4. Reagents and conditions: (i) TBSCl, imidazole, DMF, r.t., 24 h (ii) $AcOH/H_2O$ (3:1), THF, r.t., 24 h, 79-88% over 2 steps.

Scheme 5 depicts the final carbodiimide-catalyzed esterification of the phenolic/alcoholic OH groups in the various ring structures with the silyloxy benzoic acids. Removal of the protecting silyl groups yielded the final compounds **EC1**-**EC3**, **EC5, EC6**, **EC8** and **EC9** bearing two galloyloxy side chains. The methoxylated analogs **EC4** and **EC7** were obtained by directly esterifying trimethoxybenzoic acid **12d** with stilbene **7a** and diphenylmethane **13**. The mono-galloyl analogs **EC10**, **EC11**, **EC12** and **EC13** were synthesized in a similar manner as depicted in Scheme 6.

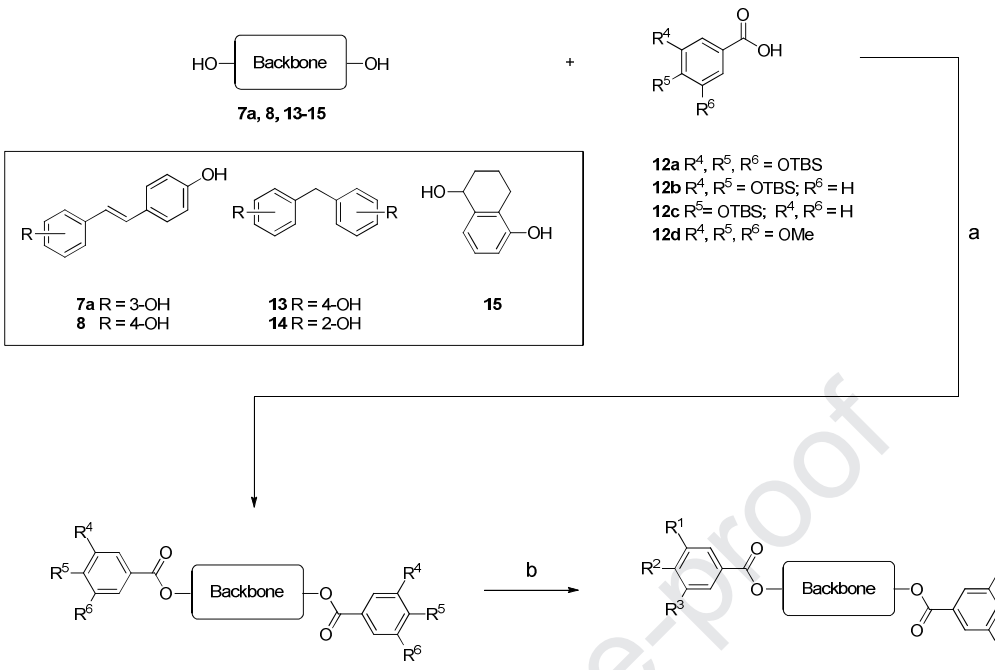

Backbone		R	R^4	R^5	R^6
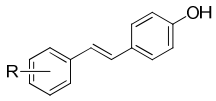	**16a**	3-OH	OTBS	OTBS	OTBS
	16b	3-OH	OTBS	OTBS	H
	16c	3-OH	H	OTBS	H
	EC4	3-OH	OMe	OMe	OMe
	16d	4-OH	OTBS	OTBS	OTBS
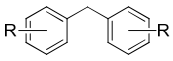	**16e**	4-OH	OTBS	OTBS	OTBS
	EC7	4-OH	OMe	OMe	OMe
	16f	2-OH	OTBS	OTBS	OTBS
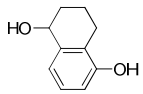	**16g**		OTBS	OTBS	OTBS

Backbone		R	R^1	R^2	R^3
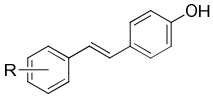	**EC1**	3-OH	OH	OH	OH
	EC2	3-OH	OH	OH	H
	EC3	3-OH	H	OH	H
	EC5	4-OH	OH	OH	OH
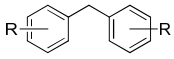	**EC6**	4-OH	OH	OH	OH
	EC8	2-OH	OH	OH	OH
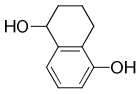	**EC9**		OH	OH	OH

Scheme 5. Reagents and conditions: (a) EDCI or DCC, DMAP, CH_2Cl_2, r.t., 12 h, 51-85% (b) TBAF or NH_4F, THF/MeOH, r.t., 6 h, 38-73%.

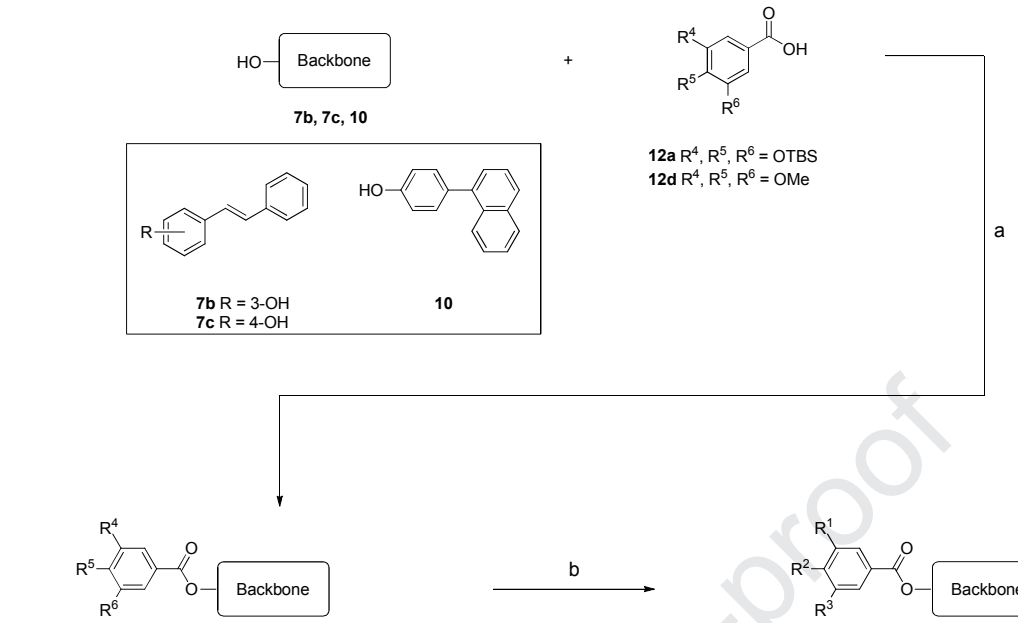

Backbone		R	R^4	R^5	R^6
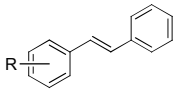	**16h**	3-OH	OTBS	OTBS	OTBS
	16i	4-OH	OTBS	OTBS	OTBS
	EC12	4-OH	OMe	OMe	OMe
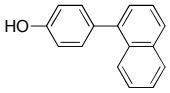	**16j**		OTBS	OTBS	OTBS

Backbone		R	R^1	R^2	R^3
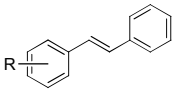	**EC10**	3-OH	OH	OH	OH
	EC11	4-OH	OH	OH	OH
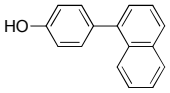	**EC13**		OH	OH	OH

Scheme 6. Reagents and conditions: (a) EDCI or DCC, DMAP, CH_2Cl_2, r.t., 12 h, 57-63% (b) TBAF or NH_4F, THF/MeOH, r.t., 6 h, 43-88%.

3. Results and Discussion

3.1. The galloyl stilbenes EC1 and EC5 potently inhibited cell proliferation across a panel of FASN expressing NSCLC cell lines

EC1-**EC13** were initially assessed for growth inhibition on the FASN expressing NSCLC H1703 cell line at a single concentration of 25 µM (Figure 3). Growth inhibition was determined after 72 h using the tetrazolium-based MTS assay and only compounds that inhibited growth by more than 50% inhibition were shortlisted as “actives”. Based on this cut-off, all the methoxylated analogs (**EC4**, **EC7**, **EC12**) were excluded, as were the monosubstituted analogs **EC10** and **EC13**.

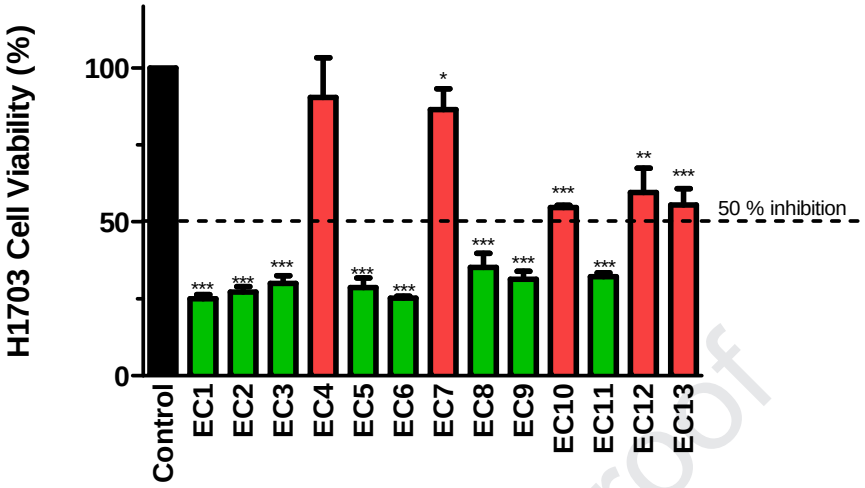

Figure 3. Viability of NSCLC H1703 cells on treatment with **EC1-EC13** at a single concentration of 25 µM. Data represents the mean ± standard deviation (SD) of *n* = 3 independent determinations. Significant difference from control was analysed by unpaired *t* test using GraphPad Prism 5 and indicated by an asterisk (*p<0.05, **p<0.001, ***p<0.0001).

The shortlisted actives were then evaluated for their growth inhibitory concentrations (IC_{50}) on H1703 cells, alongside EGCG and the reported biphenyl **1** (Table 1). Three structure-activity trends were noted from these results. First, among the four scaffolds examined, *trans*-stilbene emerged as the most promising. It is found in the two most potent analogs **EC1** and **EC5** (IC_{50} 1 µM) which gratifyingly, also exceeded **1** in terms of potency. Second, potency is conditional on di-substitution of the template with galloyloxy side chains. The requirement for di-substitution alluded to a possible regioisomeric preference but this was not apparent in **EC1** and **EC5** which were equipotent in spite of differences in the positioning of the galloyloxy entities (meta-para in **EC1**, para-para in **EC5**). On the other hand, regioselectivity was clearly demonstrated in the diphenylmethyl analogs **EC6** and **EC8**. Here, there was a distinct preference for a para-para location (**EC6**) as compared to ortho-ortho (**EC8**), implicating close proximity of the galloyloxy side chains as a structural liability. Yet another instance of regioselectivity was apparent in the monosubstituted stilbenes **EC10** and **EC11**. Here, the meta-substituted **EC10** was eliminated as an inactive in the initial single concentration screen but its para-substituted counterpart (**EC11**) retained modest potency (IC_{50} 11 µM). Lastly, all three OH groups on the galloyloxy side chain were required for optimal growth inhibition. Thus, reduction in OH groups from three (**EC1**) to two (**EC2**) and then one (**EC3**) led to progressive losses in activity.

To augment these structure-activity trends, the EC compounds were tested on two additional FASN expressing NSCLC cell lines H1299 and H1650 (Table 1). In spite of variations in IC_{50} values, the rank order of each analog was broadly similar across the three cell lines. Notably, **EC1** and **EC5** were still the most potent members although they were now comparable to **1** on H1299 (in contrast to H1703) and only **EC5** ranked above **1** on H1650. Similarly, **EC3** and **EC8** were consistently flagged out for sub-optimal growth inhibition on all cell lines. Taken together, the structure-activity trends observed in H1703 corroborated with those observed on the other cell lines.

Table 1. IC_{50} values and selective indices (**EC1**, **EC5**, EGCG only) of compounds on NSCLC cells and non-malignant lung epithelial SAEC cells.

Compound	IC_{50} (μM)[a,b]					
	H1703	**H1299**	**H1650**	**PC-9**	**A549**	**SAEC**
EC1	1.28 ± 0.02	3.1 ± 0.3	12.7 ± 0.9	5.0 ± 0.5	2.3 ± 0. 1	6.8 ± 0.6
(SI[c])	**(5.3)**	**(2.2)**	**(0.5)**	**(1.4)**	**(3.0)**	
EC2	8.9 ± 0.8	11.0 ± 0.7	14.1 ± 0.8	-[d]	-[d]	-[d]
EC3	17.2 ± 1.2	37.2 ± 2.0	40.2 ± 2.0	-[d]	-[d]	-[d]
EC5	0.97 ± 0.10	3.3 ± 0.1	2.5 ± 0.1	2.3 ± 0.1	2.1 ± 0.1	5.0 ± 1.0
(SI[c])	**(5.2)**	**(1.5)**	**(2.0)**	**(2.2)**	**(2.4)**	
EC6	6.2 ± 0.4	8.6 ± 0.3	49.7 ± 3.1	-[d]	-[d]	-[d]
EC8	39.3 ± 1.2	25.9 ± 2.1	122 ± 19	-[d]	-[d]	-[d]
EC9	6.5 ± 0.4	10.2 ± 0.3	36.0 ± 2.6	-[d]	-[d]	-[d]
EC11	11.2 ± 0.1	8.5 ± 0.4	16.0 ± 1.2	-[d]	-[d]	-[d]
EGCG	17.1 ± 1.5	20.6 ± 1.4	24.8 ± 1.9	77.4 ± 1.1	185 ± 5	110 ± 14
(SI[c])	**(6.4)**	**(5.3)**	**(4.4)**	**(1.4)**	**(0.6)**	
1	5.8 ± 0.2	4.2 ± 0.4	7.4 ± 0.4	-[d]	-[d]	-[d]

[a] IC_{50}: Concentration of compound required to reduce cell viability by 50%. Evaluated using MTS assay after 72 h at 37 °C, 5% CO_2. Data represents mean ± SD values from n = 3 independent experiments respectively. [b] The NSCLC cell lines were FASN expressing as revealed by immunoblotting (Supplementary Information, Figure S1). In contrast, non-malignant SAEC cells did not express FASN. [c] Selective index (SI) = $IC_{50\ SAEC}/IC_{50\ NSCLC}$. [d] - : Not determined.

We noted with interest that some analogs (**EC1**, **EC6**, **EC8** and **EC9**) were strikingly less potent on H1650 than on H1703 and H1299. The anomalous responses to H1650 may be linked to the absence of the tumor suppressor PTEN in this cell line [36]. PTEN moderates AKT signaling which promotes cell growth and survival [36–38]. Loss of PTEN would thus desensitize cells to cell death. Intriguingly, **EC5** maintained the same level of growth inhibition on H1650 as the two other cell lines, suggesting that it may have circumvented the loss of PTEN in H1650 by activating other cell death pathways.

EC1 and **EC5** were additionally tested on FASN-expressing NSCLC PC-9 and A549 cells (Table 1). PC-9 cells harbor the clinically relevant EGCR delE746-A750 mutation which renders them sensitive to tyrosine kinase inhibitors (TKI) such as gefitinib [39,40]. In contrast, H1703 and

A549 possess wild-type EGFR and were less sensitive to gefitinib [39,40]. Curiously, these differences in gefinitib-sensitivity did not appear to affect the susceptibility of these cells to **EC1** and **EC5** as seen from the narrow 2-4 fold variation in their growth inhibitory concentrations on these cell lines (H1703, A549, PC-9). These findings were significant in view of the close functional relationship between mutated EGFR and FASN in NSCLC [39]. Briefly, mutated EGFR relies on FASN-mediated palmitoylation to mediate TKI resistance in NSCLC. Ali *et al.* showed that pharmacological inhibition of FASN by orlistat impeded the palmitoylation of EGFR, induced EGFR ubiquitination, abrogated EGFR mutant signaling and suppressed the proliferation of TKI-resistant EGFR-mutant NSCLC cells in culture and *in vivo* [39]. Viewed in this context, the equipotent activities of **EC1** and **EC5** on NSCLC cells harboring wild type or mutated EGFR intimated their potential as pan-NSCLC growth inhibitors whose cell killing properties were ostensibly independent of the cellular EGFR status.

In summary, **EC1** and **EC5** were identified as the most promising analogs in this series, inhibiting the growth of NSCLC cells (with the exception of **EC1** on H1650) at potencies that were confined to a narrow IC_{50} window (1-5 μM). To determine if their cytotoxicities were selectively directed towards malignant cells, the compounds were evaluated on non-malignant lung epithelial SAEC cells which do not express FASN (Supplementary Information, Figure S1) Disappointingly, both **EC1** and **EC5** exhibited low IC_{50} values (< 10 μM) on the non-malignant cells although they were significantly more cytotoxic ($\geq$ 5-fold) on some (H1703) but not all of the tested NSCLC cells (Table 1). Clearly, the susceptibility of the SAEC cells to **EC1** and **EC5**, in spite of the absence of FASN, hinted at the ability of these compounds to intercept other vulnerable cellular targets besides FASN. We speculate that the polyphenolic nature of these compounds may be contributory in this regard. Notably, ortho-disubstituted phenolic groups as those found in **EC1** and **EC5** are capable of generating free radicals in the course of redox cycling [28]. Besides, phenolic groups are widely reputed to be non-specific membrane disruptors [30]. That said, we found the selective cytotoxicities of EGCG to be surprisingly comparable or even lower than those of **EC1 and EC5** (Table 1) even though it is reputed to be relatively non-toxic [41]. Clearly, other correlates of toxicity would be required to confirm the selective activities of these compounds.

3.2. The galloyl stilbenes EC1 and EC5 inhibited NSCLC cell proliferation by inducing apoptosis

Having shown that **EC1** and **EC5** potently suppressed proliferation of NSCLC cells, we asked if growth inhibition led to apoptotic cell death. To investigate, NSCLC cells (PC-9, H1703) were

incubated with **EC1** and **EC5** (5 µM) for 72 h, double stained with the Annexin V-FITC conjugate and propidium iodide (PI) and analyzed for apoptosis by fluorescence-activated cell sorting (FACS). EGCG and **EC4** (the inactive methoxylated analog of **EC1**) were similarly tested at higher concentrations of 100 µM in view of their weaker growth inhibitory effects on both cell lines. Figure 4A shows the distribution of treated cells based on their staining responses to the fluorescent probes. Cells in early apoptosis were selectively stained by the Annexin V conjugate and appeared in the lower right quadrant of Figure 4A. Cells in late apoptosis were double stained by both Annexin V and PI and localized in the upper right quadrant of the same figure. Early and late apoptotic cells were collectively expressed as a percentage of total cells in Figure 4B. We found significant apoptosis in cells treated with **EC1** and **EC5**, with most cells concentrated in the late apoptotic stage after 72 h. As anticipated, no cell death was observed among **EC4**-treated NSCLC cells. EGCG induced significant levels of late apoptosis in H1703 cells but was less apoptogenic in PC-9. These observations may reflect its greater potency on H1703 (IC_{50} 17 µM) as compared to PC-9 (IC_{50} 77 µM).

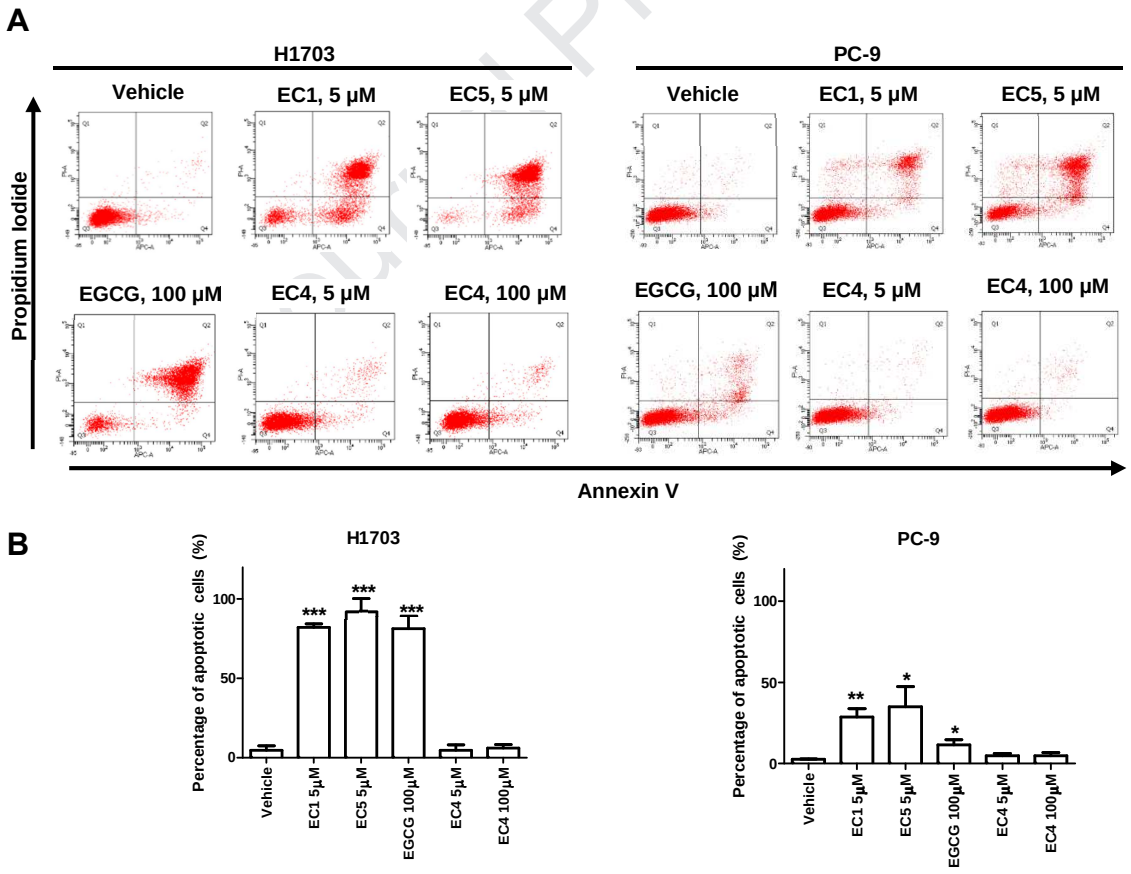

Figure 4. (A) Distribution of FACS-sorted, compound-treated H1703 and PC-9 cells that were double-stained with Annexin V and PI. Cells were sorted into 4 categories according to their staining characteristics: viable (lower left quadrant), early apoptosis (lower right quadrant), late apoptosis (upper right quadrant) and necrotic (upper left

quadrant). (B) Percentage of compound-treated cells in early and late apoptosis. Data represents mean ± SD for *n* = 3 independent determinations. Significant difference from control cells (vehicle) was analysed by unpaired *t* test using GraphPad Prism 5 and indicated by an asterisk (*p<0.05, **p<0.001, ***p<0.0001).

3.3. The galloyloxy stilbenes EC1 and EC5 are FASN inhibitors.

As **EC1** and **EC5** were designed to retain the structural features found in FASN inhibitors (EGCG and **1**), we proceeded to assess their FASN inhibitory properties. To obtain the FASN protein, FASN plasmids were transfected in lysates derived from HeLa cells using a commercial protein expression kit (1-Step Human *In Vitro* Protein Expression Kit, ThermoFisher Scientific). The success of the transcription/translation process was confirmed by the presence of FASN in immunoblots prepared from the lysates (Supplementary Information, Figure S3). To determine the loss in FASN activity, lysates were incubated with the test compound for 2 h, after which acetyl-CoA, malonyl-CoA and NADPH were added. The consumption of NADPH in the course of reaction would result in a decrease in absorbance at 340 nm but this fall would be less pronounced if the enzyme was inhibited. The compounds tested were **EC1**, **EC5** and **EC4**. Positive controls were EGCG, **1** and orlistat. All the compounds were tested at 10 µM, with the exception of EGCG, which was tested at 150 µM as well.

As seen from Figure 5, the FASN inhibitory activity of orlistat exceeded that of the other compounds while **EC1**, **EC5** and **1** had comparable potencies. Biphenyl **1** was previously identified as a potent FASN inhibitor in SK-Br3 breast cancer cells, with 90% inhibition at 4 µM [34]. In our hands, **1** exhibited only modest inhibition (20% at 10 µM), possibly due to differences in the assay protocol. Even so, we were encouraged to note that the FASN inhibitory potencies of **EC1** and **EC5** compared favorably to that of **1**. These results implied that *trans*-stilbene is a viable scaffold for FASN inhibition, equivalent to biphenyl and superior to the chroman ring found in EGCG. However, we noted that inhibitory activity required the presence of polyphenolic groups on the stilbene template. Thus, **EC4** in which the phenolic OH groups were methoxylated, was devoid of inhibitory activity. Tellingly, the polyphenolic EGCG had negligible inhibitory activity at 10 µM and required a much higher concentration (150 µM) to achieve the same level of inhibition as **EC1** and **EC5**. We posited that the close proximity of the two polyphenolic side chains in EGCG may have adversely affected FASN inhibitory activity [33]. If so, the extended configuration of *trans*-stilbene has served to advantageously space out the side chains to avoid such an occurrence.

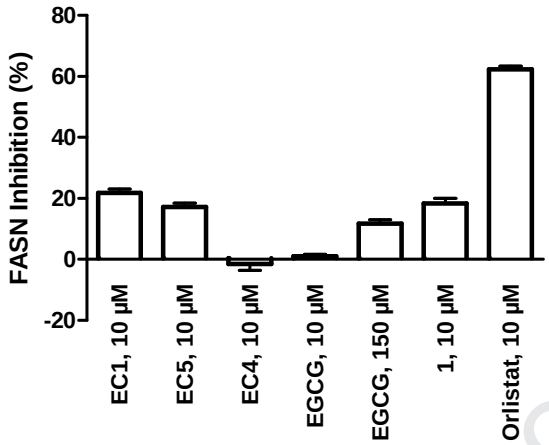

Figure 5. Inhibition of FASN by test compounds **EC1, EC4, EC5**, EGCG, biphenyl **1** and orlistat. Inhibition was determined from the decrease in NADPH absorbance in treated versus untreated HeLa cell lysates over 10 min. Compounds were tested at 10 µM to be aligned to orlistat which induced 50-60% inhibition at this concentration. Data represents mean ± SD of *n* = 3 independent determinations.

We noted with interest that **EC1** and **EC5** were more soluble than **1** when determined under similar conditions (pH 7.4, 25 °C, 24 h). The kinetic solubilities of **EC1** and **EC5** were 6 µM and 2.5 µM respectively, which exceeded that of **1** (0.4 µM) by 6-15 fold. We posited that the greater solubilities of **EC1** and **EC5** may be a consequence of diminished intermolecular packing within the extended framework of the *trans*-stilbene scaffold.

3.4. Inhibition of FASN is causal to the growth inhibitory activities of EC1 and EC5

Having shown that **EC1** and **EC5** inhibited FASN, we asked if FASN inhibition was causal to the growth inhibitory activities of these compounds. We reasoned that if this was true, reversing the lipid deprived status of the FASN-inhibited cells should restore viability. Hence, we supplemented **EC1**/**EC5**-treated PC-9 cells with a commercial lipid mixture (CD Lipid concentrate, Gibco) which contained palmitate and other essential fatty acids for 72 h, after which cell viability was assessed by the tetrazolium MTS assay. Figure 6A shows that cell viability improved upon addition of lipids to **EC1**/**EC5**-treated PC-9 cells. Similarly, lipid supplementation restored the viability of PC-9 cells treated with **EGCG** at 100 µM. The experiment was repeated on H1703 cells treated with **EC1** and **EC5** at 1 µM. Again, viability of cells was enhanced by lipid supplementation (Figure 6B).

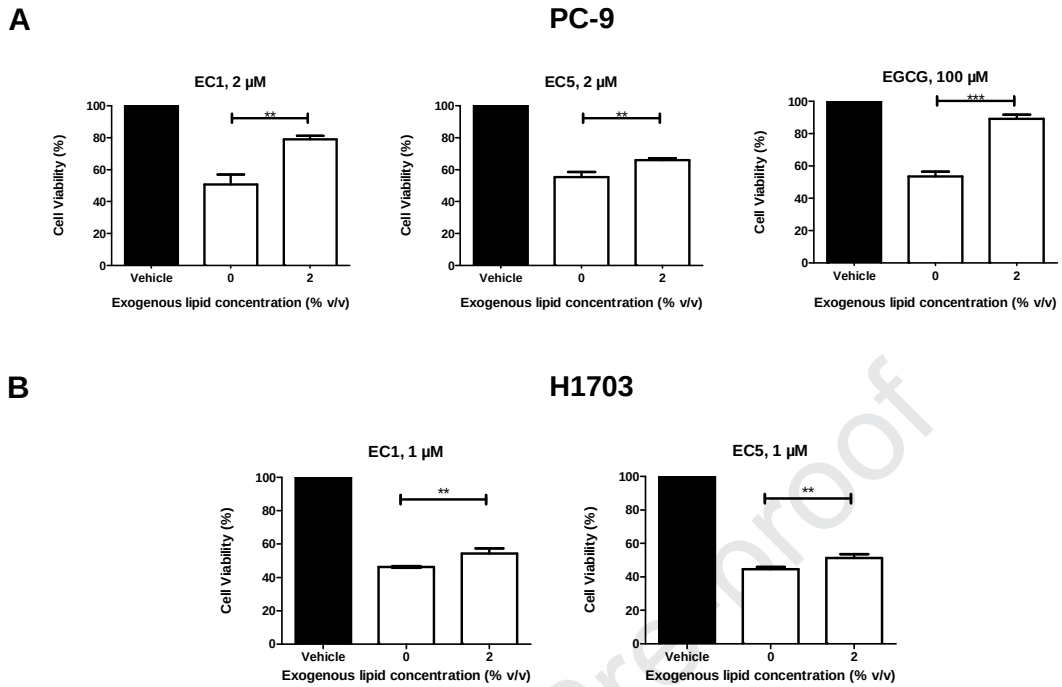

Figure 6. Viability of (A) PC-9 and (B) H1703 cells treated with test compound only and test compound + lipid concentrate (2% v/v). Compounds tested were **EC1**, **EC5** and EGCG (on PC-9 only). Compounds were tested at concentrations that fall within the range of their IC_{50} values. Cell viability was determined by the MTS assay, after 72 h incubation. Data represents mean ± SD for n = 3 independent determinations. Significant difference between the different treatments were analysed by unpaired t test using GraphPad Prism 5 and indicated by an asterisk (***p<0.0001, ** p<0.01).

3.5. Inhibition of FASN by EC1 and EC5 intercepted the FASN-AKT feedback loop in NSCLC cells

The PI3K/AKT signaling cascade has been implicated in the regulation of FASN expression in several malignant cell lines [42–45]. Specifically, Wang et al. [43] demonstrated a mutually reinforcing relationship between AKT activation and FASN expression in ovarian carcinoma cells. Briefly, constitutive activation of AKT increases FASN expression and enhances the biosynthesis of palmitate and other fatty acids. Incorporation of these fatty acids into membrane phospholipids ensures an optimal lipid balance within the membrane which is required for the functional integrity of AKT and other membrane embedded proteins. Pharmacological inhibition of FASN disrupts the positive feedback loop between AKT activation and FASN expression with two consequential outcomes. First, FASN inhibition would sensitize cells to apoptotic cell death by inactivating AKT and nullifying its role in regulating cell survival [46]. Second, inhibition would reduce the supply of palmitate and other essential fatty acids which would in turn alter

membrane composition, adversely affect the functional activity of AKT and consequently lead to suppression of FASN.

We have already shown that **EC1** and **EC5** induced apoptosis in NSCLC cells at their growth inhibitory concentrations (Figure 4) but have yet to demonstrate the ensuing losses in AKT and FASN that would be incurred as a consequence of inhibition. Hence, levels of these proteins were probed in PC-9 and H1703 cells exposed to **EC1** and **EC5** at 1 µM and 5 µM for 48 h. As seen in Figure 7, dose dependent suppression of FASN was observed on both cell lines. In addition, there were concurrent losses in total AKT and phospho-AKT levels. Tellingly, no change was observed in the levels of these proteins in cells treated with the inactive analog **EC4** which did not inhibit FASN or induce apoptotic cell death.

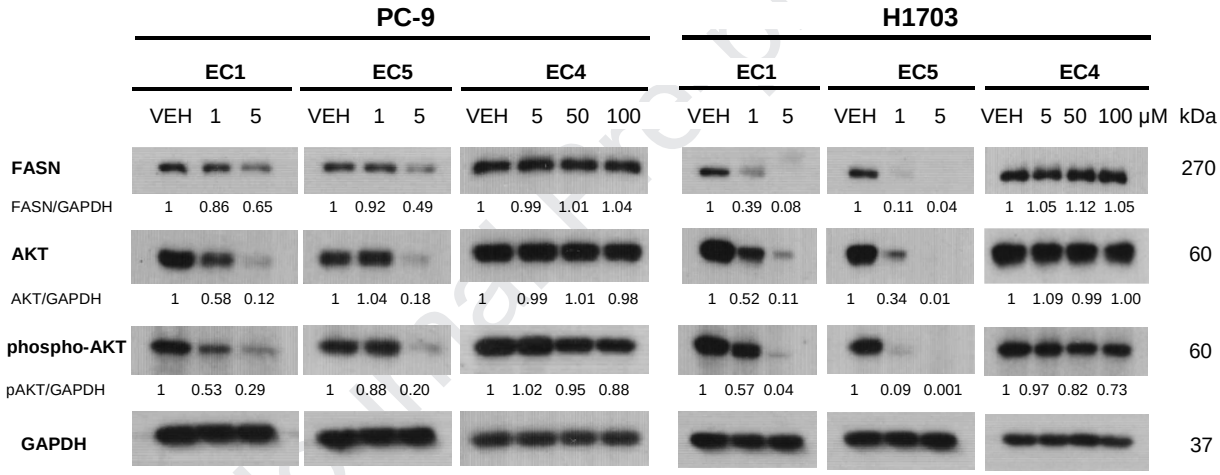

Figure 7. Representative western blots (*n* = 3) showing concentration-dependent losses in the levels of FASN, AKT and phospho-AKT S473 in PC-9 and H1703 cells treated with test compound (**EC1**, **EC5**, **EC4**) or media only (VEH) for 48 h. **EC1** and **EC5** were tested at 1 µM and 5 µM. **EC4** was tested at 5, 50 and 100 µM. Densitometric analysis was performed on ImageJ and normalised against the untreated control (VEH).

Having shown that lipid supplementation increased the viability of **EC1**/**EC5** treated PC-9 and H1703 cells (Figure 6), we reasoned that if **EC1** and **EC5** disrupted the FASN-AKT axis, compound-induced suppression of AKT and FASN should be restored to pre-inhibition levels on addition of lipids. Hence, we monitored the AKT/FASN levels in PC-9 and H1703 cells treated with **EC1** and **EC5** in the presence of the lipid concentrate. The results in Figures 8A and 8B reveal that the presence of lipids negated the suppressive effects of the test compound on FASN/AKT/phospho-AKT and restored levels to that found in control cells. Thus the strong rebound in protein levels dovetailed with the positive effects of lipid supplementation on cell viability and recapitulated the disruptive effects of **EC1** and **EC5** on the FASN-AKT axis as a consequence of their FASN inhibitory activity.

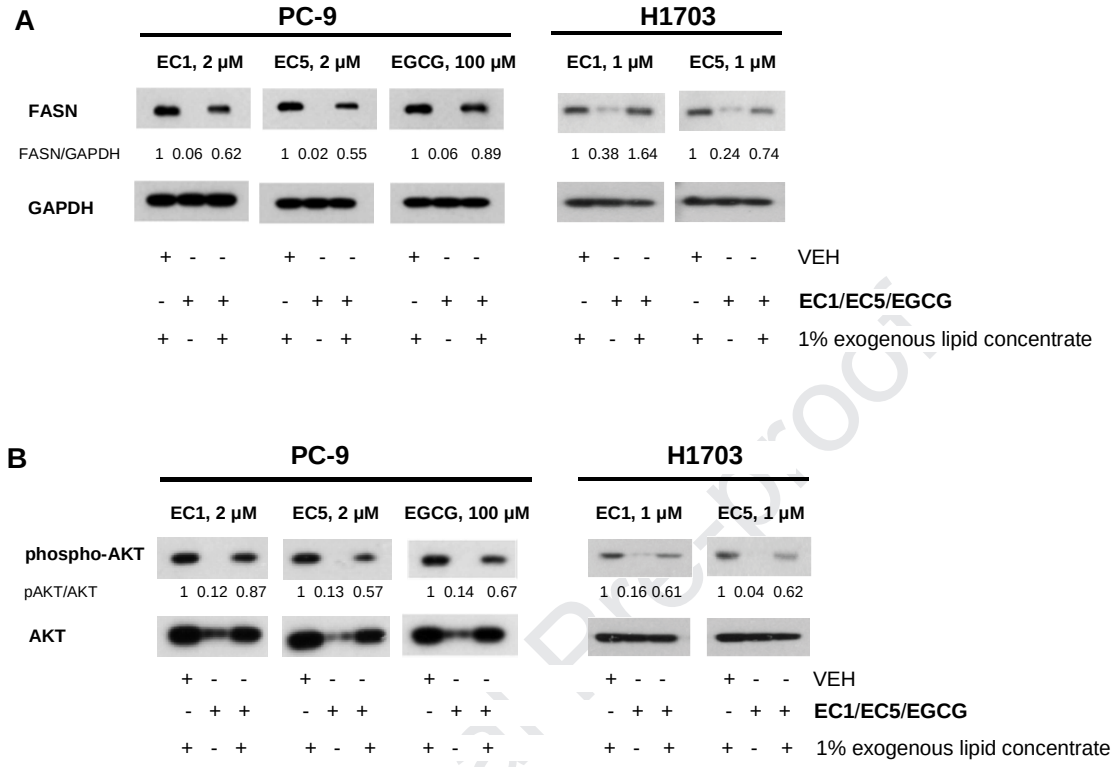

Figure 8. Representative western blots showing the recovery of (A) FASN; (B) AKT and phospho-AKT S473 levels in PC-9 and H1703 cells treated with test compound (**EC1**, **EC5**) + Lipid concentrate (1% v/v) or media only (VEH) for 48 h. EGCG (100 µM) was tested on PC-9 cells. Densitometric analysis was carried out with ImageJ and normalised against the untreated control (vehicle).

Conclusion

Two *trans*-stilbene esters bearing polyphenolic galloyloxy side chains (**EC1**, **EC5**) were identified for the first time as inhibitors of FASN. The FASN inhibitory activities of both compounds were comparable to that of EGCG at their growth inhibitory concentrations, implicating *trans*-stilbene as a viable FASN inhibitory scaffold. With its extended configuration and limited flexibility, there are more options available for positioning the essential polyphenolic side chains on *trans*-stilbene while still complying with the putative optimal distance between the said groups. Consequently *trans*-stilbene has the potential of generating more “actives” than other scaffolds that do not possess its stereochemical characteristics. Future work should focus on exploring other substituted trans-stilbenes, such as H-bonding amino as a surrogate of the phenolic hydroxyl and ring structures like indole/benzimidazole which are isosteric to catechols [47].

Mechanistically, we have shown that the FASN inhibitory properties of **EC1** and **EC5** disrupted the mutually reinforcing signaling pathway between FASN expression and AKT activation. Corroboratory evidence of this disruption is seen from the significant levels of apoptosis and diminished FASN/phospho-AKT protein levels in **EC1**/**EC5** treated cells. It is further affirmed by the "rescue" afforded by lipid supplementation which reversed the loss in cell viability and reinstated FASN/phospho-AKT expression to pre-inhibition levels.

Notwithstanding, FASN inhibition may not be the sole means by which **EC1** and **EC5** induced cell death. The structure-activity requirement for polyphenolic groups taken together with their multi-targeting potential hint at the involvement of other biological targets besides FASN. The susceptibility of the non-FASN expressing SEAC cells to **EC1** and **EC5**, as well as the contrasting growth inhibitory responses of **EC1** and **EC5** in PTEN-deficient H1650 cell line are cases in point. From the latter, we deduced that **EC1** was more dependent on the FASN-AKT signaling axis as the loss in PTEN in H1650 led to significant losses in its growth inhibitory activity. In contrast, **EC5** was as potent on H1650 as on other PTEN-bearing cell lines, possibly due to its ability to engage other cell death pathways. This raises the interesting possibility that **EC5** may be better positioned than **EC1** to act against resistant NSCLC cells in view of its pleiotropy. Future work should be directed towards identifying these additional pathways intercepted by **EC5** with the aim of understanding their functional correlations with FASN and their feasibility as co-therapeutic targets together with FASN for the treatment of NSCLC.

Materials and Methods

Chemistry

Commercially available reagents were purchased from Sigma Aldrich, Alfa Aesar and TCI Chemicals and used without further purification. Solvents (hexane, ethyl acetate, dichloromethane, methanol) were distilled before use. Moisture-sensitive reactions were conducted under N_2 environment using commercially obtained anhydrous solvents and activated molecular sieves. Thin layer chromatography (TLC) was performed using Merck silica gel 60 F254 pre-coated aluminum plates. Flash column chromatography was carried out with silica gel (Merck, 230 – 400 mesh). ^{1}H and ^{13}C NMR spectra were recorded on Bruker Avance 500 (AV500) and Bruker Avance 400 (AV400) instruments at 298K. Chemical shifts were reported in parts per million (ppm) on the δ scale using residual protio-solvent signals (^{1}H NMR, $CDCl_3$ δ 7.26, DMSO-d_6 δ 2.50, MeOH-d_4 δ 3.31; ^{13}C NMR, $CDCl_3$ δ 77.0, DMSO-d_6 δ 39.5, MeOH-d_4 δ 49.0, Acetone-d_6 δ 29.8) as internal references. Mass spectra were determined by

high resolution mass spectrometry (HRMS) electrospray ionization (ESI) or atmospheric pressure chemical ionisation (APCI). Final compounds were purified to ≥ 95% as determined by reverse-phase HPLC using Zorbax Eclipse XDB-C18 column (5 µm, 150 mm × 4.6 mm) on two solvent systems (Supplementary Information, S5).

*3-Vinylphenyl acetate (**4a**)*

The Wittig synthesis of intermediate **3** was carried out following a reported method [48]. Briefly, methyltriphenylphosphonium bromide (14.6 g, 2.5 eq.) was dissolved in dry THF (140 mL) and cooled to 0 °C under N_2. To the stirred mixture was added 2M *n*-butyllithium (20.4 mL, 2.5 eq.) dropwise, stirring was continued for 1 h at 0 °C after which the reaction was cooled to -78 °C. A solution of 3-hydroxybenzaldehyde (2 g, 1 eq.) in dry THF (2.4 mL) was then added dropwise to the stirred mixture. Thereafter the reaction mixture was sequentially warmed to room temperature, stirred for 4 h, cooled to 0 °C and quenched with saturated NH_4Cl. The aqueous layer was extracted with diethyl ether, dried with anhydrous Na_2SO_4, filtered and evaporated under vacuum to give crude 3-vinylphenol **3**. The latter was purified by column chromatography using hexane: ethyl acetate (8:1) as eluting solvent. The subsequent acetylation of **3** was carried out following a reported method [49]. **3** was dissolved in DCM (30 mL), 4-dimethylaminopyridine (DMAP) (0.115 g, 0.05 eq.) and triethylamine (TEA) (2.11 mL, 0.8 eq.) were added, followed by dropwise addition of acetic anhydride (2.14 mL, 1.2 eq.) dissolved in DCM (5 mL). The reaction mixture was then stirred at room temperature (25^{o}C) for 1.5 h and diluted with water. The aqueous layer was extracted several times with DCM, the combined organic layer was washed with brine, dried with anhydrous Na_2SO_4, filtered after which the organic solvent was removed under reduced pressure. The product was then purified by column chromatography with hexane: ethyl acetate (20:1) as eluting solvent. The acetylated product **4a** was obtained as an oil in 93% yield (2.47 g). ^{1}H NMR (400 MHz, $CDCl_3$) δ 7.21 (t, J = 7.8 Hz, 1H), 7.15 (dt, J = 7.7, 1.1 Hz, 1H), 7.05 (s, 1H), 6.89 (dd, J = 7.9, 1.0 Hz, 1H), 6.64 – 6.52 (m, 1H), 5.64 (d, J = 17.6 Hz, 1H), 5.17 (d, J = 10.9 Hz, 1H), 2.15 (s, 3H). ^{13}C NMR (101 MHz, $CDCl_3$) δ 169.1, 150.8, 139.0, 135.8, 129.2, 123.6, 120.7, 118.9, 114.6, 20.8. HRMS (APCI, M+H): m/z calculated for [$C_{10}H_{11}O_2$]: 163.0754; found 163.0750.

*4-Iodophenyl acetate (**5a**)*

The acetylation of **5a** was carried out as described for **3**. DMAP (0.056 g, 0.05 eq.) and TEA (1.01 mL, 0.8 eq.) were added to a stirred solution of 4-iodophenol (2 g, 1 eq.) in DCM (20 mL). This was followed by dropwise addition of acetic anhydride (1.03 mL, 1.2 eq.) in DCM (5 mL),

followed by stirring at room temperature for 1.5 h and then dilution with water. The same workup method was followed to give the crude product **5a** which was purified by column chromatography with hexane: ethyl acetate (20:1). **5a** was used for the next step of the synthesis without further characterization.

*General procedure for the synthesis of acetylated stilbenes (**6a-c**)* [50]

The respective styrenes (**4a** or **4b**) (1 eq.) and iodoarenes (**5a** or **5b**) (1 eq.) were dissolved in dry DMF. The solution was purged with N_2 for 10 min. $Pd(OAc)_2$ (0.01 eq.) and triphenylphosphine (0.045 eq.) were then added and the reaction was heated with stirring to 80 °C for 18 h. Thereafter, it was quenched with 1M HCl at 0 °C, extracted with diethyl ether and the combined organic layer worked up in the usual way. The crude product was purified by column chromatography.

*General procedure for the synthesis of hydroxylated stilbenes (**7a-c**)*

To a stirred solution of the acetylated stilbene (**6a**-**c**) in THF was added 1M LiOH. The reaction was stirred at 95°C for 4 h after which 1M HCl was added to quench the reaction. The aqueous layer was extracted with ethyl acetate and the combined organic layer worked up in the usual way to give the crude product which was purified by column chromatography.

*(E)-4,4'-(Ethene-1,2-diyl)diphenol (**8**)*

8 was synthesized following a reported method with modifications [51]. 4-Hydroxybenzaldehyde (0.15 g, 1 eq.) and 4-hydroxyphenylacetic acid (0.243 g, 1.3 eq.) were stirred in the presence of piperidine (0.90 mL, 7.5 eq.) and 1-methylimidazole (0.73 mL, 7.5 eq.) in polyethylene glycol 4600 (0.75 g) as solvent, under microwave conditions at 160 °C for 25 min. On cooling, the reaction was acidified with 1M HCl and extracted with ethyl acetate. The combined organic layer was worked up in the usual way to give crude **8** which was purified by column chromatography using hexane: ethyl acetate (8:1). **8** was obtained as a solid in 3% (0.009 g) yield. ^{1}H NMR (400 MHz, DMSO) δ 9.50 (s, 2H), 7.36 (d, J = 8.5 Hz, 4H), 6.91 (s, 2H), 6.78 (d, J = 8.4 Hz, 4H). ^{13}C NMR (101 MHz, DMSO) δ 156.8, 128.7, 127.4, 125.3, 115.6. HRMS (ESI, M-H): m/z calculated for $[C_{14}H_{11}O_2]$: 211.0765; found 211.0769.

*1-(4-Methoxyphenyl)naphthalene (**9**)*

9 was synthesized following a reported method with modifications [52]**.** 1-Naphthaleneboronic acid (0.2 g, 1 eq.) and 4-bromoanisole (0.16 mL, 1.1 eq.) were stirred in the presence of $Pd(OAc)_2$ (0.011 g, 0.042 eq.) and $Ba(OH)_2$ (0.55 g, 1.5 eq.) in 95% ethanol (14 mL) for 17 h at

room temperature. The reaction mixture was then quenched with 1M HCl, extracted with DCM and worked up in the usual way. The crude product was purified by column chromatography with hexane: DCM (100:1) to give **9** as a solid (0.20 g, 74%). ^{1}H NMR (400 MHz, CDCl3) δ 7.83 (d, J = 8.3 Hz, 1H), 7.79 (d, J = 7.9 Hz, 1H), 7.73 (d, J = 8.2 Hz, 1H), 7.39 (ddd, J = 9.7, 8.1, 4.2 Hz, 2H), 7.34 – 7.28 (m, 4H), 6.95 – 6.89 (m, 2H), 3.78 (s, 3H). ^{13}C NMR (101 MHz, CDCl3) δ 158.9, 139.9, 133.8, 133.1, 131.8, 131.1, 128.2, 127.3, 126.9, 126.0, 125.9, 125.7, 125.4, 113.7, 55.3. HRMS (APCI, M+H): m/z calculated for [$C_{17}H_{15}O$]: 235.1117; found 235.1119.

*4-(Naphthalen-1-yl)phenol (**10**)*

Boron tribromide (1M in DCM) (2.56 mL, 3 eq.) was added dropwise to a stirred solution of **9** (0.2 g, 1 eq.) in DCM (8 mL) at 0 ^{o}C. The reaction was then warmed to room temperature, stirred for 12 h, quenched with water and extracted with DCM. The combined organic layer was worked up in the usual way to give the crude product which was purified by column chromatography using hexane: ethyl acetate (10:1). **10** was obtained as a solid in 96% (0.18g) yield. ^{1}H NMR (500 MHz, $CDCl_3$) δ 7.79 (d, J = 8.4 Hz, 1H), 7.74 (d, J = 8.1 Hz, 1H), 7.68 (d, J = 8.2 Hz, 1H), 7.33 (dd, J = 15.0, 7.1 Hz, 2H), 7.29 – 7.19 (m, 4H), 6.81 (d, J = 8.3 Hz, 2H). ^{13}C NMR (126 MHz, CDCl3) δ 154.7, 139.7, 133.8, 133.3, 131.7, 131.3, 128.2, 127.3, 126.9, 125.9, 125.9, 125.7, 125.4, 115.2. HRMS (ESI, M-H): m/z calculated for [$C_{16}H_{11}O$]: 219.0815; found 219.0811.

*General procedure for synthesis of silyloxy benzoic acids (**12a-c**)*

Reported methods were followed with some modifications [53,54]. The respective commercially available benzoic acid (**11a-c**) (1 eq.) was dissolved in DMF, *tert*-butyldimethylsilyl chloride (TBSCl) (1.4 eq. per TBS group added) and imidazole (2.5 eq. per TBS group added) were added and the reaction mixture stirred for 24 h at room temperature. The reaction was then diluted with diethyl ether, washed with water, and the organic layer worked up in the usual way. The residue was dissolved in THF, a solution of acetic acid: water (3:1) was added and stirred (24 h, room temperature) to selectively effect hydrolysis of the silyloxy ester. The reaction mixture was diluted with water, extracted with ethyl acetate and the combined organic layer worked up in the usual way to give the desired silyloxybenzoic acid (**12a-c**).

*General procedure for synthesis of disubstituted silyloxy esters **16a-g, EC4, EC7***

Procedure A was used for the synthesis of **16a**, **16c**, **EC4**, **16d** and **EC7**. The respective diol (1 eq.) and substituted benzoic acid (2.4 eq.) were dissolved in DCM.

N,N'-Dicyclohexylcarbodiimide (DCC) (3.4 eq.) and DMAP (0.2 eq.) were added and the reaction mixture stirred for 12 h at room temperature. The solvent was removed under reduced pressure and the compound purified by column chromatography.

Procedure B was used for the synthesis of **16b** and **16e-g**. The respective diol (1 eq.) and substituted benzoic acid (4 eq.) were dissolved in DCM. N-(3-Dimethylaminopropyl)-N'-ethylcarbodiimide hydrochloride (EDCI) (4 eq.) and DMAP (4 eq.) were added, the mixture stirred for 12 h at room temperature and DCM was subsequently added to stop the reaction. The organic layer was washed with $NaHCO_3$ and worked up in the usual way to give the crude product which was purified by column chromatography.

*General procedure for synthesis of monosubstituted silyloxy esters **16h-j, EC12***

The respective acid (**12a** or **12d**) (2 eq.), EDCI (2 eq.) and DMAP (2 eq.) were dissolved in DCM and cooled to 0 °C. The respective alcohol (1 eq) dissolved in DCM was added dropwise and stirring was continued for 12h at room temperature. The reaction mixture was diluted with DCM and worked up as described in the preceding paragraph (Procedure B).

*General procedure for the desilylation of **16a-j** to hydroxylated esters **EC1-3, EC5-6, EC8-11, EC13***

Procedure A was used for the synthesis of **EC11** and **EC13**. The silylated ester (**16i** and **16j**) (1 eq.) was dissolved in THF. 1M tetrabutylammonium fluoride (TBAF) (4 eq.) was added to the reaction mixture, stirred for 4 h at room temperature, and diluted with ethyl acetate. The organic layer was washed with water and worked up in the usual way. The crude product was purified by column chromatography.

Procedure B was used for the synthesis of **EC6**, **EC9** and **EC10**.The silylated ester (**16e**, **16g** and **16h**) (1 eq.) was dissolved in THF. 1M TBAF (5 eq.) and NH_4F (5 eq.) were added to the reaction mixture, stirred for 4 h at room temperature and diluted with ethyl acetate. The organic layer was washed with water and worked up in the usual way. The crude product was purified by column chromatography.

Procedure C was used for the synthesis of **EC1-3**, **EC5** and **EC8**. The silylated ester (**16a-d** and **16f**) (1 eq.) was dissolved in THF/methanol (ratios stated in Supplementary Information, S7), NH_4F (1.5 eq. per TBS group) was added to the reaction mixture, stirred for 4 h at room temperature (unless otherwise stated in Supplementary Information, S7) and diluted with ethyl

acetate. The organic layer was washed with water and worked up in the usual way. The crude product was purified by column chromatography.

General Biology

Human NSCLC cells (H1299, H1650, H1703, PC-9, A549) and SAEC cell lines were purchased from the American Type Culture Collection (ATCC). H1299, H1650, H1703 and PC-9 cells were maintained in RPMI 1640 (HyClone), supplemented with 10% fetal bovine serum (FBS) (HyClone) and 1% penicillin/streptomycin, while A549 cells were maintained in Dulbecco's Modified Eagle Medium (DMEM) with high glucose (HyClone) and supplemented with 10% FBS, 1% penicillin/streptomycin and 1 mM sodium pyruvate. SAEC cells were maintained in Bronchial Epithelial Cell Growth Medium (BEGM), supplemented with growth factors and supplements from BEGM Bronchial Epithelial SingleQuots Kit (Lonza). All cell lines were grown at 37°C in a humidified incubator with 5% CO_2. CellTiter 96® AQueous One Solution Cell Proliferation Assay (MTS) reagent (#G3582) was purchased from Promega (Madison, WI, USA). FITC Annexin V Apoptosis Detection kit (#556547) was obtained from BD Biosciences (Franklin Lakes, NJ). Human FASN plasmids (#OHu24141D) were prepared by GenScript (Piscataway, NJ). 1-Step Human Coupled IVT Kit - DNA (#88882) was obtained from Thermo Scientific. RIPA buffer (#89900) was obtained from Pierce and cOmplete Mini EDTA-free Protease Inhibitor Cocktail Tablets (#4693159001) were obtained from Merck. Pierce™ BCA Protein Assay Kit was obtained from ThermoFischer Scientific. Phospho-AKT Ser473 (#9271, 1:1,000) and total AKT (#9272, 1:1,000) antibodies were obtained from Cell Signaling Technology Inc. (Danvers, MA, USA), while FASN (#20140, 1:2,000) and GAPDH (#25778, 1: 2, 000) antibodies were obtained from Santa Cruz Biotechnologies Inc. (Santa Cruz, CA, USA). PVDF membranes (#88520) were obtained from Thermo Scientific. WesternBright ECL detection kit (K-12045-D50) was obtained from Advansta (San Jose, CA). Malonyl-CoA (#M1762), acetyl-CoA (#A2056) and NADPH were purchased from Sigma Aldrich. Chemically defined (CD) Lipid concentrate (#11905031) was obtained from Gibco.

Determination of cell viability

Cell viability was assessed using CellTitre 96® Aqueous One Solution (Promega, Madison, WI) containing the tetrazolium salt 3-(4.5-dimethylthiazol-2-yl)-5-(3-carboxymethoxyphenyl)-2-(4-sulfophenyl)-2H-tetrazolium (MTS). Cells were seeded at densities of 3×10^3 cells/100 µL (except H1650 and SEAC which were seeded at 3.5×10^3 cells / 100 µL and 4×10^6 cells/100 µL respectively) in 96-well format and incubated overnight for attachment to occur. Stock solutions of test compounds were prepared in DMSO and serially diluted with media to give

solutions covering a range of concentrations. Aliquots (50 µL) were then added to the wells to give the desired final concentrations. DMSO was kept at 0.1% v/v per well. The treated cells were incubated for 72 h (37 °C. 5% CO_2). The plates were then centrifuged at 500*g* for 5 min, supernatant were removed from the wells and replaced with fresh aliquots of media (150 µL). MTS reagent (20 µL) was added to each well and the plates were then read at 490 nm on a microplate reader (Tecan) after 2 h incubation at room temperature. Cell viability at each concentration was determined from the following equation:

$$\%\ \text{Cell viability} = \frac{\text{Mean absorbance}_{\text{compound}}}{\text{Mean absorbance}_{\text{control}}}\ \text{x}\ 100\%$$

Where Mean absorbance$_{compound}$ and Mean absorbance$_{control}$ were the average readings (from 4 technical repeats) of wells containing treated cells at a known concentration of test compound and cells not exposed to test compound respectively. Readings were corrected for control wells containing media only. Growth inhibitory IC_{50} (concentration of test compound required to inhibit cell growth by 50% relative to control untreated cells) was determined by plotting % viability against logarithmic concentration of test compound (GraphPad Prism 5).The experiments were repeated on 3 separate occasions to give mean IC_{50}. Statistical analysis was done using GraphPad Prism 5 (GraphPad Software, San Diego, CA).

Determination of apoptosis

Apoptosis was monitored using the FITC Annexin V Apoptosis Detection kit (#556547) (BD Biosciences, Franklin Lakes, NJ). H1703 and PC-9 cells were prepared at densities of 1.5×10^5 cells/2 mL medium in 6-well plates and allowed to attach overnight. The cells were incubated with **EC1** and **EC5** at 5 µM, **EC4** at 5 µM and 100 µM, EGCG at 100 uM or 0.1 % DMSO in media (control) for 48 h (37 °C, 5% CO_2). After this time, cells were harvested, rinsed with ice-cold PBS and cell pellets were resuspended in a mixture containing 1× Annexin V binding buffer, Annexin V and propidium iodide following manufacturer's protocol. The Becton-Dickinson LSR II FACS analyzer was used for the detection and FACSAria FACS sorter was used for analyses (BD Biosciences, Franklin Lakes, NJ). Experiments were done in triplicates. Statistical analysis was done using GraphPad Prism 5 (GraphPad Software, San Diego, CA).

Inhibition of FASN

The method was modified from a protocol described by Bays et al. [55] The 1-Step Human Coupled IVT Kit - DNA (#88882, Thermo Scientific) was used to obtain FASN proteins. Briefly, 1.2 µg of FASN plasmid (#OHu24141D, GenScript) was used for the in vitro translation of FASN

protein in accordance to manufacturer's guidelines. The freshly translated protein was immediately diluted with potassium phosphate buffer (100 mM, pH 6.5, containing 1 mM EDTA) in the ratio 3 parts lysate to 7 parts buffer and an aliquot (10 µL) was added to test compound (35 µL) contained in a 96-well plate and incubated for 2 h at 37°C, 5% CO_2. The final concentration of test compound per well was 10 µM. Thereafter, an aliquot (45 µL) of the NADPH activity buffer containing acetyl Co-A (55 µM) and NADPH (330 µM) prepared in the above mentioned phosphate buffer was added. The FASN catalytic reaction was started by adding an aliquot (10 µL) of malonyl-CoA (500 µM) in phosphate buffer to the compound-lysate mixture in the well. Absorbances at 340 nm were recorded on a microplate reader (Tecan) at the point of addition (0 min) and 10 min later. FASN inhibition was determined using the expression:

$$\%\ \text{FASN inhibition} = \left[1 - \frac{\text{Mean absorbance}_{\text{compound at 10 min}} - \text{Mean absorbance}_{\text{compound at 0 min}}}{\text{Mean absorbance}_{\text{control at 10 min}} - \text{Mean absorbance}_{\text{control at 0 min}}}\right] \text{x } 100\%$$

Experiments were done in triplicates.

Protein analysis using western immunoblotting

H1703 and PC-9 cells were seeded at densities of 8 × 10^5 cells/plate in 100 mm Petri dishes and incubated overnight for attachment. They were then treated with test compound at their indicated concentrations for 48h or 72 h, after which cells were harvested and lysed directly in RIPA buffer (#89900, Pierce) with protease inhibitors (#4693159001, Merck). Proteins were quantified using Pierce™ BCA Protein Assay Kit (ThermoFischer Scientific). Approximately 20-50 µg of proteins were loaded into wells of 8% SDS-PAGE gels and electrophoresed until the bromophenol blue dye reaches the bottom of gel. Proteins were then transferred onto PVDF membranes (#88520, Thermo Scientific). Membranes were blocked with 5% w/v milk in TBS-T (for AKT and phospho-AKT) or PBS-T (for FASN and GAPDH), and then incubated with the required primary and peroxidase conjugated secondary antibodies. Protein bands were detected using the WesternBright ECL detection kit (K-12045-D50, Advansta). Densitometric analysis was done using ImageJ.

Lipid rescue assay

PC-9 cells were seeded at densities of 3 × 10^3 cells/100 µL (for cell viability assay) or 1 × 10^5 cells/2 mL in RPMI 1640 medium and allowed to attach overnight. Cells were treated with test compound as described earlier for the determination of cell viability except that after 6 h of incubation (37 °C, 5% CO_2), 1× chemically defined lipid concentrate (#11905031, Gibco) was

added to the treated cells to give a final concentration of 2 % v/v in the well. Incubation was continued for another 72 h after which the cells were procressed for cell viability determinations or Western analysis. All experiments were done in triplicates. Statistical analysis was done using GraphPad Prism 5 (GraphPad Software, San Diego, CA).

Determination of solubility

Determination of aqueous solubility was carried out on MultiScreen Solubility filter plates (Millipore MSSLBPC10) from Millipore Corporation (MA, USA). The manufacturer's protocol (PC2445EN00, Millipore Corporation) was followed.

Acknowledgements

The authors gratefully acknowledge funding support from Ministry of Education, Republic of Singapore and National University of Singapore (ML Go R148000234 114; YL Lam R143000681112, AA R713000216720), Ministry of Education for provision of the National University of Singapore President Graduate Fellowship to YJ Tan and the NUS Drug Development Unit for carrying out solubility determinations on the test compounds.

References

[1] S.J. Wakil, Fatty Acid Synthase, A Proficient Multifunctional Enzyme, Biochemistry. 28 (1989) 4523–4530. doi:10.1021/bi00437a001.

[2] T. Maier, S. Jenni, N. Ban, Architecture of Mammalian Fatty Acid Synthase at 4.5 Å Resolution, Science. 311 (2006) 1258–1262. doi:10.1126/science.1123248.

[3] T. Maier, M. Leibundgut, N. Ban, The Crystal Structure of a Mammalian Fatty Acid Synthase, Science. 321 (2008) 1315–1322. doi:10.1126/science.1161269.

[4] S.S. Chirala, S.J. Wakil, Structure and Function of Animal Fatty Acid Synthase, Lipids. 39 (2004) 1045–1053. doi:10.1007/s11745-004-1329-9.

[5] L. Weiss, G.E. Hoffmann, R. Schreiber, H. Andres, E. Fuchs, E. Körber, H.J. Kolb, Fatty-Acid Biosynthesis in Man, a Pathway of Minor Importance. Purification, Optimal Assay Conditions, and Organ Distribution of Fatty-Acid Synthase, Biol. Chem. Hoppe. Seyler. 367 (1986) 905–912. doi:10.1515/bchm3.1986.367.2.905.

[6] G. Medes, A. Thomas, S. Weinhouse, Metabolism of Neoplastic Tissue. IV. A Study of

Lipid Synthesis in Neoplastic Tissue Slices in Vitro, Cancer Res. 13 (1953) 27–29.

[7] K.E. Hopperton, R.E. Duncan, R.P. Bazinet, M.C. Archer, Fatty acid synthase plays a role in cancer metabolism beyond providing fatty acids for phospholipid synthesis or sustaining elevations in glycolytic activity, Exp. Cell Res. 320 (2014) 302–310. doi:10.1016/j.yexcr.2013.10.016.

[8] M.S. Shurbaji, J.H. Kalbfleisch, T.S. Thurmond, Immunohistochemical Detection of a Fatty Acid Synthase (OA-519) as a Predictor of Progression of Prostate Cancer, Hum. Pathol. 27 (1996) 917–921. doi:10.1016/S0046-8177(96)90218-X.

[9] P.L. Alò, P. Visca, G. Trombetta, A. Mangoni, L. Lenti, S. Monaco, C. Botti, D.E. Serpieri, U. Di Tondo, Fatty Acid Synthase (FAS) Predictive Strength in Poorly Differentiated Early Breast Carcinomas, Tumori. 85 (1999) 35–40. doi:10.1177/030089169908500108.

[10] V. Jensen, M. Ladekarl, P. Holm-Nielsen, F. Melsen, F.B. Soerensen, The Prognostic Value of Oncogenic Antigen 519 (OA-519) Expression and Proliferative Activity Detected By Antibody MIB-1 in Node-Negative Breast Cancer, J. Pathol. 176 (1995) 343–352. doi:10.1002/path.1711760405.

[11] J.A. Menendez, B.P. Oza, E. Atlas, V.A. Verma, I. Mehmi, R. Lupu, Inhibition of tumor-associated fatty acid synthase activity antagonizes estradiol- and tamoxifen-induced agonist transactivation of estrogen receptor (ER) in human endometrial adenocarcinoma cells, Oncogene. 23 (2004) 4945–4958. doi:10.1038/sj.onc.1207476.

[12] J.A. Menendez, L. Vellon, I. Mehmi, B.P. Oza, S. Ropero, R. Colomer, R. Lupu, Inhibition of fatty acid synthase (FAS) suppresses HER2/neu (erbB-2) oncogene overexpression in cancer cells, Proc. Natl. Acad. Sci. USA. 101 (2004) 10715–10720. doi:10.1073/pnas.0403390101.

[13] J.A. Menendez, R. Lupu, Fatty acid synthase regulates estrogen receptor-α signaling in breast cancer cells, Oncogenesis. 6 (2017) e299. doi:10.1038/oncsis.2017.4.

[14] A. Vazquez-Martin, R. Colomer, J. Brunet, R. Lupu, J.A. Menendez, Overexpression of fatty acid synthase gene activates HER1/HER2 tyrosine kinase receptors in human breast epithelial cells, Cell Prolif. 41 (2008) 59–85. doi:10.1111/j.1365-2184.2007.00498.x.

[15] E. De Schrijver, K. Brusselmans, W. Heyns, G. Verhoeven, J. V. Swinnen, RNA

interference-mediated Silencing of the Fatty Acid Synthase Gene Attenuates Growth and Induces Morphological Changes and Apoptosis of LNCaP prostate Cancer Cells, Cancer Res. 63 (2003) 3799–3804.

[16] J.A. Menendez, L. Vellon, R. Colomer, R. Lupu, Pharmacological and small interference RNA-mediated inhibition of breast cancer-associated fatty acid synthase (oncogenic antigen-519) synergistically enhances Taxol (Paclitaxel)-induced cytotoxicity, Int. J. Cancer. 115 (2005) 19–35. doi:10.1002/ijc.20754.

[17] A.M. Gonzalez-Guerrico, I. Espinoza, B. Schroeder, C.H. Park, C.M. KVP, A. Khurana, B. Corominas-Faja, E. Cuyàs, T. Alarcón, C. Kleer, J.A. Menendez, R. Lupu, Suppression of endogenous lipogenesis induces reversion of the malignant phenotype and normalized differentiation in breast cancer, Oncotarget. 7 (2016) 71151–71168. doi:10.18632/oncotarget.9463.

[18] J.A. Menendez, R. Lupu, Fatty acid synthase (FASN) as a therapeutic target in breast cancer, Expert Opin. Ther. Targets. 21 (2017) 1001–1016. doi:10.1080/14728222.2017.1381087.

[19] G.E. Mullen, L. Yet, Progress in the development of fatty acid synthase inhibitors as anticancer targets, Bioorganic Med. Chem. Lett. 25 (2015) 4363–4369.

[20] S. Ōmura, The Antibiotic Cerulenin, a Novel Tool for Biochemistry an Inhibitor of Fatty Acid Synthesis, Bacteriol. Rev. 40 (1976) 681–697.

[21] J.M. McFadden, S.M. Medghalchi, J.N. Thupari, M.L. Pinn, A. Vadlamudi, K.I. Miller, F.P. Kuhajda, C.A. Townsend, Application of a Flexible Synthesis of (5R)-Thiolactomycin to Develop New Inhibitors of Type I Fatty Acid Synthase, J. Med. Chem. 48 (2005) 946–961. doi:10.1021/jm049389h.

[22] K. Brusselmans, E. De Schrijver, W. Heyns, G. Verhoeven, J. V. Swinnen, Epigallocatechin-3-gallate is a Potent Natural Inhibitor of Fatty Acid Synthase in Intact Cells and Selectively Induces Apoptosis in Prostate Cancer Cells, Int. J. Cancer. 106 (2003) 856–862. doi:10.1002/ijc.11317.

[23] M. Putteeraj, W.L. Lim, S.L. Teoh, M.F. Yahaya, Flavonoids and its Neuroprotective Effects on Brain Ischemia and Neurodegenerative Diseases, Curr. Drug Targets. 19 (2018) 1710–1720. doi:10.2174/1389450119666180326125252.

[24] R. Colomer, A. Sarrats, R. Lupu, T. Puig, Natural Polyphenols and their Synthetic Analogs as Emerging Anticancer Agents, Curr. Drug Targets. 18 (2017) 147–159. doi:10.2174/1389450117666160112113930.

[25] Q.Y. Eng, P.V. Thanikachalam, S. Ramamurthy, Molecular understanding of Epigallocatechin gallate (EGCG) in cardiovascular and metabolic diseases, J. Ethnopharmacol. 210 (2018) 296–310. doi:10.1016/j.jep.2017.08.035.

[26] W.C. Reygaert, The antimicrobial possibilities of green tea, Front. Microbiol. 5 (2014) 434. doi:10.3389/fmicb.2014.00434.

[27] A. Golonko, T. Pienkowski, R. Swislocka, R. Lazny, M. Roszko, W. Lewandowski, Another look at phenolic compounds in cancer therapy the effect of polyphenols on ubiquitin-proteasome system, Eur. J. Med. Chem. 167 (2019) 291–311. doi:10.1016/j.ejmech.2019.01.044.

[28] M.C. Foti, Antioxidant properties of phenols, J. Pharm. Pharmacol. 59 (2007) 1673–1685. doi:10.1211/jpp.59.12.0010.

[29] J.B. Baell, Feeling Nature's PAINS: Natural Products, Natural Product Drugs, and Pan Assay Interference Compounds (PAINS), J. Nat. Prod. 79 (2016) 616–628. doi:10.1021/acs.jnatprod.5b00947.

[30] H.I. Ingólfsson, P. Thakur, K.F. Herold, E.A. Hobart, N.B. Ramsey, X. Periole, D.H. De Jong, M. Zwama, D. Yilmaz, K. Hall, T. Maretzky, H.C. Hemmings, C. Blobel, S.J. Marrink, A. Koçer, J.T. Sack, O.S. Andersen, Phytochemicals perturb membranes and promiscuously alter protein function, ACS Chem. Biol. 9 (2014) 1788–1798. doi:10.1021/cb500086e.

[31] X. Wang, W.X. Tian, Green Tea Epigallocatechin Gallate: A Natural Inhibitor of Fatty-Acid Synthase, Biochem. Biophys. Res. Commun. 288 (2001) 1200–1206. doi:10.1006/bbrc.2001.5923.

[32] T. Wei-Xi, Inhibition of Fatty Acid Synthase by Polyphenols, Curr. Med. Chem. 13 (2006) 967–977. doi:10.2174/092986706776361012.

[33] B.H. Li, X.F. Ma, Y. Wang, W.X. Tian, Structure-Activity Relationship of Polyphenols That Inhibit Fatty Acid Synthase, J. Biochem. 138 (2005) 679–685. doi:10.1093/jb/mvi171.

[34] C. Turrado, T. Puig, J. García-Cárceles, M. Artola, B. Benhamú, S. Ortega-Gutiérrez, J.

Relat, G. Oliveras, A. Blancafort, D. Haro, P.F. Marrero, R. Colomer, M.L. López-Rodríguez, New Synthetic Inhibitors of Fatty Acid Synthase with Anticancer Activity, J. Med. Chem. 55 (2012) 5013–5023.

[35] K. Brusselmans, R. Vrolix, G. Verhoeven, J. V. Swinnen, Induction of Cancer Cell Apoptosis by Flavonoids Is Associated with Their Ability to Inhibit Fatty Acid Synthase Activity, J. Biol. Chem. 280 (2005) 5636–5645. doi:10.1074/jbc.M408177200.

[36] S. V Sharma, D.W. Bell, J. Settleman, D.A. Haber, Epidermal growth factor receptor mutations in lung cancer, Nat. Rev. Cancer. 7 (2007) 169–181. doi:10.1038/nrc2088.

[37] S. Matsuda, A. Nakanishi, Y. Wada, Y. Kitagishi, Roles of PI3K/AKT/PTEN Pathway as a Target for Pharmaceutical Therapy, Open Med. Chem. J. 7 (2013) 23–29. doi:10.2174/1874104501307010023.

[38] M.-M. Georgescu, PTEN Tumor Suppressor Network in PI3K-Akt Pathway Control, Genes Cancer. 1 (2011) 1170–1177. doi:10.1177/1947601911407325.

[39] A. Ali, E. Levantini, J.T. Teo, J. Goggi, J.G. Clohessy, C.S. Wu, L. Chen, H. Yang, I. Krishnan, O. Kocher, J. Zhang, R.A. Soo, K. Bhakoo, T.M. Chin, D.G. Tenen, Fatty acid synthase mediates EGFR palmitoylation in EGFR mutated non-small cell lung cancer, EMBO Mol. Med. 10 (2018) e8313. doi:10.15252/emmm.201708313.

[40] M. Ono, A. Hirata, T. Kometani, M. Miyagawa, S. Ueda, H. Kinoshita, T. Fujii, M. Kuwano, Sensitivity to gefitinib (Iressa , ZD1839) in non-small cell lung cancer cell lines correlates with dependence on the epidermal growth factor (EGF) receptor/extracellular signal-regulated kinase 1/2 and EGF receptor/Akt pathway for proliferation, Mol. Cancer Ther. 3 (2004) 465–472.

[41] M. Younes, P. Aggett, F. Aguilar, R. Crebelli, B. Dusemund, M. Filipič, M.J. Frutos, P. Galtier, D. Gott, U. Gundert-Remy, C. Lambré, J.C. Leblanc, I.T. Lillegaard, P. Moldeus, A. Mortensen, A. Oskarsson, I. Stankovic, I. Waalkens-Berendsen, R.A. Woutersen, R.J. Andrade, C. Fortes, P. Mosesso, P. Restani, D. Arcella, F. Pizzo, C. Smeraldi, M. Wright, Scientific Opinion on the Safety of Green Tea Catechins, EFSA J. 16 (2018) 5239. doi:10.2903/j.efsa.2018.5239.

[42] T. Van De Sande, E. De Schrijver, W. Heyns, G. Verhoeven, J. V Swinnen, Role of the Phosphatidylinositol 3'-Kinase/PTEN/Akt Kinase Pathway in the Overexpression of Fatty Acid Synthase in LNCaP Prostate Cancer Cells, Cancer Res. 62 (2002) 642–646.

[43] H.Q. Wang, D.A. Altomare, K.L. Skele, P.I. Poulikakos, F.P. Kuhajda, A. Di Cristofano, J.R. Testa, Positive feedback regulation between AKT activation and fatty acid synthase expression in ovarian carcinoma cells, Oncogene. 24 (2005) 3574–3582. doi:10.1038/sj.onc.1208463.

[44] Y.-A. Yang, W.F. Han, P.J. Morin, F.J. Chrest, E.S. Pizer, Activation of Fatty Acid Synthesis during Neoplastic Transformation: Role of Mitogen-Activated Protein Kinase and Phosphatidylinositol 3-Kinase, Exp. Cell Res. 279 (2002) 80–90. doi:10.1006/excr.2002.5600.

[45] K. Tomek, R. Wagner, F. Varga, C.F. Singer, H. Karlic, T.W. Grunt, Blockade of Fatty Acid Synthase Induces Ubiquitination and Degradation of Phosphoinositide-3-Kinase Signaling Proteins in Ovarian Cancer, Mol. Cancer Res. 9 (2011) 1767–1779. doi:10.1158/1541-7786.MCR-10-0467.

[46] S.R. Datta, A. Brunet, M.E. Greenberg, Cellular survival: a play in three Akts, Genes Dev. 13 (1999) 2905–2927.

[47] P. Ciapetti, B. Giethlen, Molecular variations based on isosteric replacements, in: C. Wermuth (Ed.), Pract. Med. Chem. 3rd Ed., Academic Press London, 2008: pp. 318–320.

[48] K.J. Hock, R. Spitzner, R.M. Koenigs, Towards nitrile-substituted cyclopropanes – a slow-release protocol for safe and scalable applications of diazo acetonitrile, Green Chem. 19 (2017) 2118–2122. doi:10.1039/C7GC00602K.

[49] C. Xu, W. Du, Y. Zeng, B. Dai, H. Guo, Reactivity Switch Enabled by Counterion: Highly Chemoselective Dimerization and Hydration of Terminal Alkynes, Org. Lett. 16 (2014) 948–951. doi:10.1021/ol403684a.

[50] A. Farina, C. Ferranti, C. Marra, An improved synthesis of resveratrol, Nat. Prod. Res. 20 (2006) 247–252. doi:10.1080/14786410500059532.

[51] A.K. Sinha, V. Kumar, A. Sharma, A. Sharma, R. Kumar, An unusual, mild and convenient one-pot two-step access to (E)-stilbenes from hydroxy-substituted benzaldehydes and phenylacetic acids under microwave activation: a new facet of the classical Perkin reaction, Tetrahedron. 63 (2007) 11070–11077. doi:10.1016/j.tet.2007.08.034.

[52] E.M. Campi, W.R. Jackson, S.M. Marcuccio, C.G.M. Naeslund, High Yields of

Unsymmetrical Biaryls via Cross Coupling of Arylboronic Acids with Haloarenes Using a Modified Suzuki-Beletskaya Procedure, J. Chem. Soc. Chem. Commun. (1994) 2395. doi:10.1039/C39940002395.

[53] A.H. De Groot, R.A. Dommisse, G.L. Lemière, Selective Cleavage of tert-Butyldimethylsilylethers ortho to a Carbonyl Group by Ultrasound, Tetrahedron. 56 (2000) 1541–1549. doi:10.1016/S0040-4020(00)00053-3.

[54] K.S. Feldman, S.M. Ensel, Ellagitannin Chemistry. Preparative and Mechanistic Studies of the Biomimetic Oxidative Coupling of Galloyl Esters, J. Am. Chem. Soc. 116 (1994) 3357–3366. doi:10.1021/ja00087a022.

[55] N.W. Bays, A.D. Hill, I. Kariv, A Simplified Scintillation Proximity Assay for Fatty Acid Synthase Activity: Development and Comparison with Other FAS Activity Assays, J. Biomol. Screen. 14 (2009) 636–642. doi:10.1177/1087057109335746.

Highlights

- FASN activity plays an important role in cancer progression
- *trans*-Stilbene galloyl esters **EC1** and **EC5** are pan-growth inhibitors of NSCLC cells
- **EC1** and **EC5** cause apoptosis in NSCLC cells through FASN inhibition
- FASN inhibition disrupts FASN-AKT axis and reduces phospho-AKT levels
- Lipid supplementation rescues NSCLC cells from inhibitory effects of **EC1** and **EC5**

Supplementary Information: NMR Spectra

Galloyl esters of *trans*-stilbenes are inhibitors of FASN with anticancer activity on non-small cell lung cancer cells

Yu-Jia Tan [a #], Azhar Ali [b #], Sheng-Yang Tee [a], Jun-Ting Teo [b], Xi Yu [c], Mei-Lin Go [c *], Yulin Lam [a *]

[a] Department of Chemistry, National University of Singapore, 3 Science Drive 3, 117543, Singapore. [b] Cancer Science Institute of Singapore, Yong Loo Lin School of Medicine, 14 Medical Drive, 117599, Singapore; [c] Department of Pharmacy, National University of Singapore, 18 Science Drive 4, 117543, Singapore.

Co-First Authors; * Co-Corresponding authors.

Table of Contents

(A) ^{1}H and ^{13}C NMR spectra of intermediate of and final compound 1

[1,1'-Biphenyl]-4,4'-diyl bis(3,4,5-tris((*tert*-butyldimethylsilyl)oxy)benzoate) (**17**)

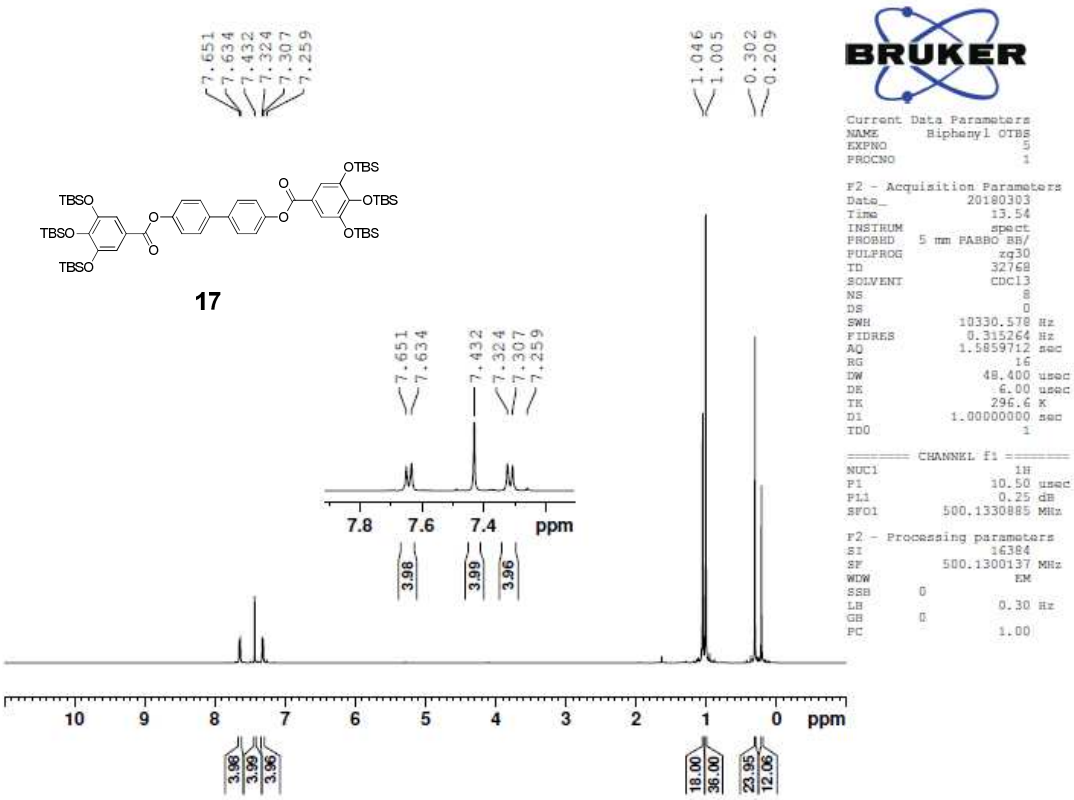

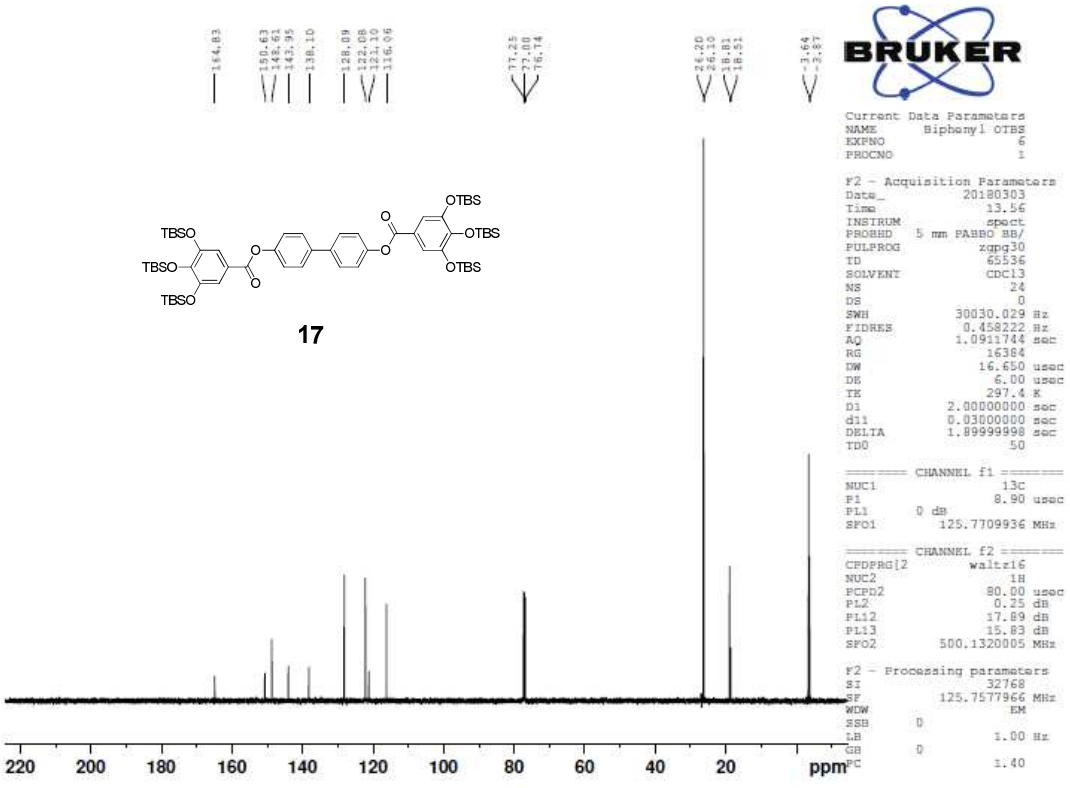

[1,1'-Biphenyl]-4,4'-diyl bis(3,4,5-trihydroxybenzoate) **(1)**

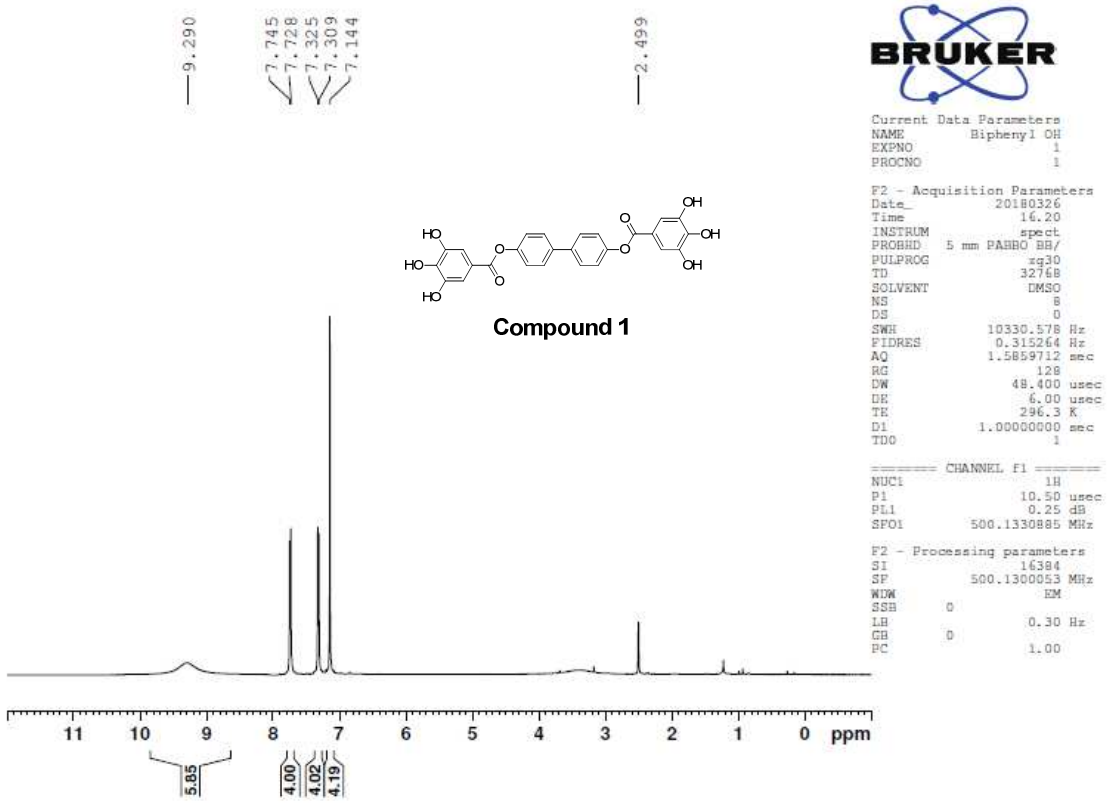


```
Current Data Parameters
NAME          Biphenyl OH
EXPNO                   1
PROCNO                  1

F2 - Acquisition Parameters
Date_            20180326
Time                16.20
INSTRUM             spect
PROBHD   5 mm PABBO BB/
PULPROG             zg30
TD                 32768
SOLVENT             DMSO
NS                     8
DS                     0
SWH          10330.578 Hz
FIDRES        0.315264 Hz
AQ           1.5859712 sec
RG                   128
DW              48.400 usec
DE               6.00 usec
TE              296.3 K
D1           1.00000000 sec
TD0                    1

======== CHANNEL f1 ========
NUC1                  1H
P1              10.50 usec
PL1              0.25 dB
SFO1       500.1330885 MHz

F2 - Processing parameters
SI                 16384
SF         500.1300053 MHz
WDW                   EM
SSB       0
LB               0.30 Hz
GB        0
PC               1.00
```

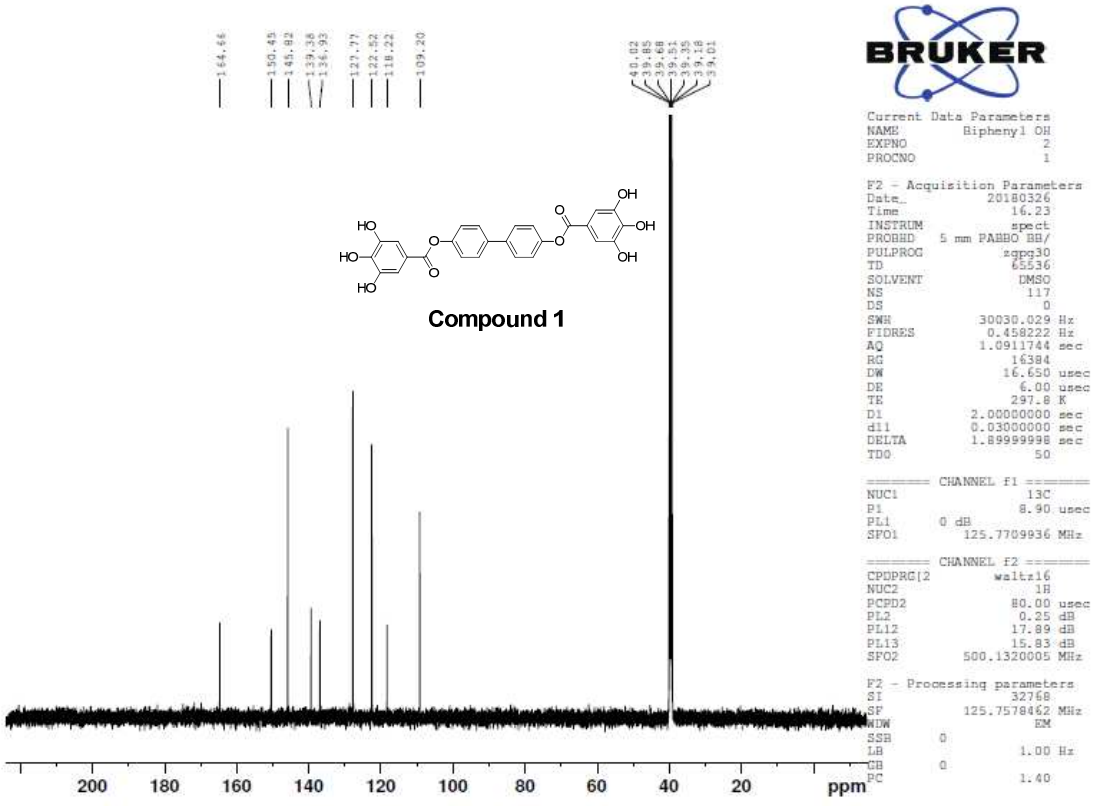


```
Current Data Parameters
NAME          Biphenyl OH
EXPNO                   2
PROCNO                  1

F2 - Acquisition Parameters
Date_            20180326
Time                16.23
INSTRUM             spect
PROBHD   5 mm PABBO BB/
PULPROG          zgpg30
TD                 65536
SOLVENT             DMSO
NS                   117
DS                     0
SWH          30030.029 Hz
FIDRES        0.458222 Hz
AQ           1.0911744 sec
RG                 16384
DW              16.650 usec
DE               6.00 usec
TE              297.8 K
D1           2.00000000 sec
d11          0.03000000 sec
DELTA        1.89999998 sec
TD0                   50

======== CHANNEL f1 ========
NUC1                 13C
P1               8.90 usec
PL1        0 dB
SFO1       125.7709936 MHz

======== CHANNEL f2 ========
CPDPRG[2          waltz16
NUC2                  1H
PCPD2           80.00 usec
PL2              0.25 dB
PL12            17.89 dB
PL13            15.83 dB
SFO2       500.1320005 MHz

F2 - Processing parameters
SI                 32768
SF         125.7578462 MHz
WDW                   EM
SSB       0
LB               1.00 Hz
GB        0
PC               1.40
```

(B) ^{1}H and ^{13}C NMR spectra of intermediates

3-Vinylphenyl acetate (**4a**)

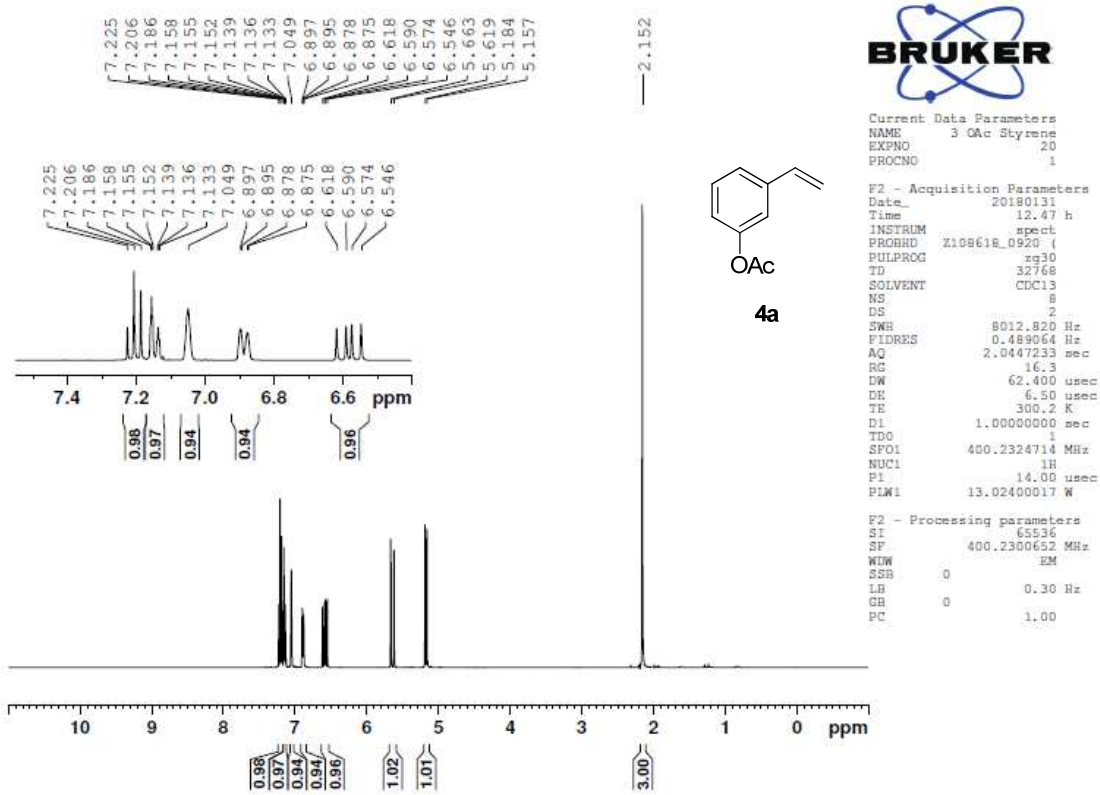

BRUKER

```
Current Data Parameters
NAME        3 OAc Styrene
EXPNO                  20
PROCNO                  1

F2 - Acquisition Parameters
Date_            20180131
Time                12.47 h
INSTRUM              spect
PROBHD    Z108618_0920 (
PULPROG              zg30
TD                  32768
SOLVENT             CDCl3
NS                      8
DS                      2
SWH              8012.820 Hz
FIDRES           0.489064 Hz
AQ               2.0447233 sec
RG                   16.3
DW                62.400 usec
DE                 6.50 usec
TE                300.2 K
D1             1.00000000 sec
TD0                     1
SFO1          400.2324714 MHz
NUC1                   1H
P1                 14.00 usec
PLW1          13.02400017 W

F2 - Processing parameters
SI                  65536
SF            400.2300652 MHz
WDW                    EM
SSB        0
LB                  0.30 Hz
GB         0
PC                  1.00
```

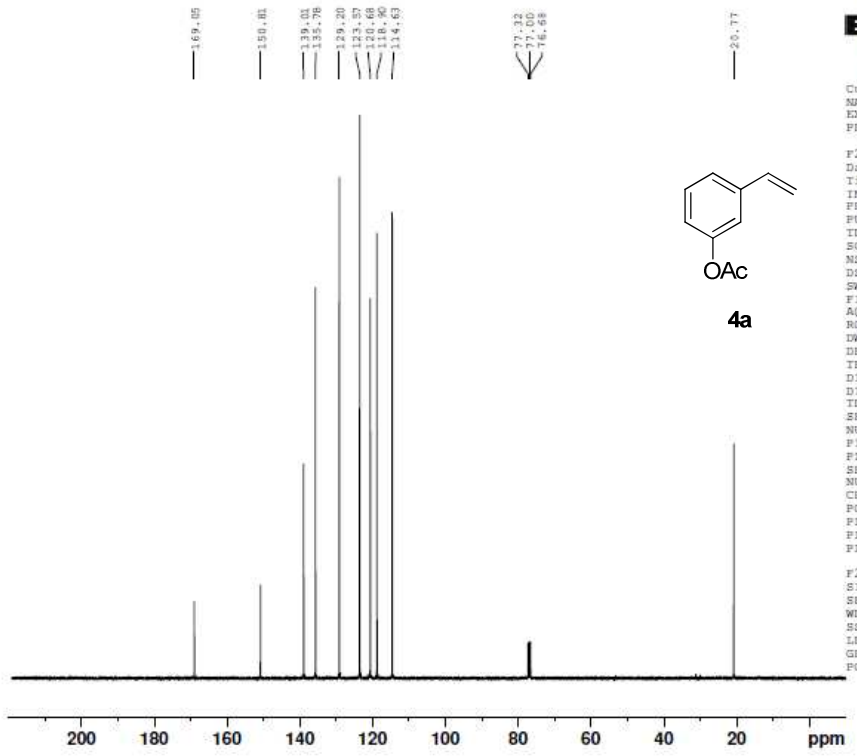

BRUKER

```
Current Data Parameters
NAME        3 OAc Styrene
EXPNO                  21
PROCNO                  1

F2 - Acquisition Parameters
Date_            20180131
Time                12.54 h
INSTRUM              spect
PROBHD    Z108618_0920 (
PULPROG            zgpg30
TD                  65536
SOLVENT             CDCl3
NS                    100
DS                      4
SWH             24038.461 Hz
FIDRES           0.733596 Hz
AQ               1.3631488 sec
RG                  205.55
DW                20.800 usec
DE                 6.50 usec
TE                301.1 K
D1             2.00000000 sec
D11            0.03000000 sec
TD0                     1
SFO1          100.6479773 MHz
NUC1                   13C
P1                 15.00 usec
PLW1          26.83600044 W
SFO2          400.2316009 MHz
NUC2                   1H
CPDPRG[2          waltz16
PCPD2              90.00 usec
PLW2          13.02400017 W
PLW12          0.31628889 W
PLW13          0.15852401 W

F2 - Processing parameters
SI                  32768
SF            100.6379431 MHz
WDW                    EM
SSB        0
LB                  1.00 Hz
GB         0
PC                  1.40
```

(*E*)-3-(4-Acetoxystyryl)phenyl acetate (**6a**)

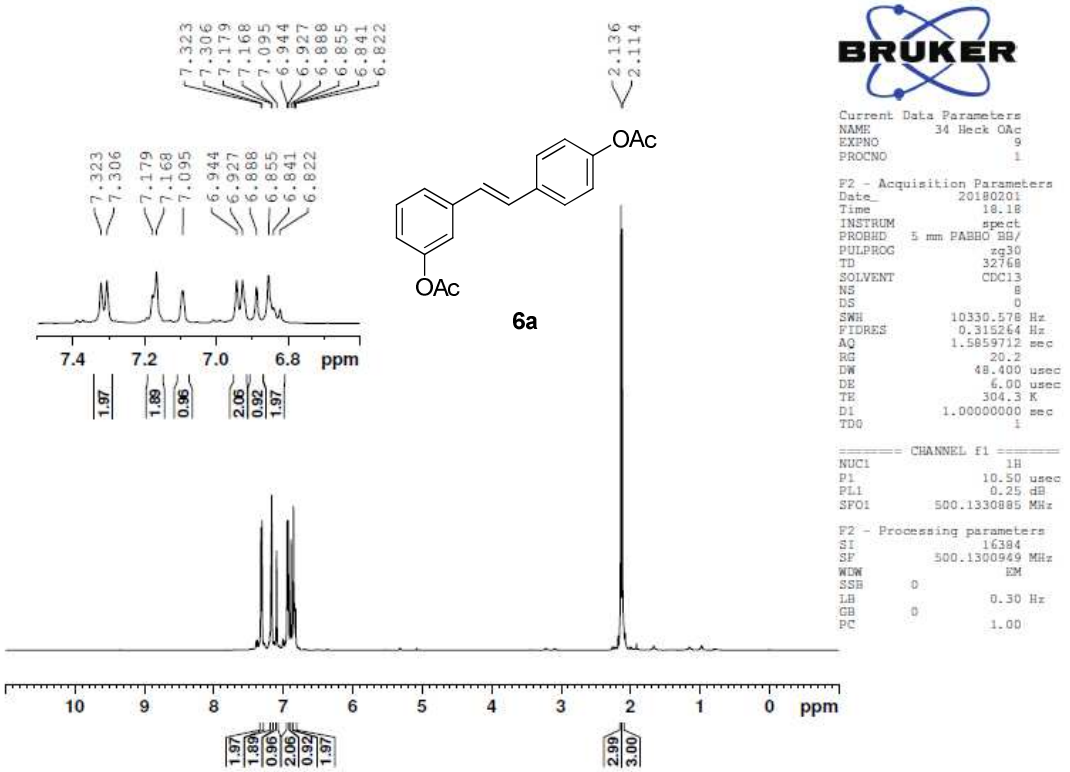

BRUKER

```
Current Data Parameters
NAME          34 Heck OAc
EXPNO                   9
PROCNO                  1

F2 - Acquisition Parameters
Date_           20180201
Time               18.18
INSTRUM            spect
PROBHD   5 mm PABBO BB/
PULPROG            zg30
TD                32768
SOLVENT           CDCl3
NS                    8
DS                    0
SWH           10330.578 Hz
FIDRES        0.315264 Hz
AQ            1.5859712 sec
RG                 20.2
DW                48.400 usec
DE                 6.00 usec
TE                304.3 K
D1            1.00000000 sec
TD0                   1

======== CHANNEL f1 ========
NUC1                  1H
P1                10.50 usec
PL1                0.25 dB
SFO1         500.1330885 MHz

F2 - Processing parameters
SI                16384
SF          500.1300949 MHz
WDW                  EM
SSB          0
LB                 0.30 Hz
GB           0
PC                 1.00
```

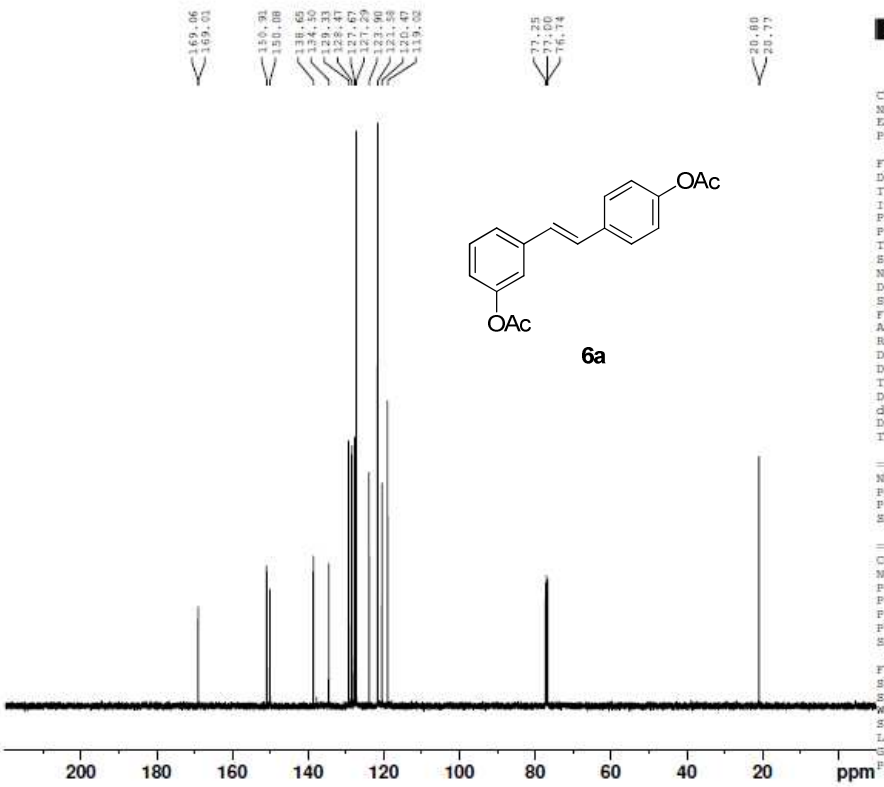

BRUKER

```
Current Data Parameters
NAME          34 Heck OAc
EXPNO                  10
PROCNO                  1

F2 - Acquisition Parameters
Date_           20180201
Time               18.19
INSTRUM            spect
PROBHD   5 mm PABBO BB/
PULPROG          zgpg30
TD                65536
SOLVENT           CDCl3
NS                   32
DS                    0
SWH           30030.029 Hz
FIDRES        0.458222 Hz
AQ            1.0911744 sec
RG                16384
DW               16.650 usec
DE                 6.00 usec
TE                305.2 K
D1            2.00000000 sec
d11           0.03000000 sec
DELTA         1.89999998 sec
TD0                  50

======== CHANNEL f1 ========
NUC1                 13C
P1                 8.90 usec
PL1        0 dB
SFO1         125.7709936 MHz

======== CHANNEL f2 ========
CPDPRG[2          waltz16
NUC2                  1H
PCPD2             80.00 usec
PL2                0.25 dB
PL12              17.89 dB
PL13              15.83 dB
SFO2         500.1320005 MHz

F2 - Processing parameters
SI                32768
SF          125.7578259 MHz
WDW                  EM
SSB          0
LB                 1.00 Hz
GB           0
PC                 1.40
```

(*E*)-3-Styrylphenyl acetate (**6b**)

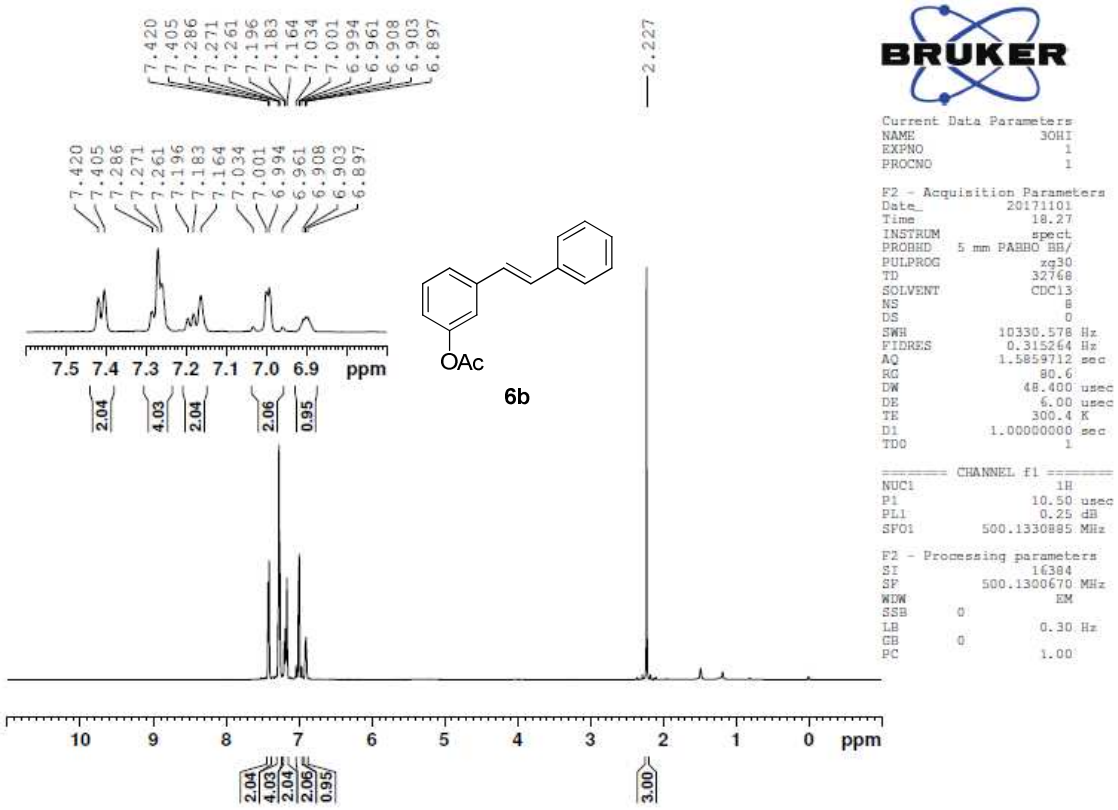

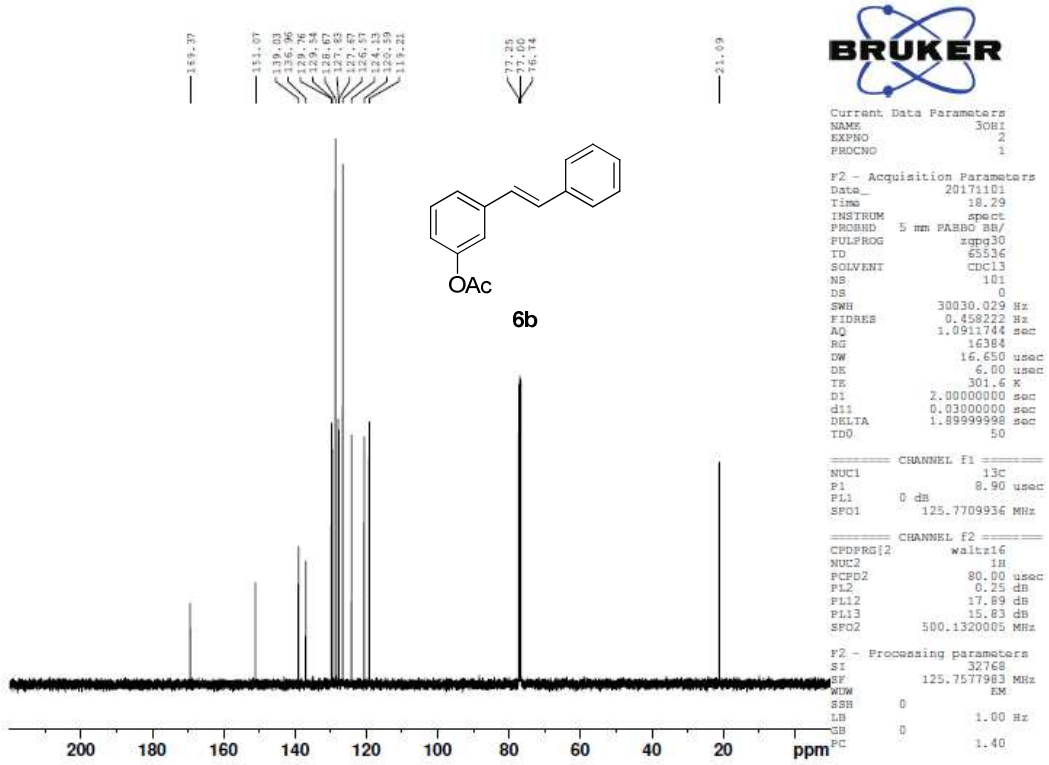

(*E*)-4-Styrylphenyl acetate (**6c**)

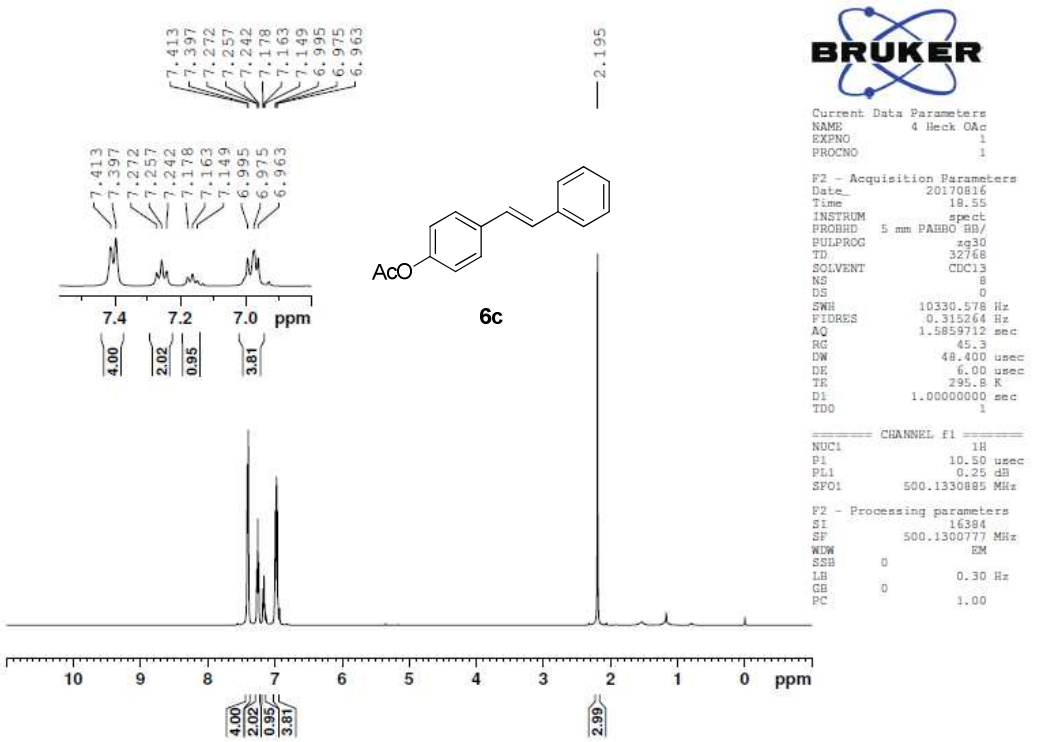


```
Current Data Parameters
NAME                  4 Heck OAc
EXPNO                          1
PROCNO                         1

F2 - Acquisition Parameters
Date_               20170816
Time                   18.55
INSTRUM                spect
PROBHD    5 mm PABBO BB/
PULPROG                zg30
TD                    32768
SOLVENT               CDCl3
NS                        8
DS                        0
SWH                10330.578 Hz
FIDRES             0.315264 Hz
AQ                 1.5859712 sec
RG                      45.3
DW                    48.400 usec
DE                     6.00 usec
TE                    295.8 K
D1                 1.00000000 sec
TD0                       1

======== CHANNEL f1 ========
NUC1                      1H
P1                     10.50 usec
PL1                     0.25 dB
SFO1              500.1330885 MHz

F2 - Processing parameters
SI                        16384
SF                500.1300777 MHz
WDW                        EM
SSB                       0
LB                     0.30 Hz
GB                        0
PC                     1.00
```

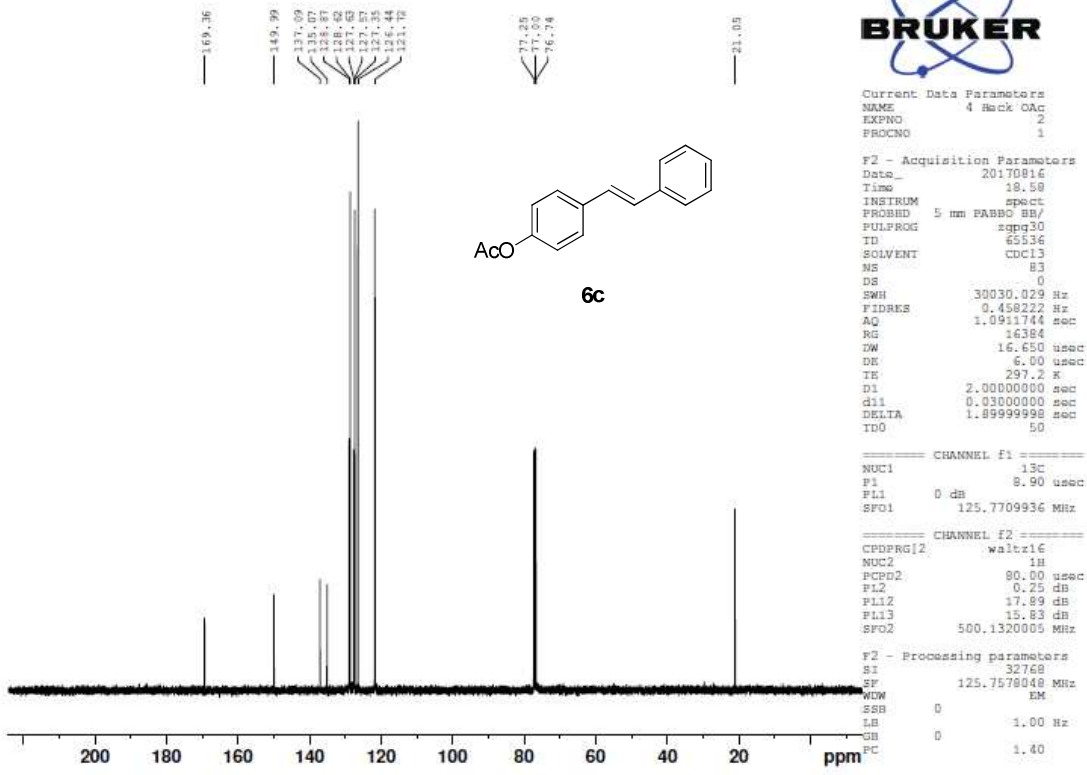


```
Current Data Parameters
NAME                  4 Heck OAc
EXPNO                          2
PROCNO                         1

F2 - Acquisition Parameters
Date_               20170816
Time                   18.50
INSTRUM                spect
PROBHD    5 mm PABBO BB/
PULPROG             zgpg30
TD                    65536
SOLVENT               CDCl3
NS                       83
DS                        0
SWH                30030.029 Hz
FIDRES             0.458222 Hz
AQ                 1.0911744 sec
RG                     16384
DW                    16.650 usec
DE                     6.00 usec
TE                    297.2 K
D1                 2.00000000 sec
d11                0.03000000 sec
DELTA              1.89999998 sec
TD0                       50

======== CHANNEL f1 ========
NUC1                      13C
P1                     8.90 usec
PL1                    0 dB
SFO1             125.7709936 MHz

======== CHANNEL f2 ========
CPDPRG[2                waltz16
NUC2                      1H
PCPD2                  80.00 usec
PL2                     0.25 dB
PL12                   17.89 dB
PL13                   15.83 dB
SFO2              500.1320005 MHz

F2 - Processing parameters
SI                        32768
SF               125.7578048 MHz
WDW                        EM
SSB                       0
LB                     1.00 Hz
GB                        0
PC                     1.40
```

(*E*)-3-(4-Hydroxystyryl)phenol (**7a**)

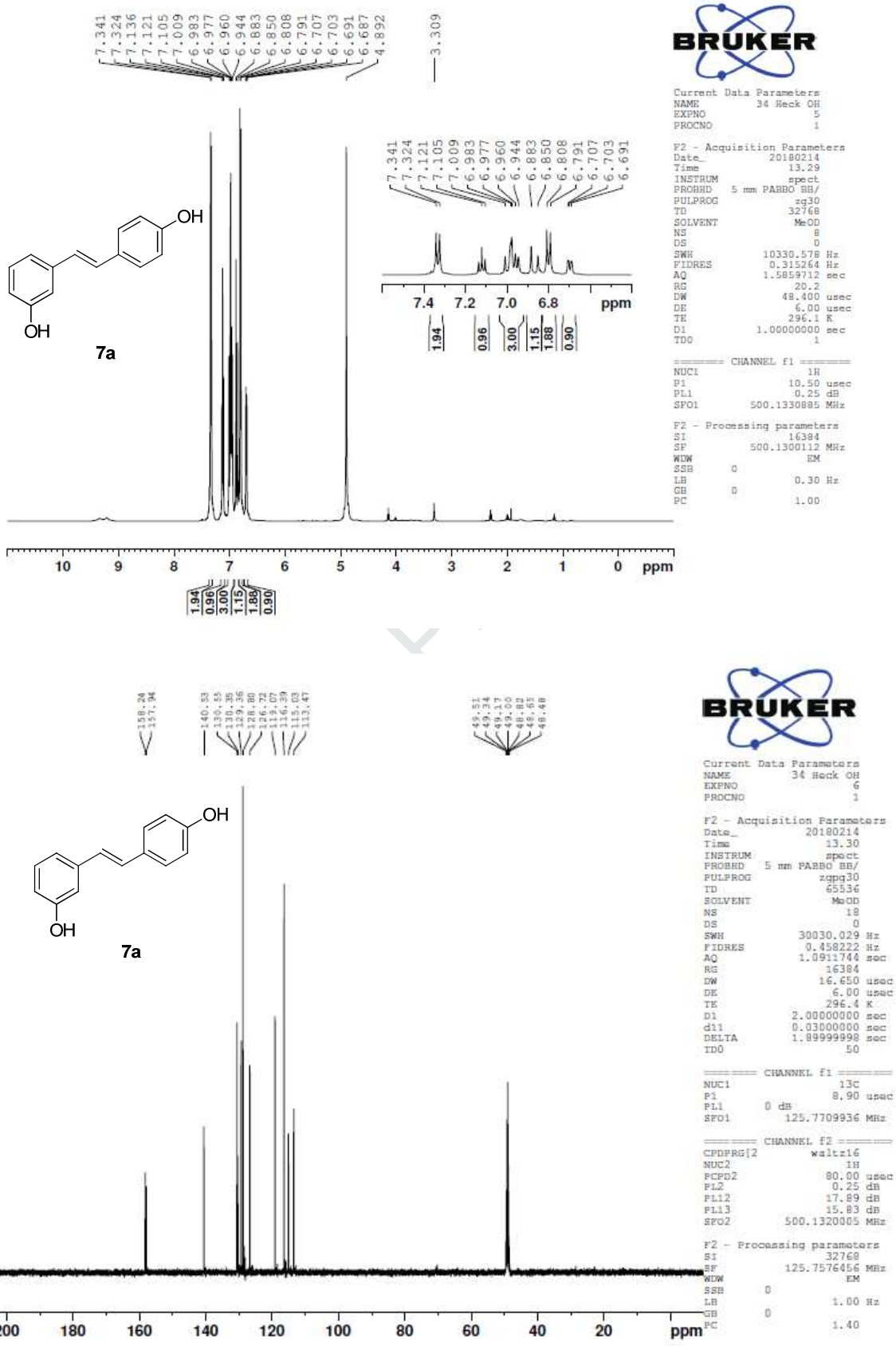

(*E*)-3-Styrylphenol (**7b**)

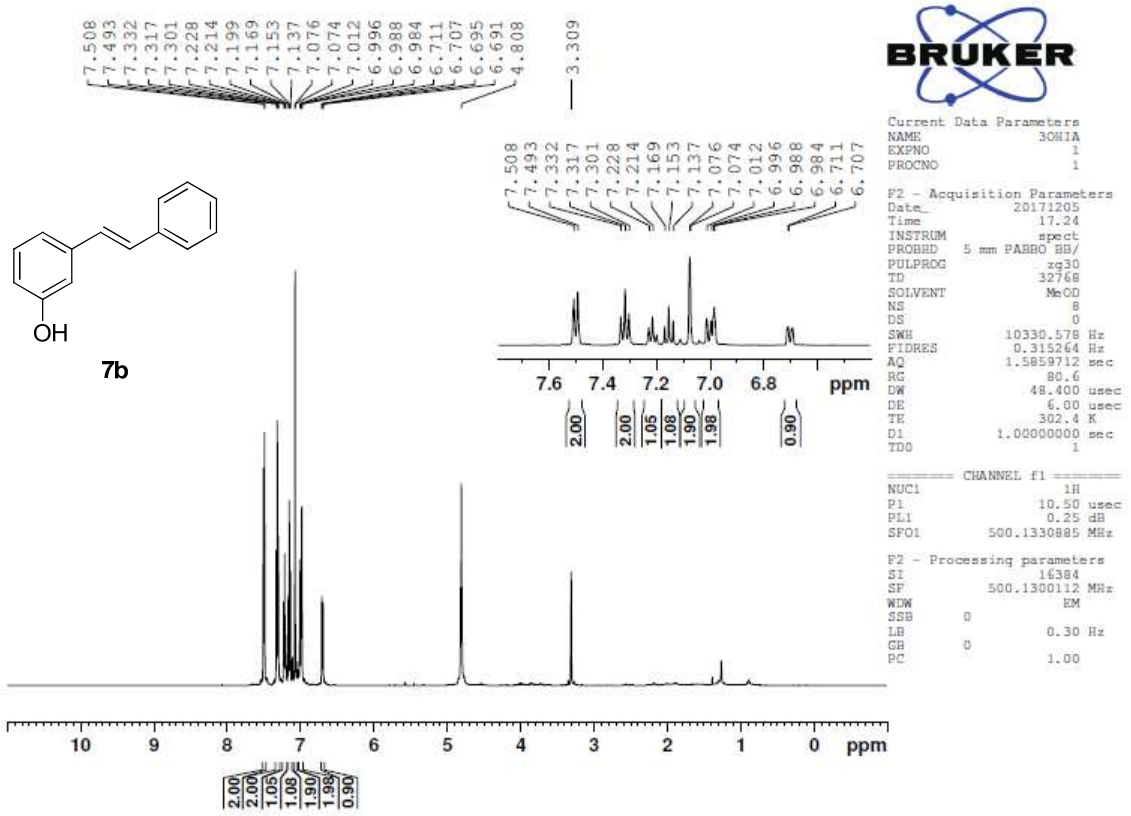

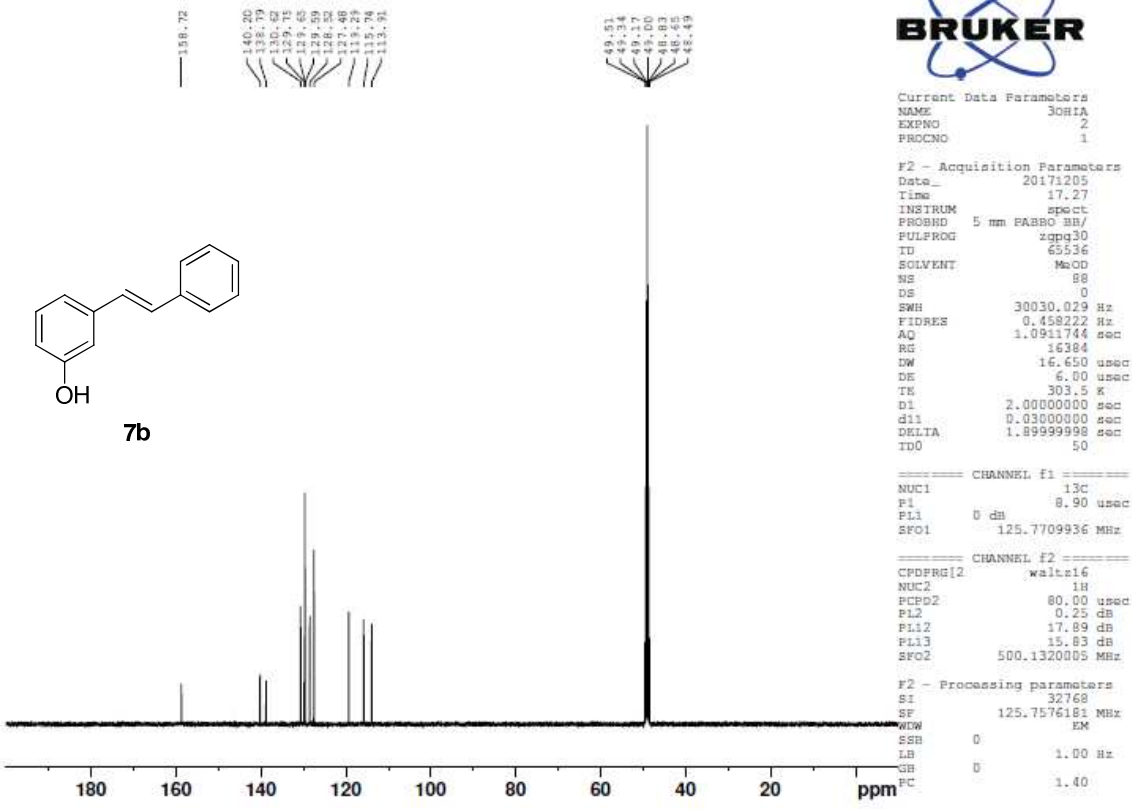

(*E*)-4-Styrylphenol (**7c**)

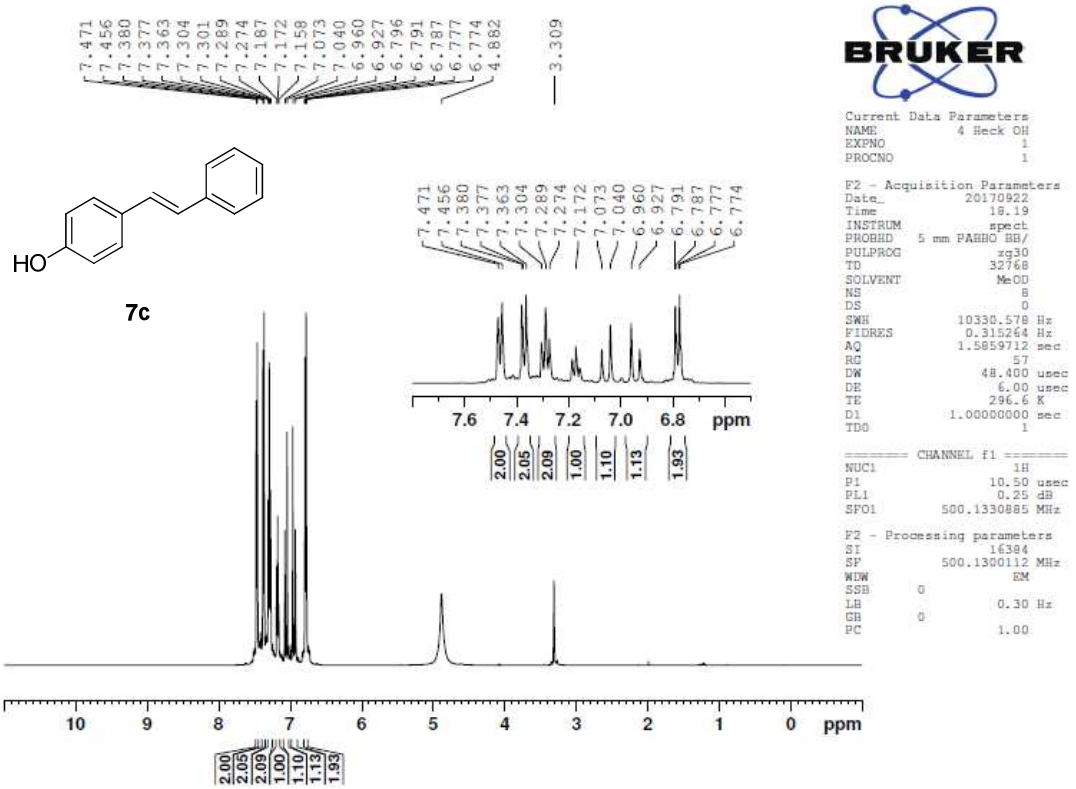

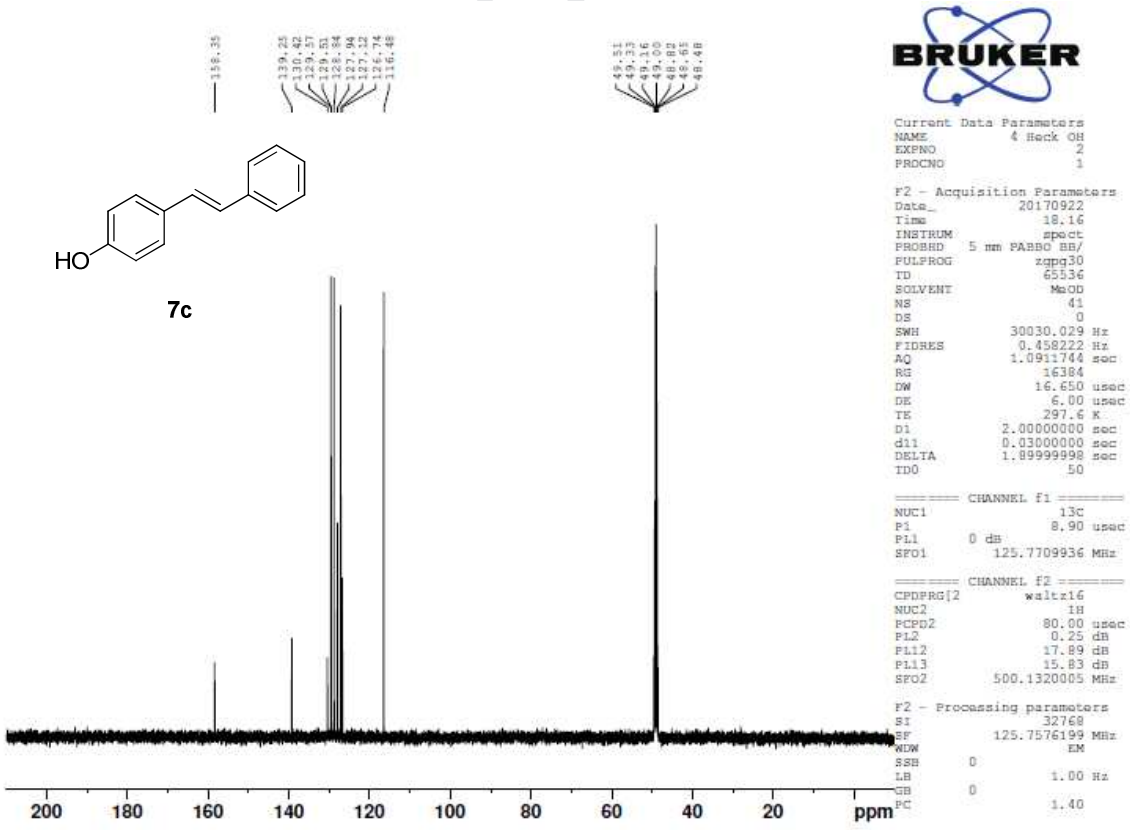

(*E*)-4,4'-(Ethene-1,2-diyl)diphenol (**8**)

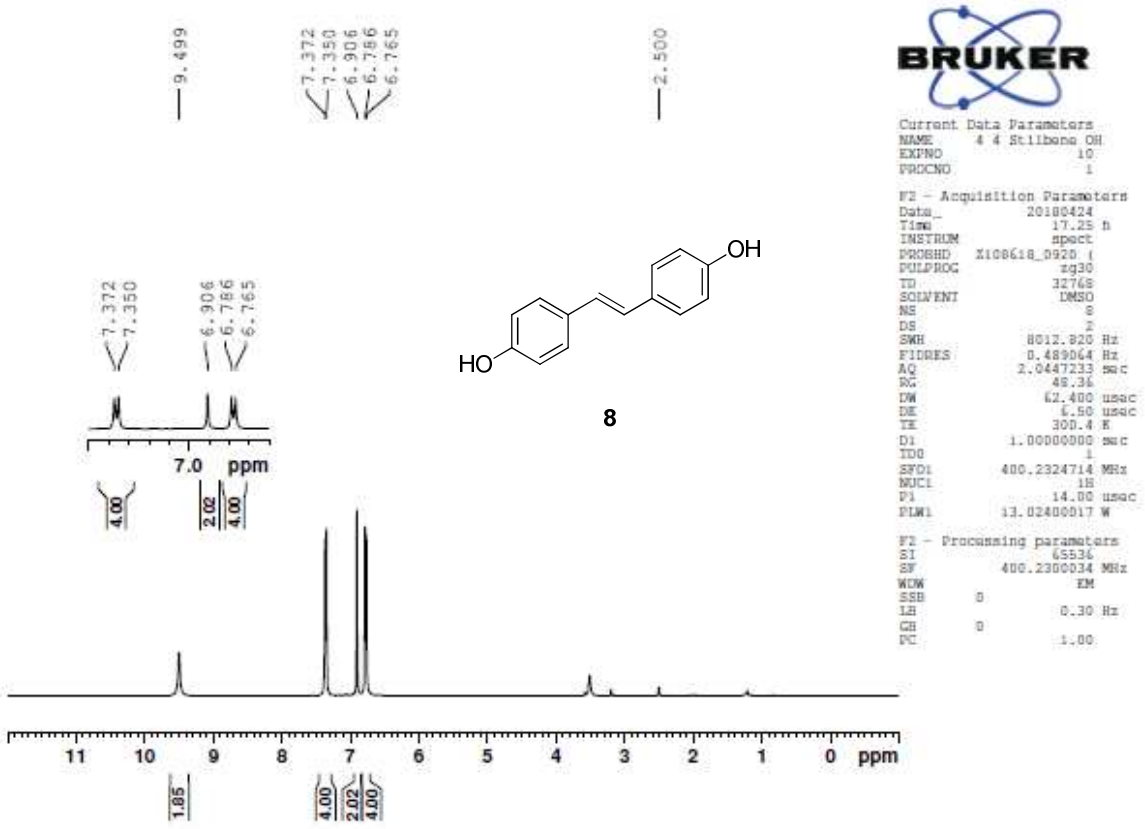

BRUKER

```
Current Data Parameters
NAME      4 4 Stilbene OH
EXPNO               10
PROCNO               1

F2 - Acquisition Parameters
Date_         20180424
Time              17.25 h
INSTRUM           spect
PROBHD   Z108618_0920 (
PULPROG           zg30
TD               32768
SOLVENT           DMSO
NS                   8
DS                   2
SWH            8012.820 Hz
FIDRES         0.489064 Hz
AQ             2.0447233 sec
RG                48.36
DW               62.400 usec
DE                6.50 usec
TE              300.4 K
D1             1.00000000 sec
TD0                  1
SFO1         400.2324714 MHz
NUC1               1H
P1                14.00 usec
PLW1          13.02400017 W

F2 - Processing parameters
SI                65536
SF           400.2300034 MHz
WDW                EM
SSB       0
LB                0.30 Hz
GB        0
PC                1.00
```

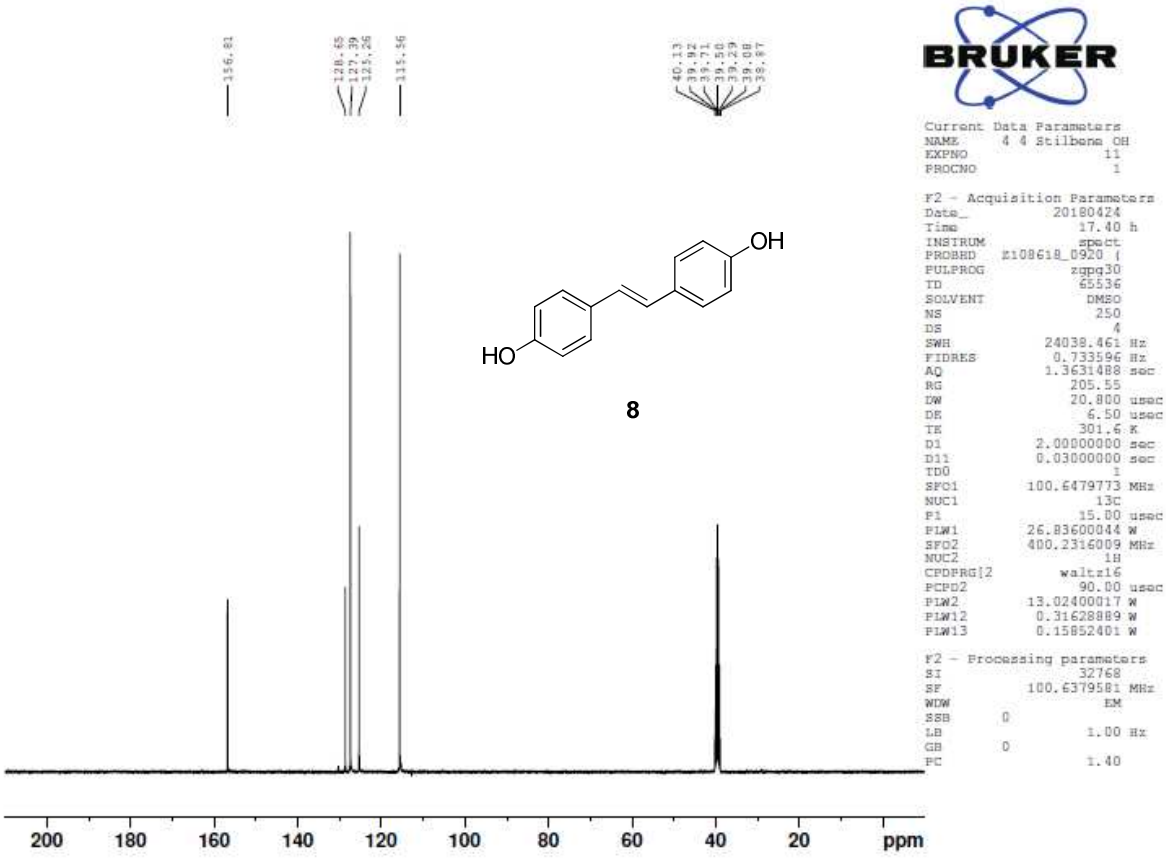

BRUKER

```
Current Data Parameters
NAME      4 4 Stilbene OH
EXPNO               11
PROCNO               1

F2 - Acquisition Parameters
Date_         20180424
Time              17.40 h
INSTRUM           spect
PROBHD   Z108618_0920 (
PULPROG          zgpg30
TD               65536
SOLVENT           DMSO
NS                 250
DS                   4
SWH           24038.461 Hz
FIDRES         0.733596 Hz
AQ             1.3631488 sec
RG                205.55
DW               20.800 usec
DE                6.50 usec
TE              301.6 K
D1             2.00000000 sec
D11            0.03000000 sec
TD0                  1
SFO1         100.6479773 MHz
NUC1               13C
P1                15.00 usec
PLW1          26.83600044 W
SFO2         400.2316009 MHz
NUC2               1H
CPDPRG[2         waltz16
PCPD2             90.00 usec
PLW2          13.02400017 W
PLW12          0.31628889 W
PLW13          0.15852401 W

F2 - Processing parameters
SI                32768
SF           100.6379581 MHz
WDW                EM
SSB       0
LB                1.00 Hz
GB        0
PC                1.40
```

1-(4-Methoxyphenyl)naphthalene (**9**)

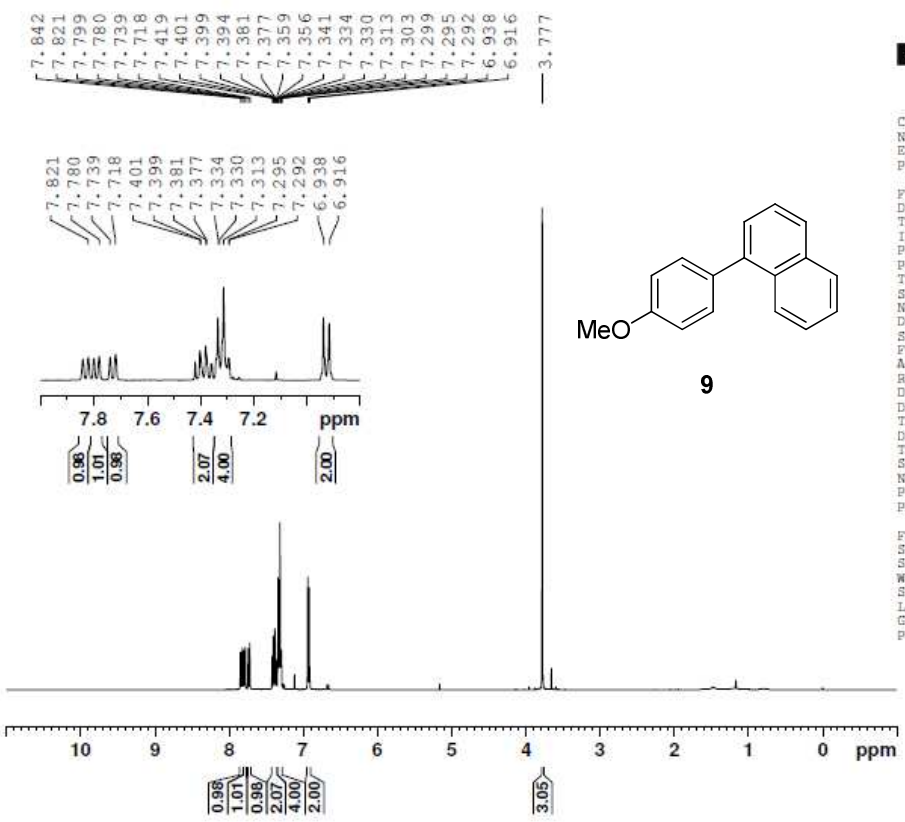

9

```
Current Data Parameters
NAME      Phen Naphth OMe
EXPNO                 10
PROCNO                 1

F2 - Acquisition Parameters
Date_           20170913
Time              18.05 h
INSTRUM             spect
PROBHD   Z108618_0920 (
PULPROG             zg30
TD                 32768
SOLVENT            CDCl3
NS                     8
DS                     2
SWH             8012.820 Hz
FIDRES          0.489064 Hz
AQ              2.0447233 sec
RG                  80.4
DW                62.400 usec
DE                 6.50 usec
TE                299.6 K
D1           1.00000000 sec
TD0                    1
SFO1          400.2324714 MHz
NUC1                  1H
P1                14.00 usec
PLW1         13.02400017 W

F2 - Processing parameters
SI                 65536
SF          400.2300679 MHz
WDW                   EM
SSB       0
LB                 0.30 Hz
GB        0
PC                 1.00
```

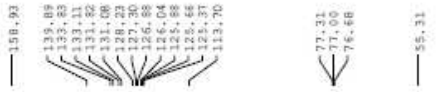

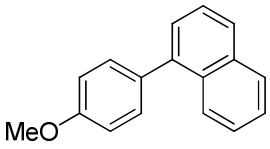

9

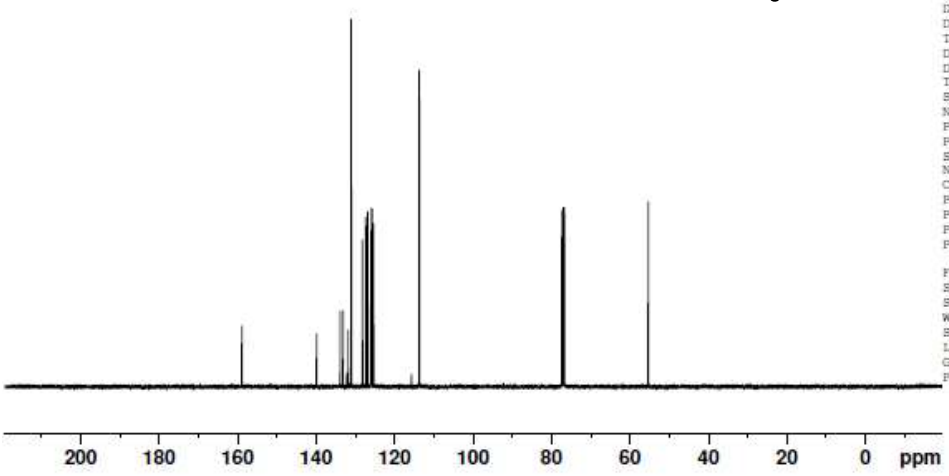

```
Current Data Parameters
NAME      Phen Naphth OMe
EXPNO                 11
PROCNO                 1

F2 - Acquisition Parameters
Date_           20170913
Time              18.16 h
INSTRUM             spect
PROBHD   Z108618_0920 (
PULPROG           zgpg30
TD                 65536
SOLVENT            CDCl3
NS                   200
DS                     4
SWH            24038.461 Hz
FIDRES          0.733596 Hz
AQ              1.3631488 sec
RG                 205.55
DW                20.800 usec
DE                 6.50 usec
TE                300.8 K
D1           2.00000000 sec
D11          0.03000000 sec
TD0                    1
SFO1          100.6479773 MHz
NUC1                  13C
P1                15.00 usec
PLW1         26.83600044 W
SFO2          400.2316009 MHz
NUC2                  1H
CPDPRG[2          waltz16
PCPD2             90.00 usec
PLW2         13.02400017 W
PLW12         0.31628889 W
PLW13         0.15852401 W

F2 - Processing parameters
SI                 32768
SF          100.6379225 MHz
WDW                   EM
SSB       0
LB                 1.00 Hz
GB        0
PC                 1.40
```

4-(Naphthalen-1-yl)phenol (**10**)

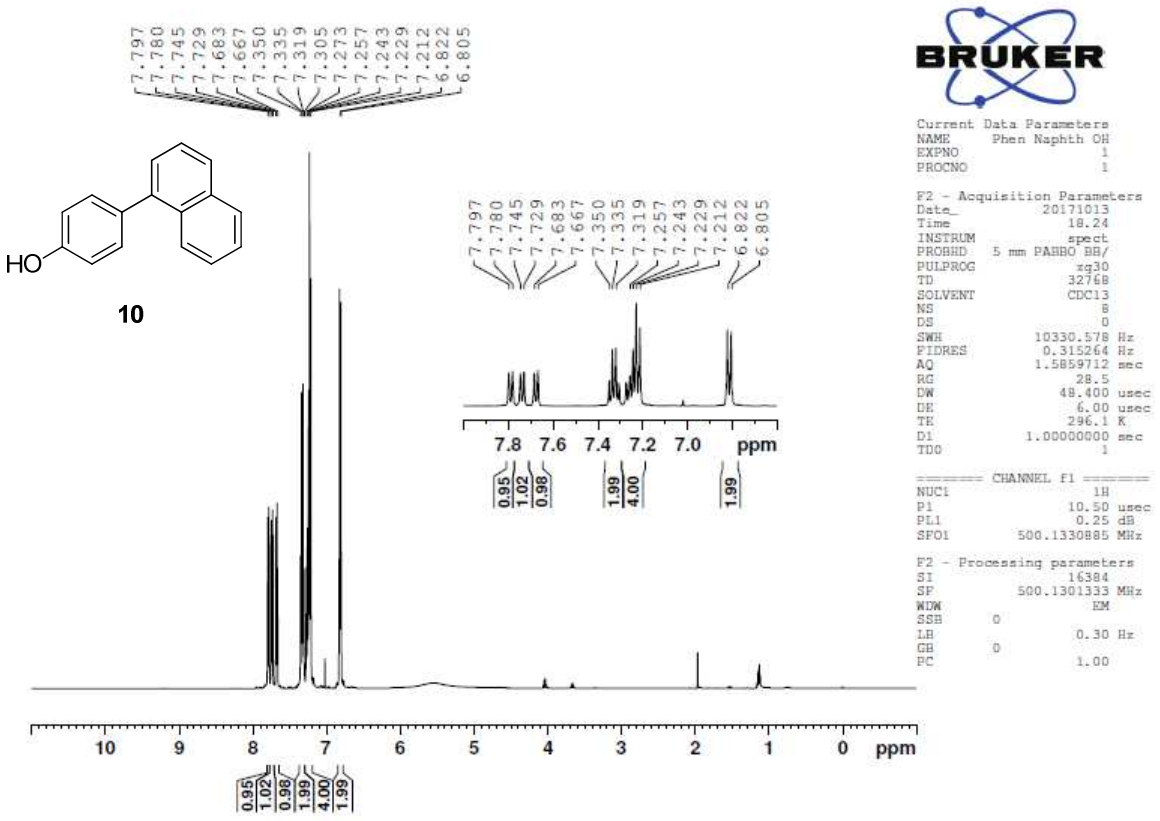

BRUKER

```
Current Data Parameters
NAME      Phen Naphth OH
EXPNO                1
PROCNO               1

F2 - Acquisition Parameters
Date_          20171013
Time              18.24
INSTRUM           spect
PROBHD   5 mm PABBO BB/
PULPROG           zg30
TD               32768
SOLVENT          CDCl3
NS                   8
DS                   0
SWH          10330.578 Hz
FIDRES        0.315264 Hz
AQ           1.5859712 sec
RG                28.5
DW              48.400 usec
DE               6.00 usec
TE              296.1 K
D1           1.00000000 sec
TD0                  1

======== CHANNEL f1 ========
NUC1                 1H
P1                10.50 usec
PL1                0.25 dB
SFO1        500.1330885 MHz

F2 - Processing parameters
SI                16384
SF          500.1301333 MHz
WDW                  EM
SSB       0
LB                0.30 Hz
GB        0
PC                1.00
```

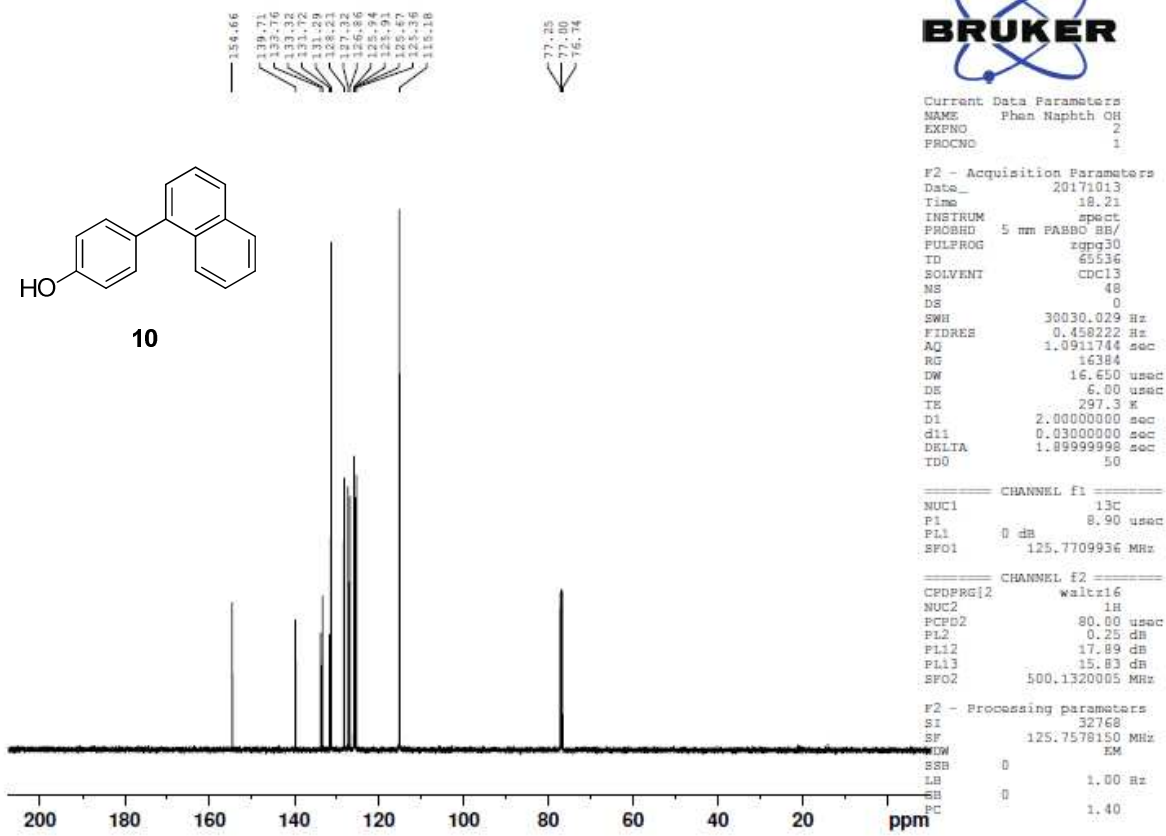

BRUKER

```
Current Data Parameters
NAME      Phen Naphth OH
EXPNO                2
PROCNO               1

F2 - Acquisition Parameters
Date_          20171013
Time              18.21
INSTRUM           spect
PROBHD   5 mm PABBO BB/
PULPROG         zgpg30
TD               65536
SOLVENT          CDCl3
NS                  48
DS                   0
SWH          30030.029 Hz
FIDRES        0.458222 Hz
AQ           1.0911744 sec
RG               16384
DW              16.650 usec
DE               6.00 usec
TE              297.3 K
D1           2.00000000 sec
d11          0.03000000 sec
DELTA        1.89999998 sec
TD0                 50

======== CHANNEL f1 ========
NUC1                13C
P1                8.90 usec
PL1       0 dB
SFO1       125.7709936 MHz

======== CHANNEL f2 ========
CPDPRG[2         waltz16
NUC2                 1H
PCPD2             80.00 usec
PL2                0.25 dB
PL12              17.89 dB
PL13              15.83 dB
SFO2        500.1320005 MHz

F2 - Processing parameters
SI                32768
SF          125.7578150 MHz
WDW                  EM
SSB       0
LB                1.00 Hz
GB        0
PC                1.40
```

3,4,5-Tris((*tert*-butyldimethylsilyl)oxy)benzoic acid (**12a**)

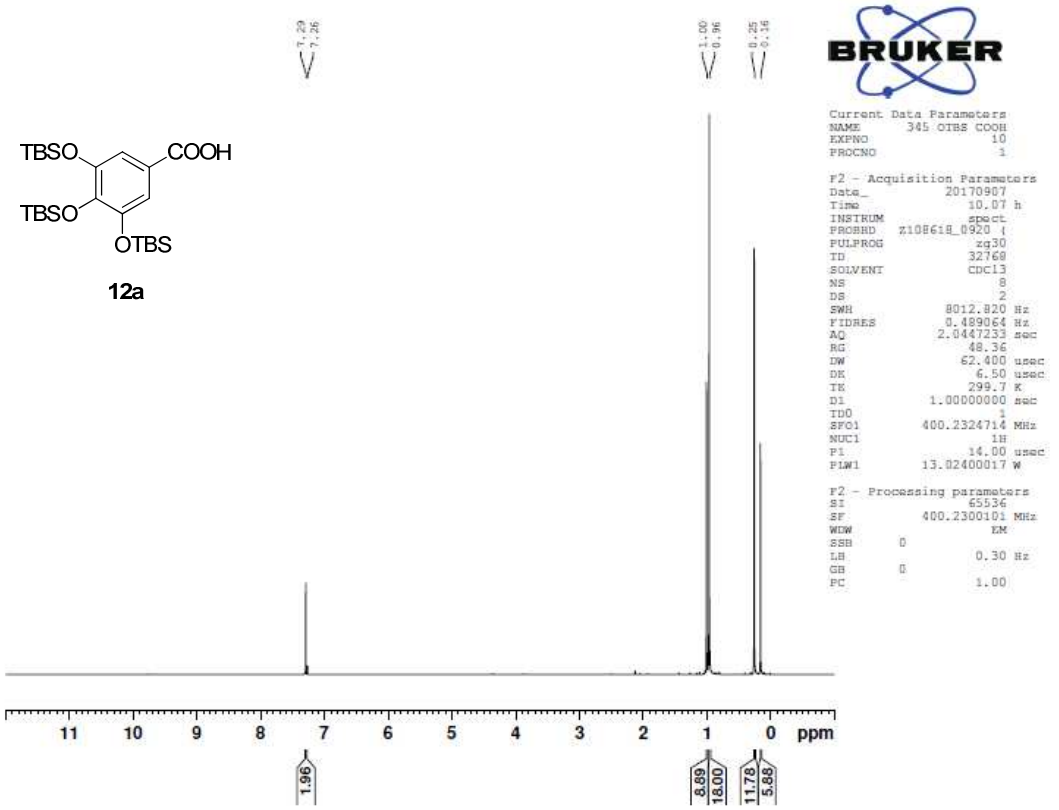

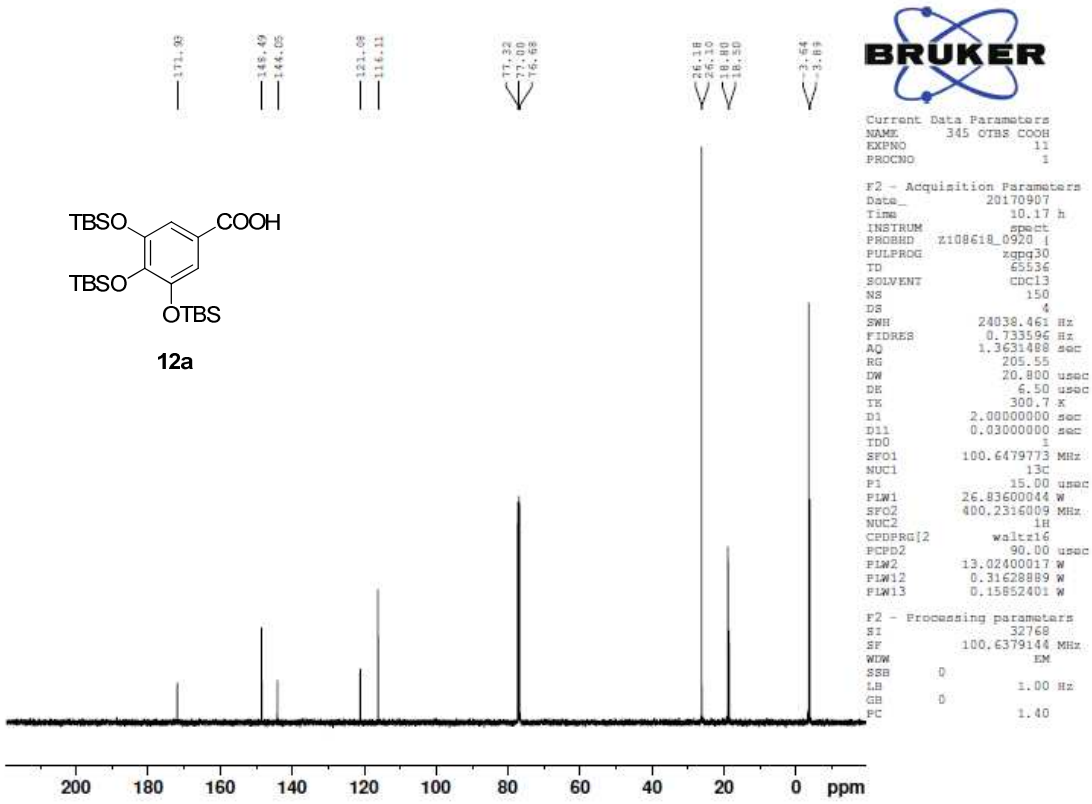

3,4-Bis((*tert*-butyldimethylsilyl)oxy)benzoic acid (**12b**)

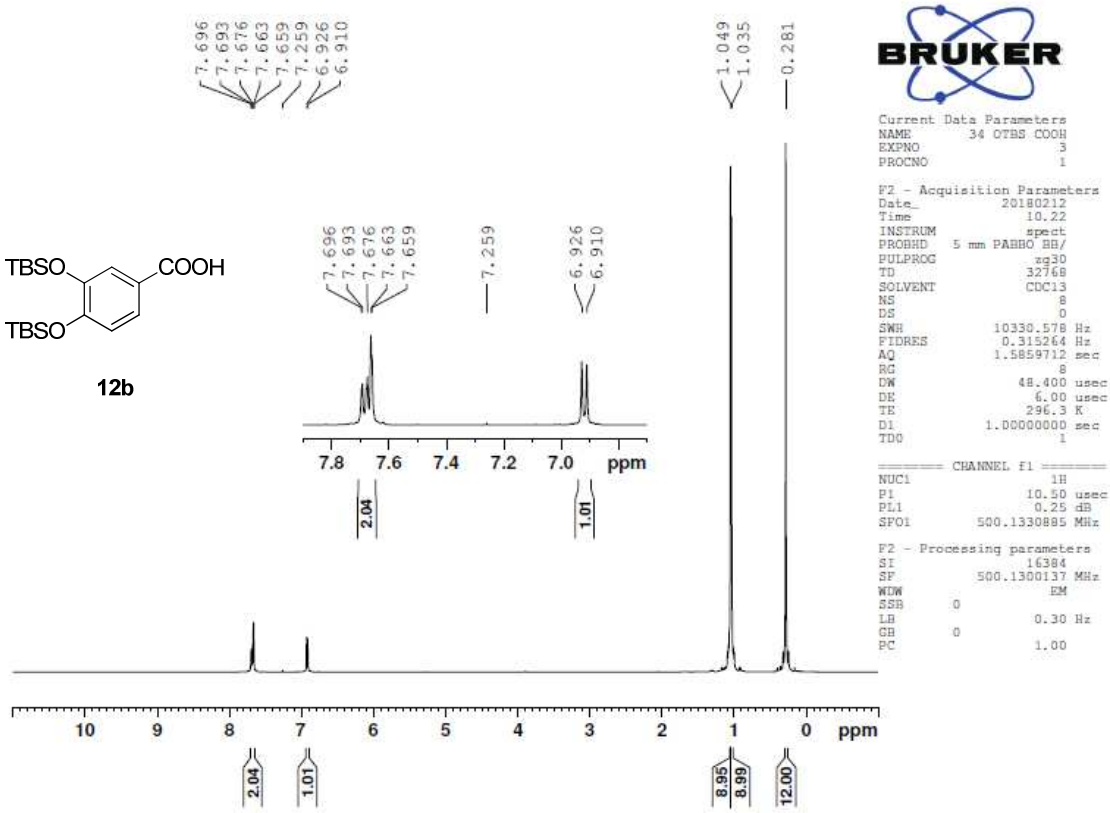

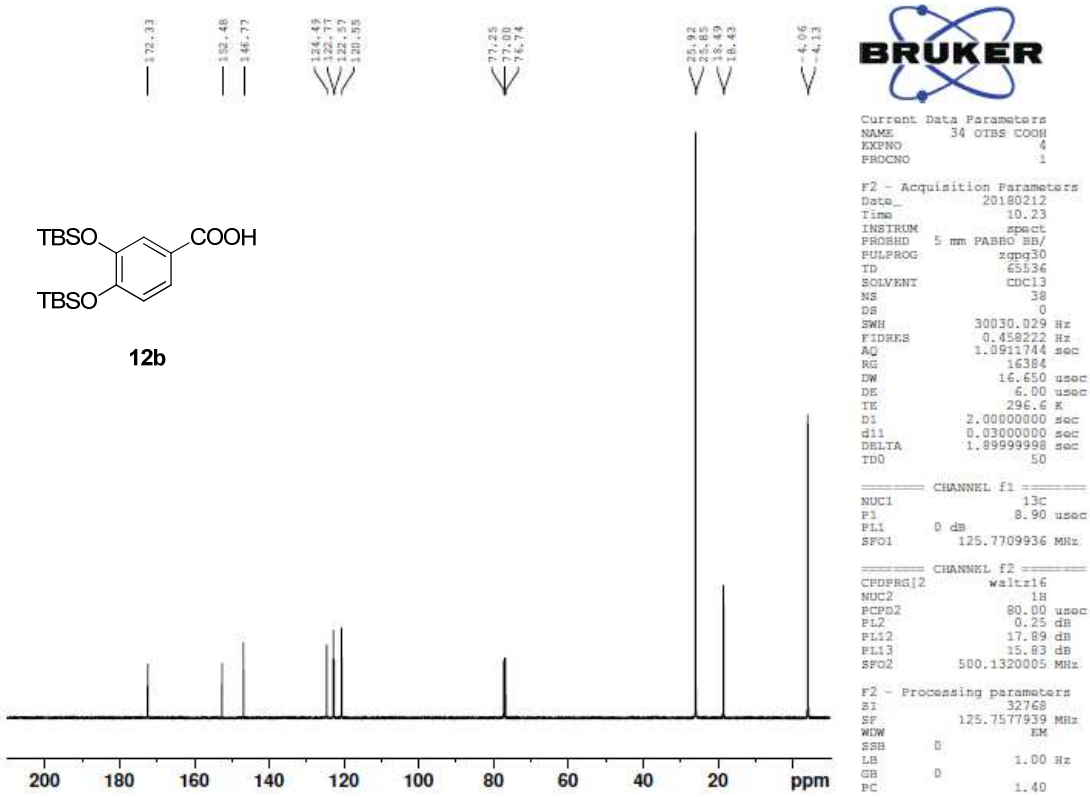

4-((*tert*-Butyldimethylsilyl)oxy)benzoic acid (**12c**)

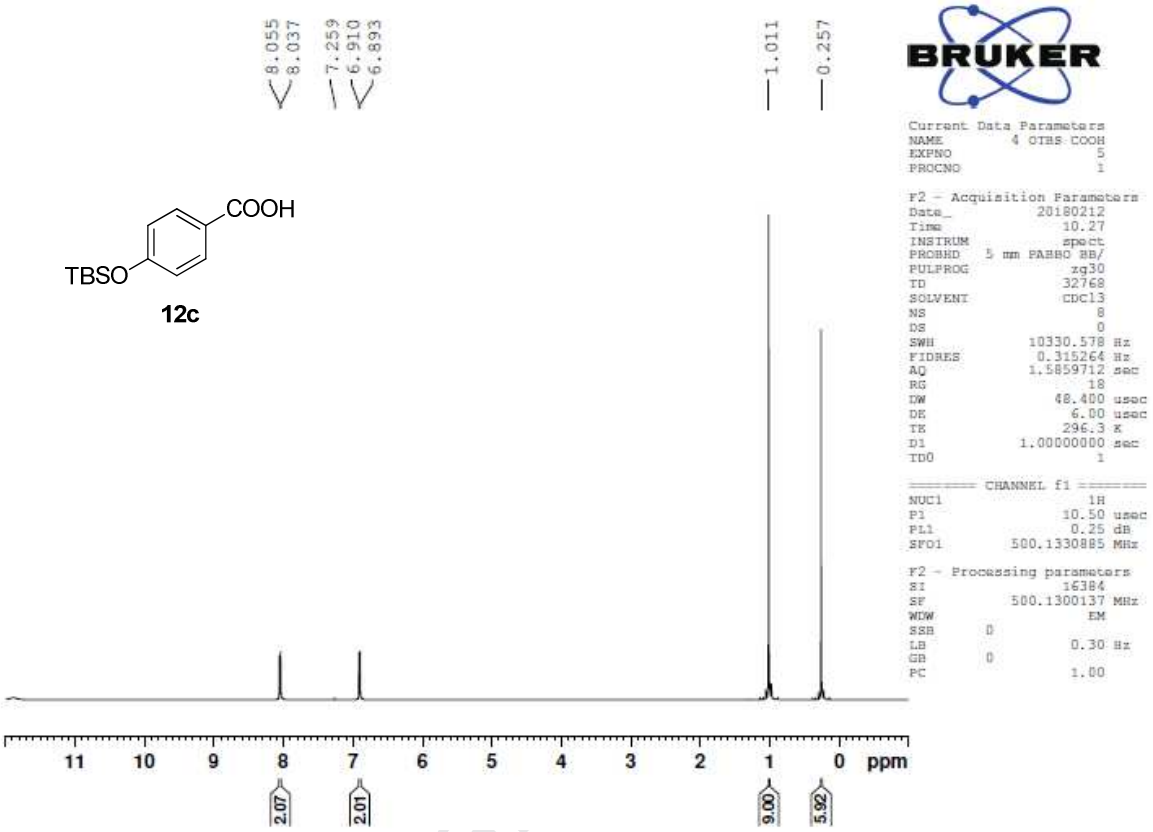

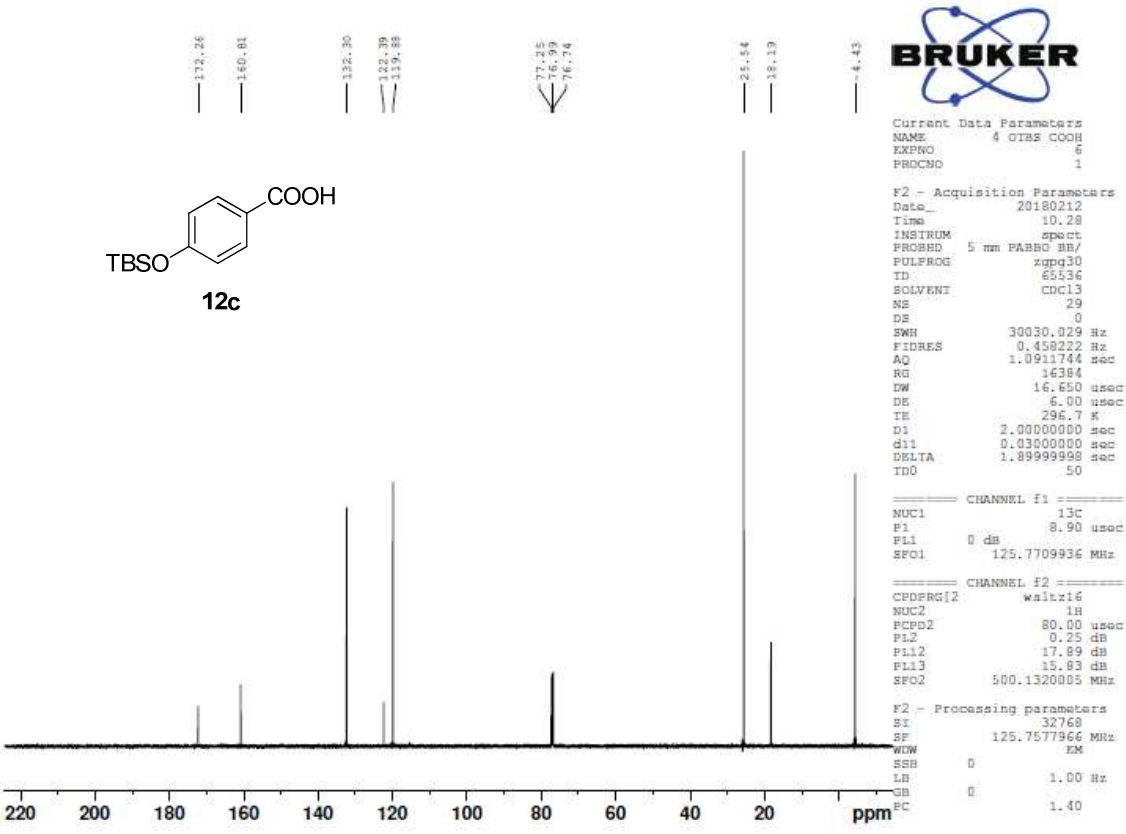

(*E*)-3-(4-((3,4,5-Tris((*tert*-butyldimethylsilyl)oxy)benzoyl)oxy)styryl)phenyl 3,4,5-tris((*tert*-butyldimethylsilyl)oxy)benzoate (**16a**)

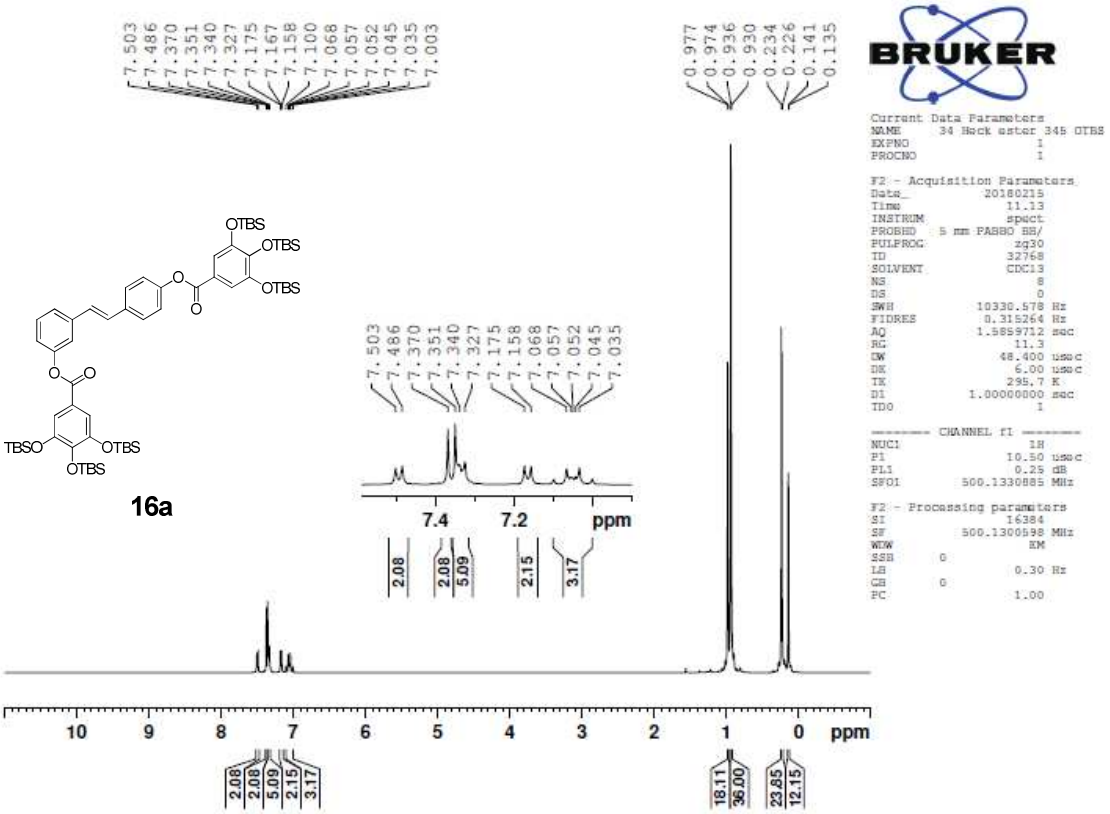

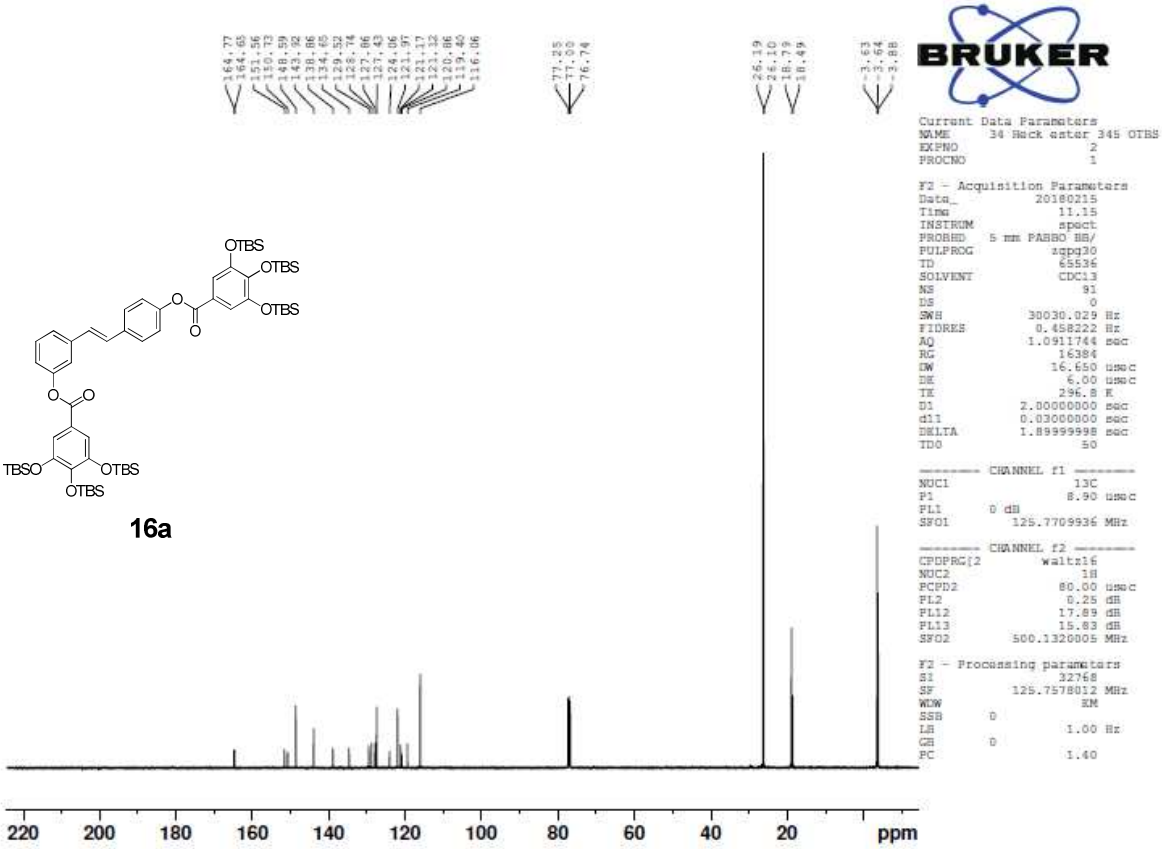

(*E*)-3-(4-((3,4-Bis((*tert*-butyldimethylsilyl)oxy)benzoyl)oxy)styryl)phenyl 3,4-bis((*tert*-butyldimethylsilyl)oxy)benzoate (**16b**)

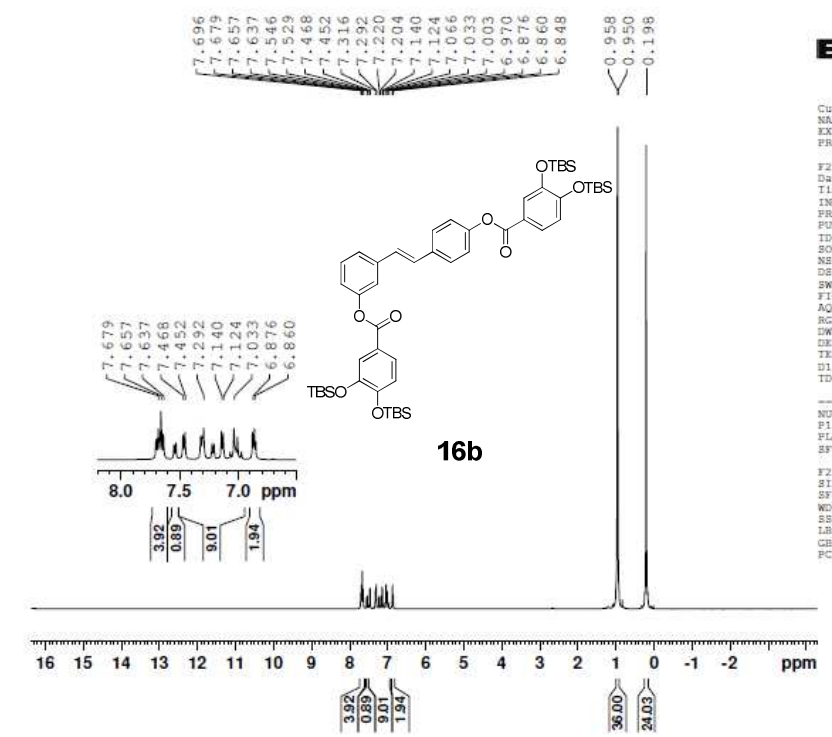

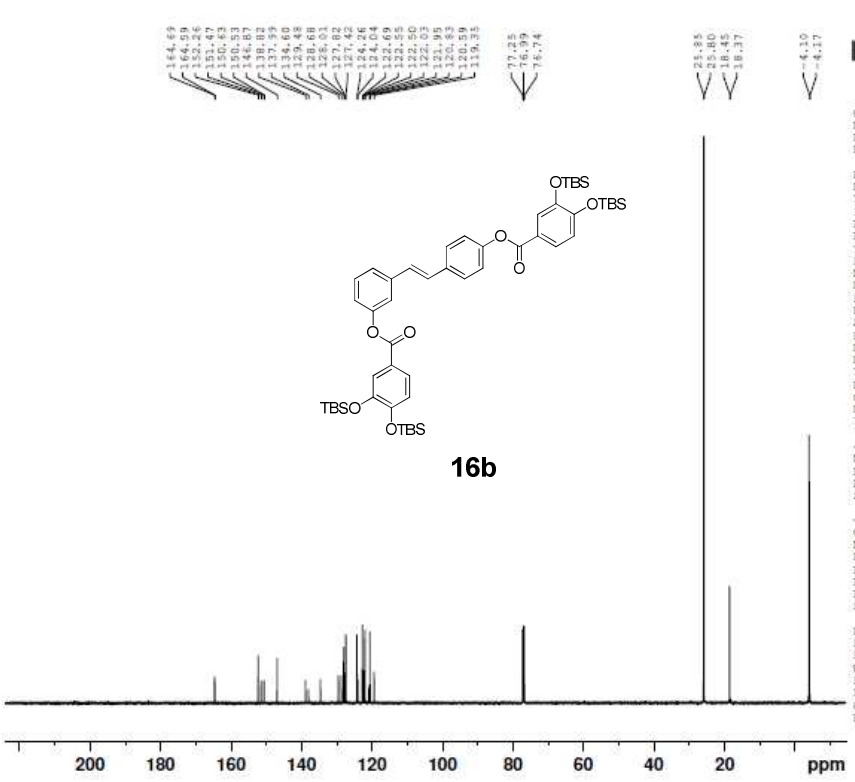

(*E*)-3-(4-((4-((*tert*-Butyldimethylsilyl)oxy)benzoyl)oxy)styryl)phenyl 4-((*tert*-butyldimethylsilyl)oxy)benzoate (**16c**)

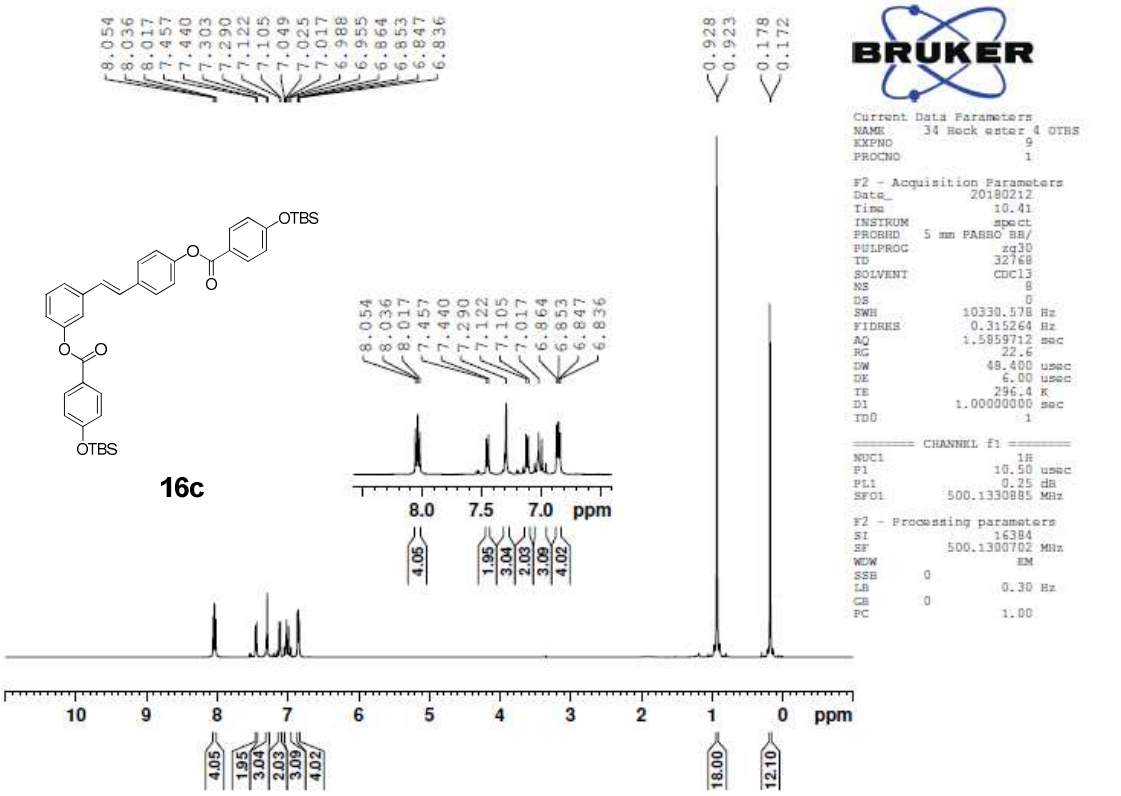

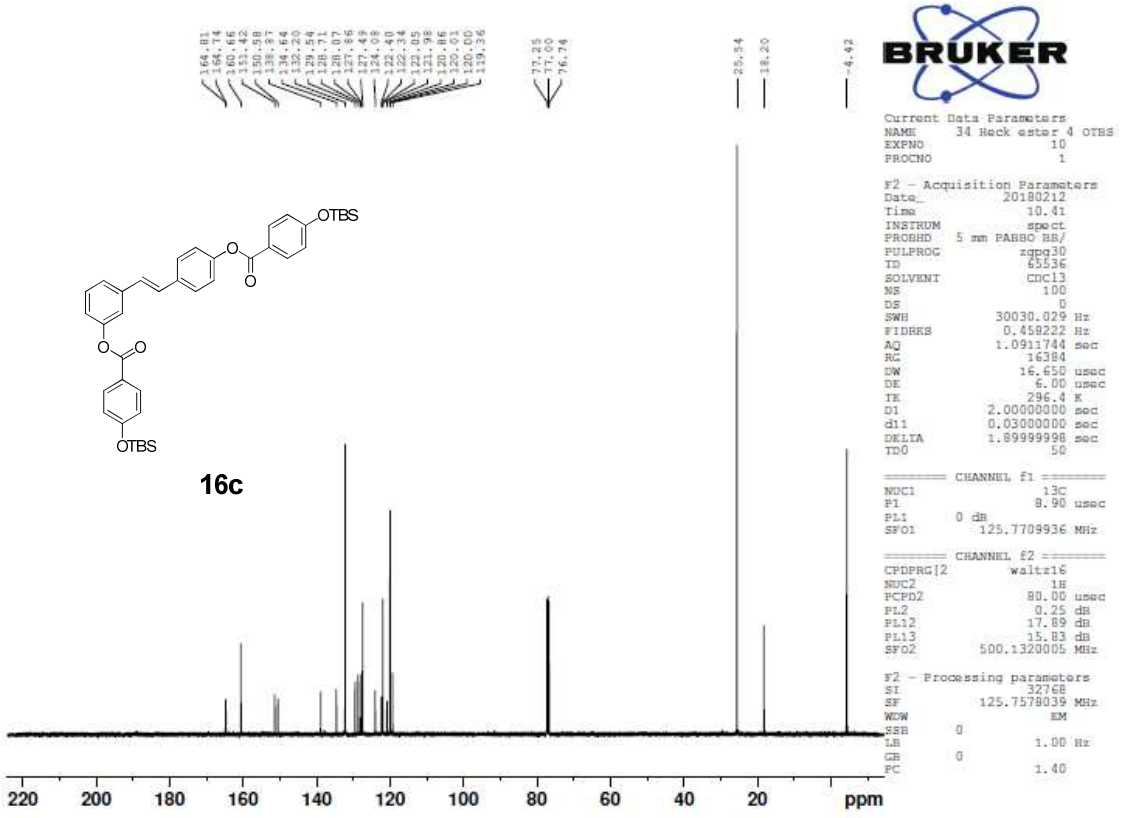

(*E*)-Ethene-1,2-diylbis(4,1-phenylene) bis(3,4,5-tris((*tert*-butyldimethylsilyl)oxy)benzoate) (**16d**)

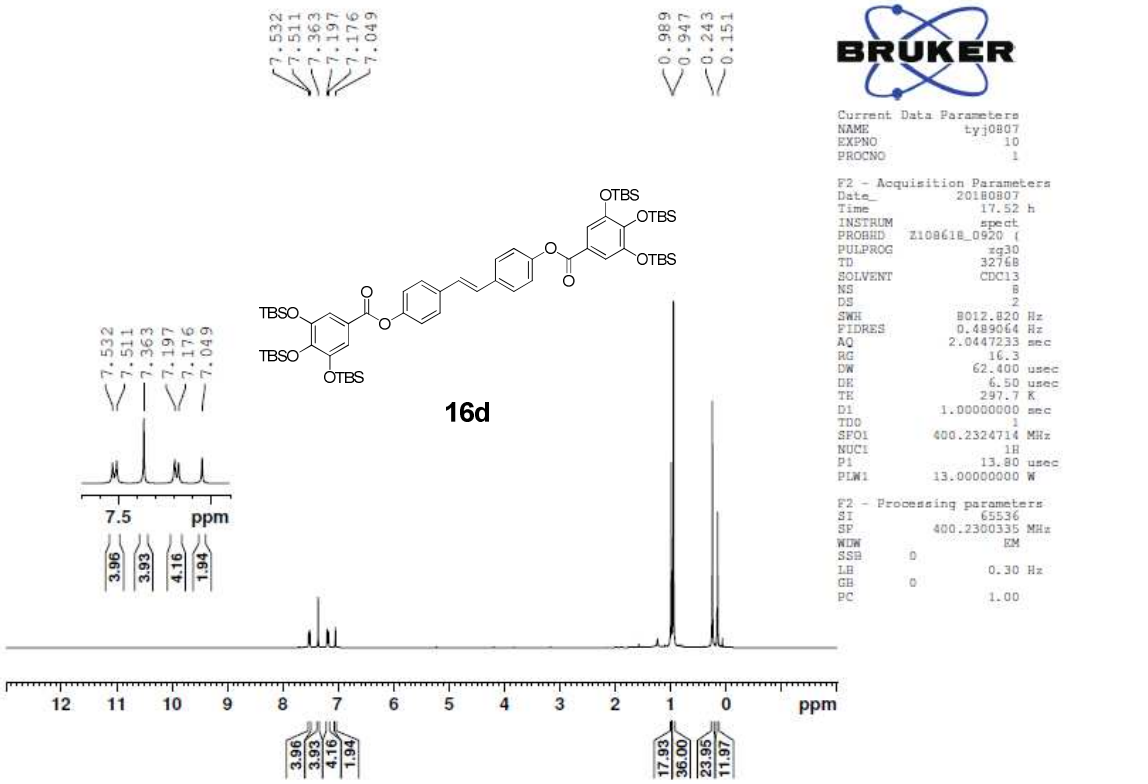

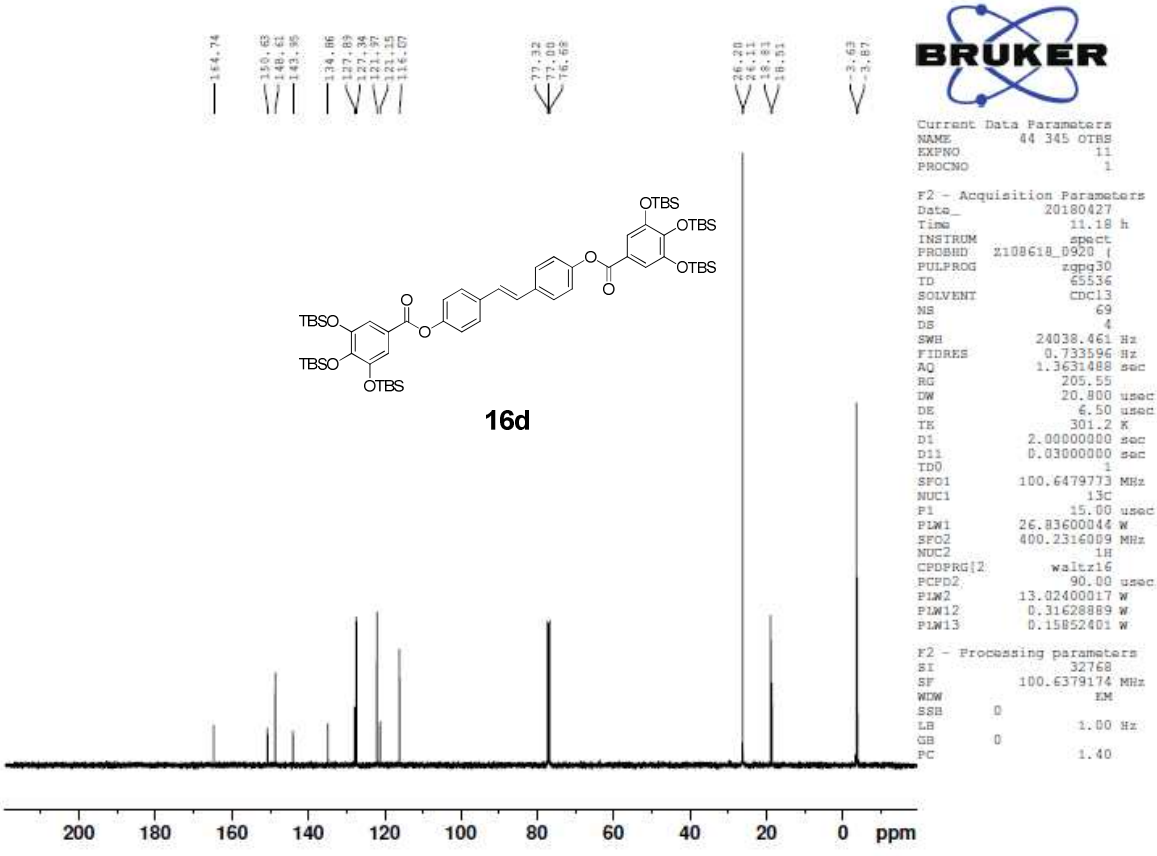

Methylenebis(4,1-phenylene) bis(3,4,5-tris((*tert*-butyldimethylsilyl)oxy)benzoate) (**16e**)

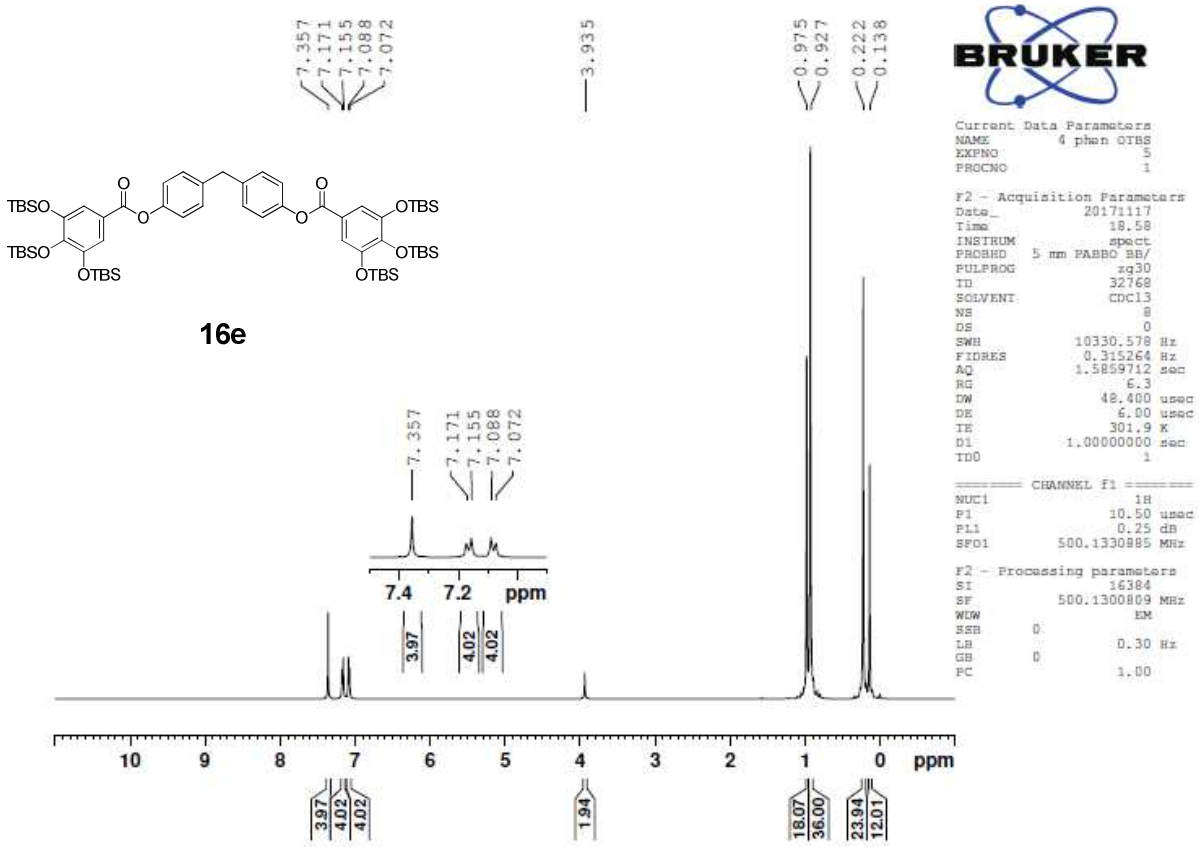

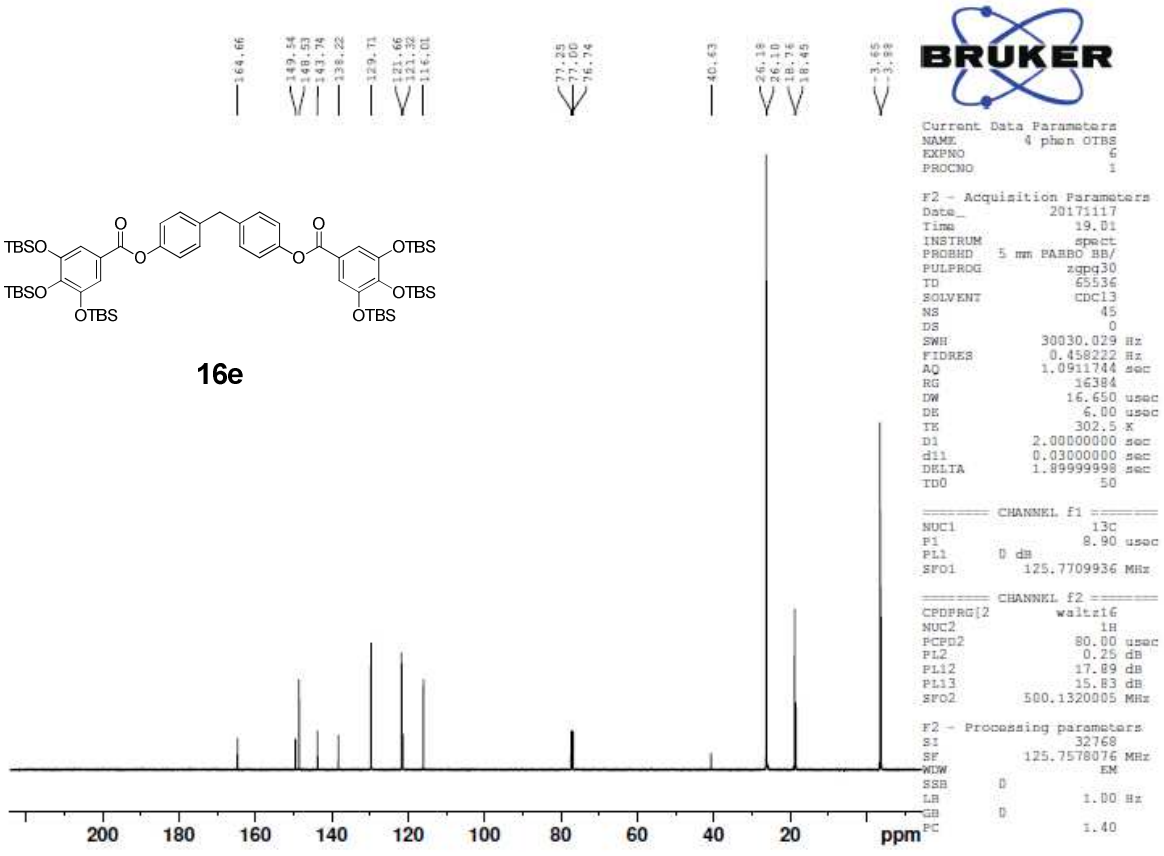

Methylenebis(2,1-phenylene) bis(3,4,5-tris((*tert*-butyldimethylsilyl)oxy)benzoate) (**16f**)

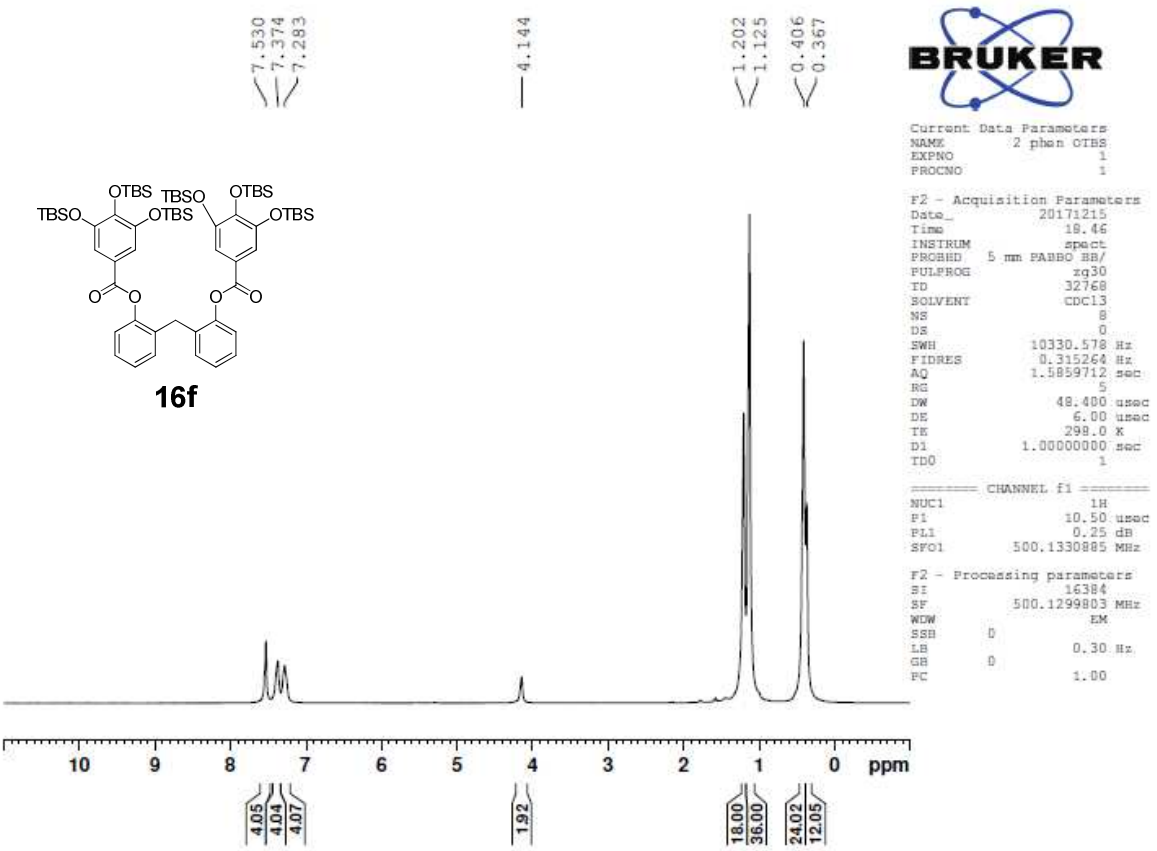

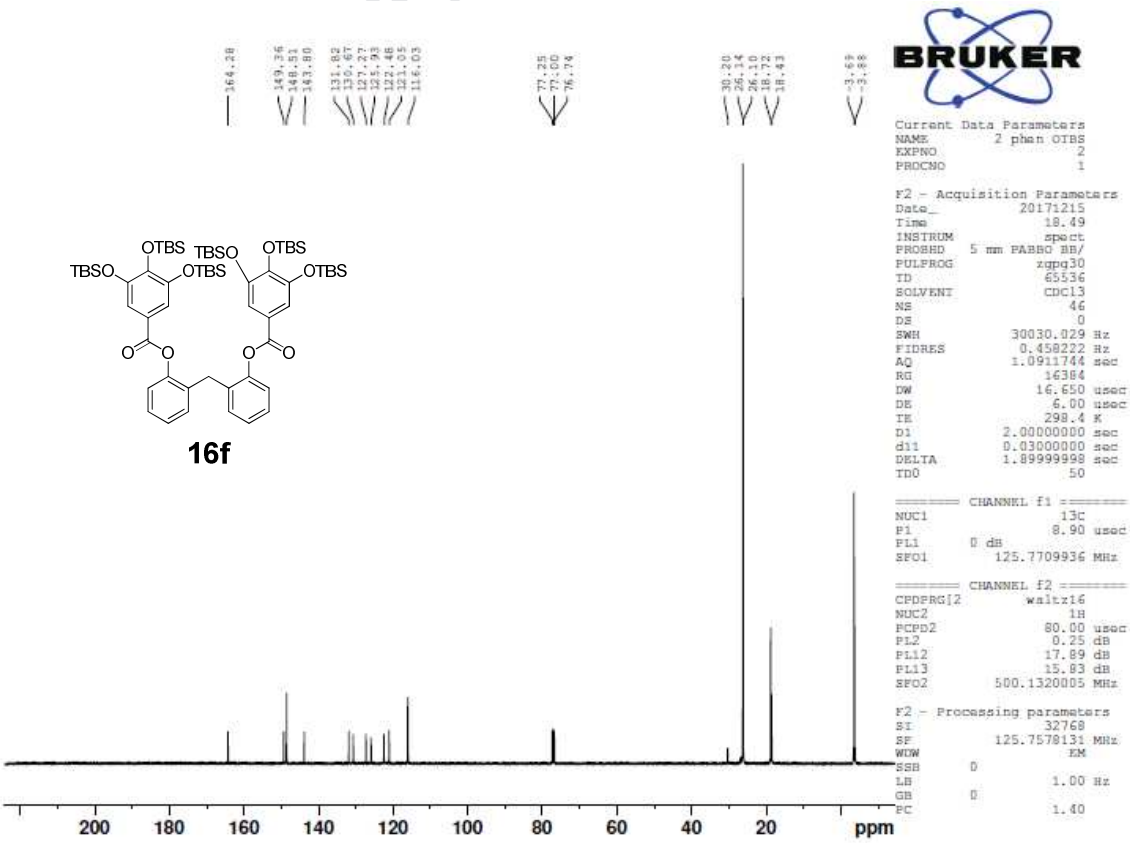

1,2,3,4-Tetrahydronaphthalene-1,5-diyl bis(3,4,5-tris((*tert*-butyldimethylsilyl)oxy)benzoate) (**16g**)

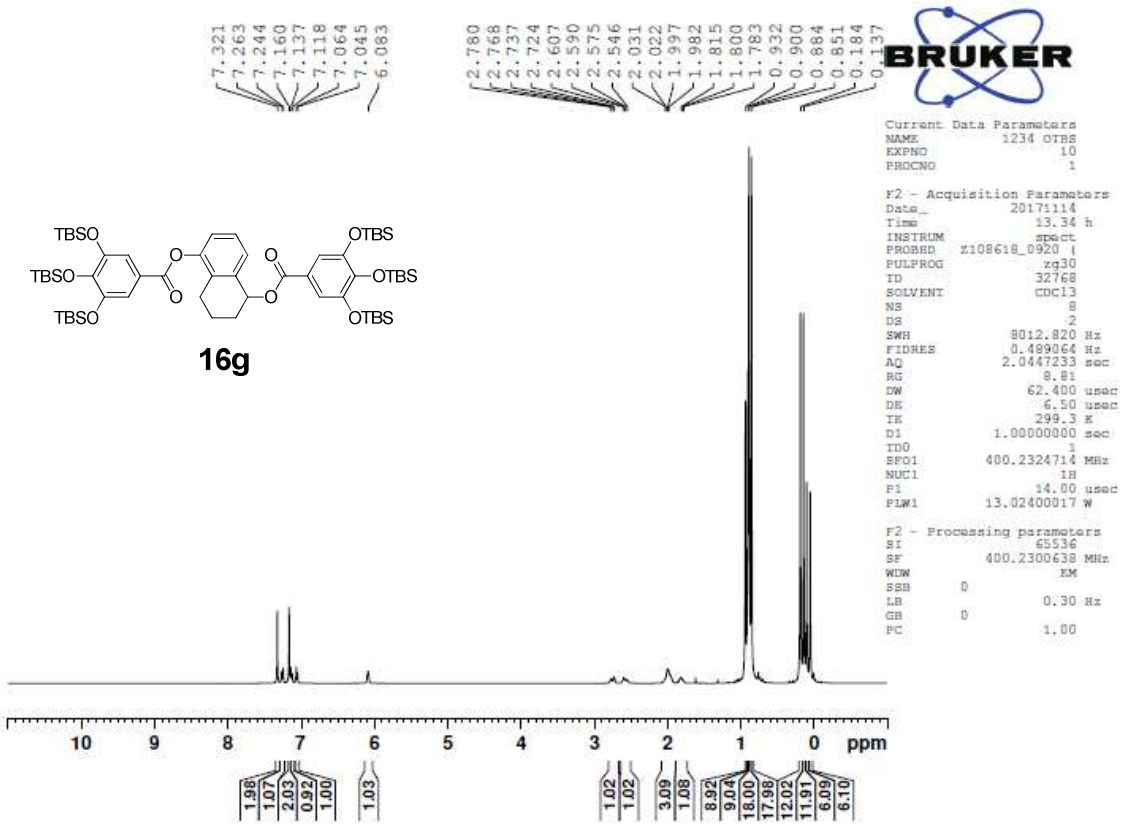

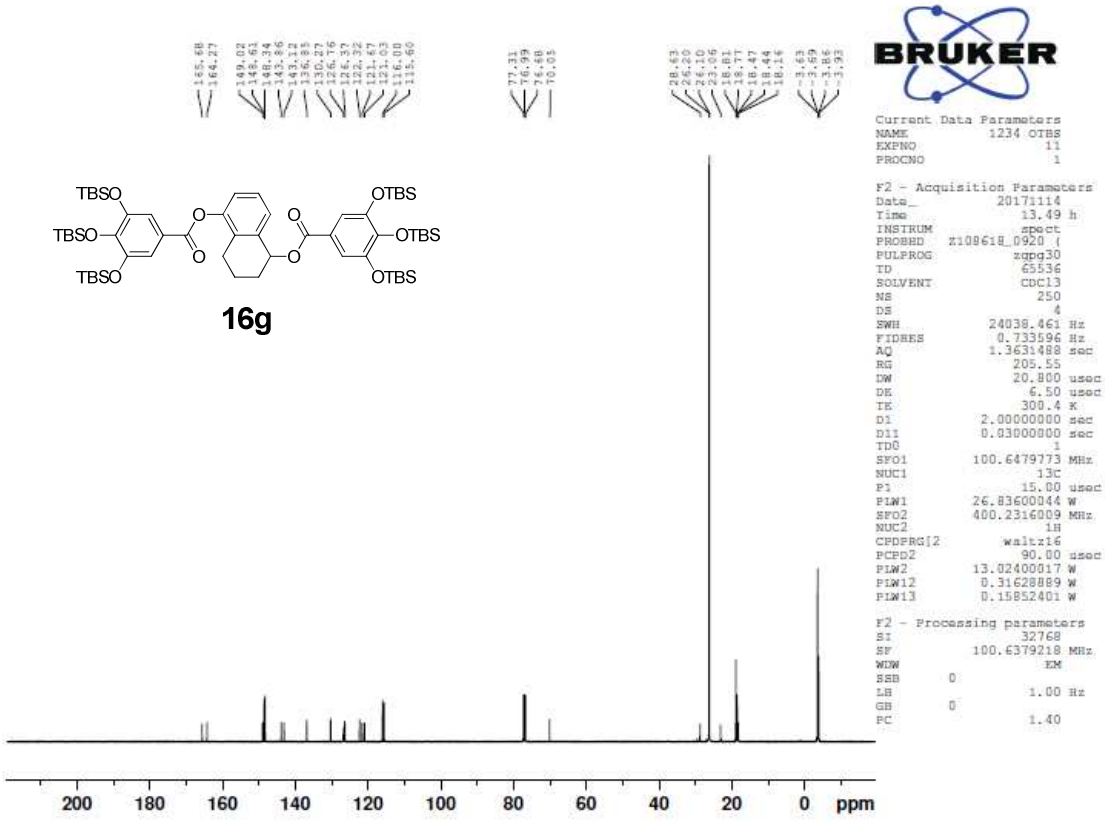

(*E*)-3-Styrylphenyl 3,4,5-tris((*tert*-butyldimethylsilyl)oxy)benzoate (**16h**)

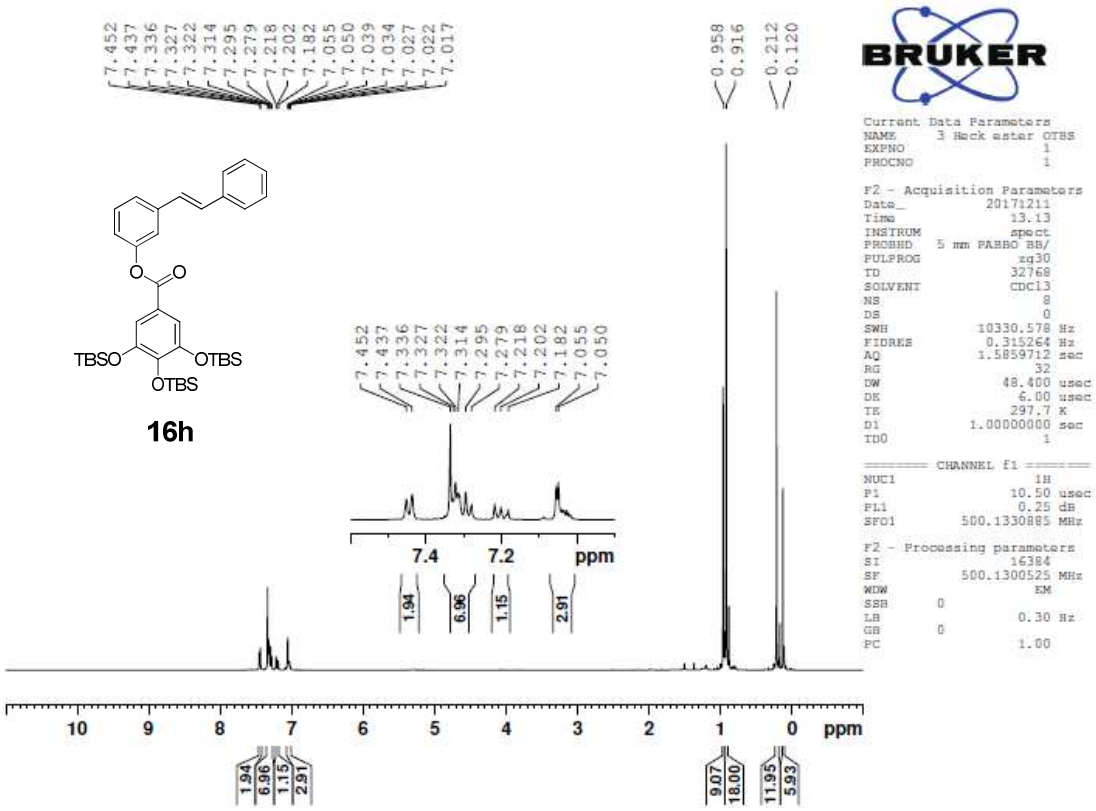

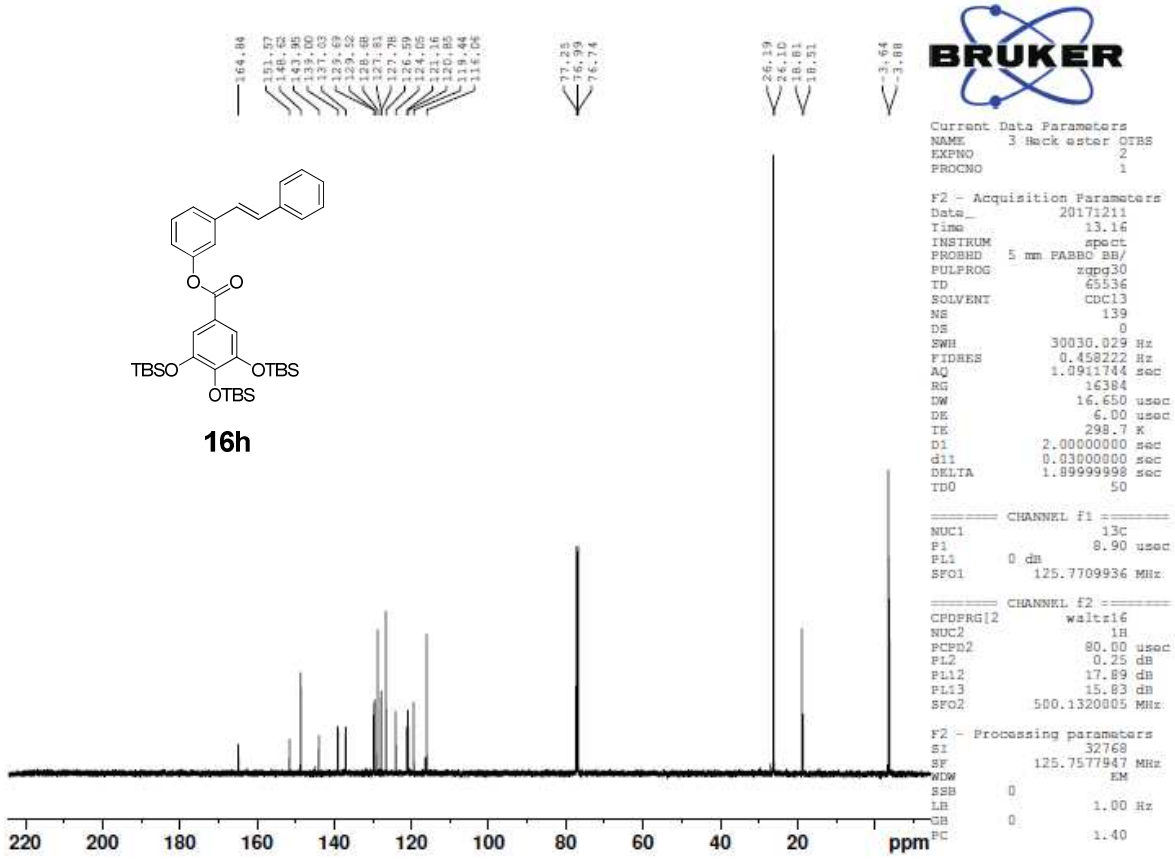

(*E*)-4-Styrylphenyl 3,4,5-tris((*tert*-butyldimethylsilyl)oxy)benzoate (**16i**)

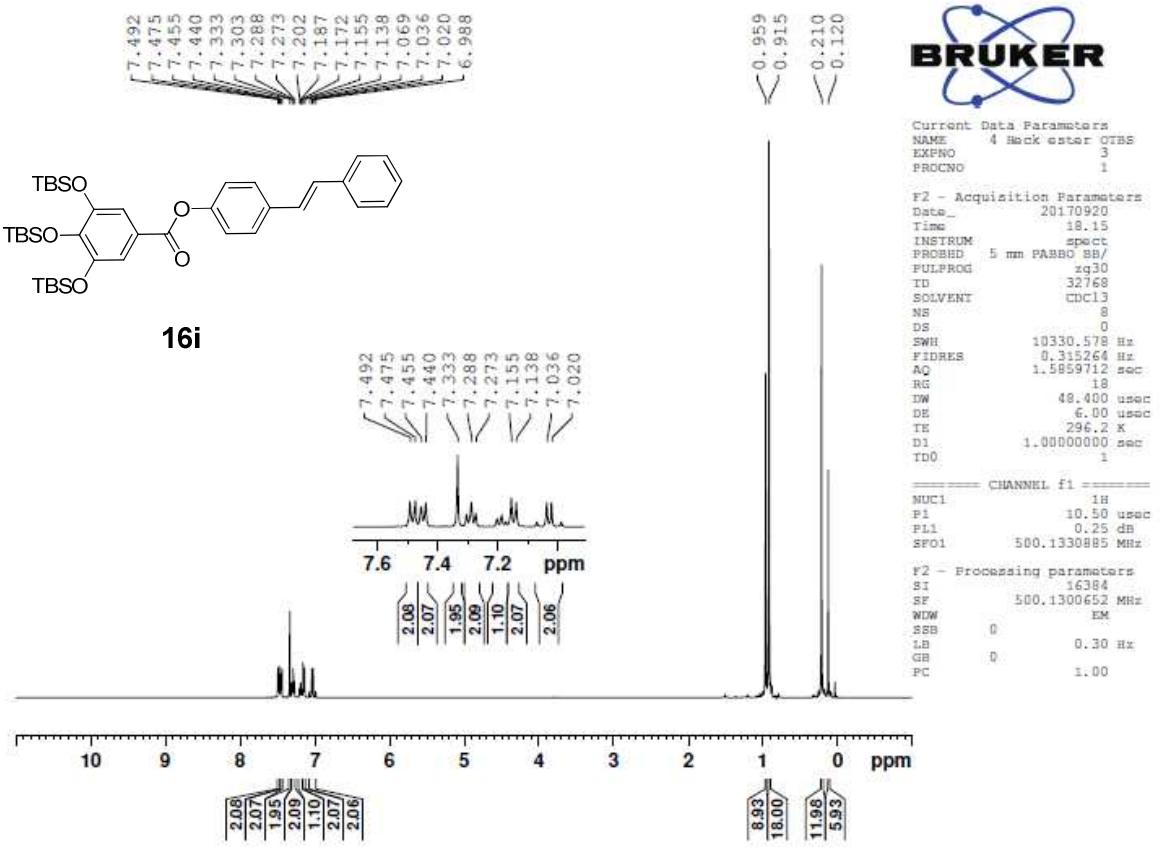

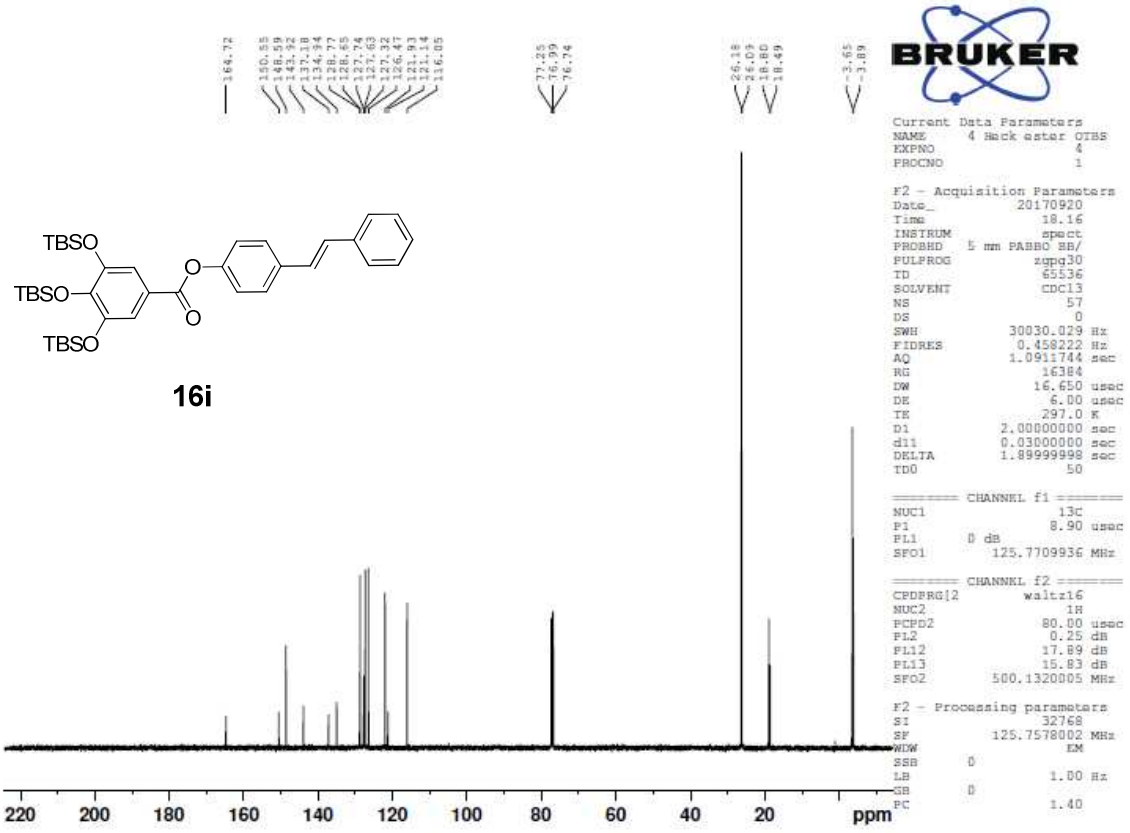

4-(Naphthalen-1-yl)phenyl 3,4,5-tris((*tert*-butyldimethylsilyl)oxy)benzoate (**16j**)

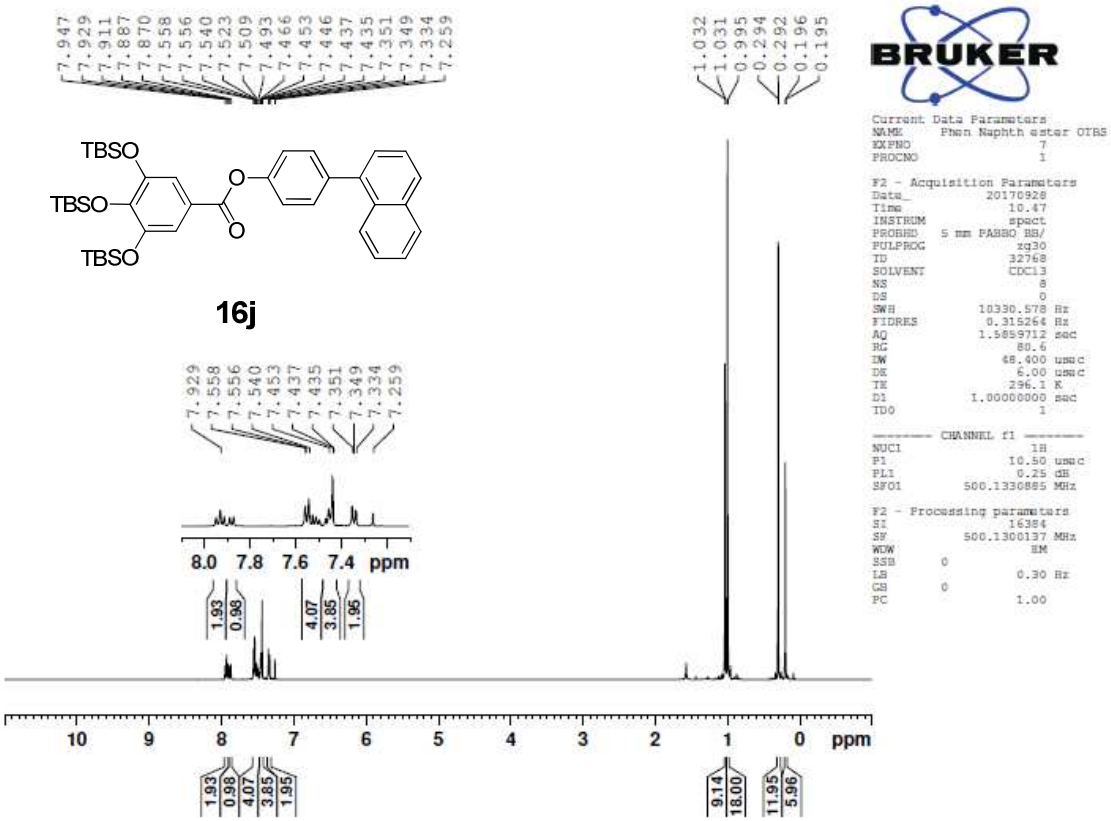

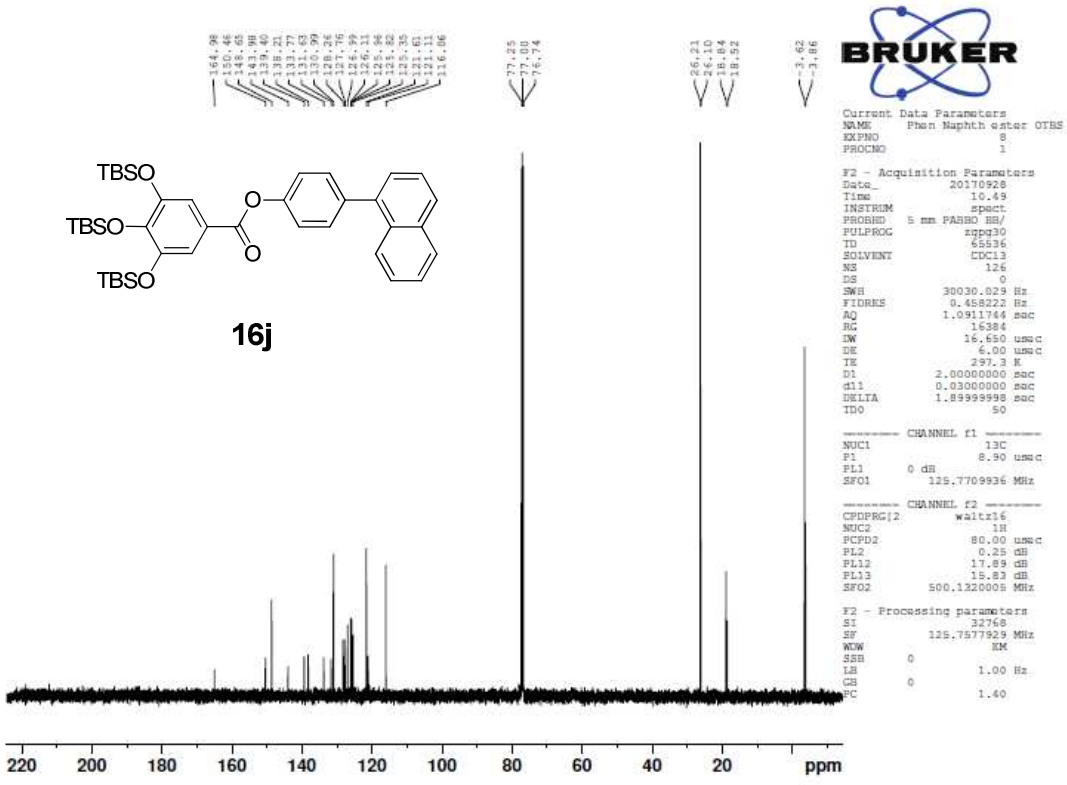

(C) ^{1}H and ^{13}C NMR spectra of final compounds

(*E*)-3-(4-((3,4,5-Trihydroxybenzoyl)oxy)styryl)phenyl 3,4,5-trihydroxybenzoate (**EC1**)

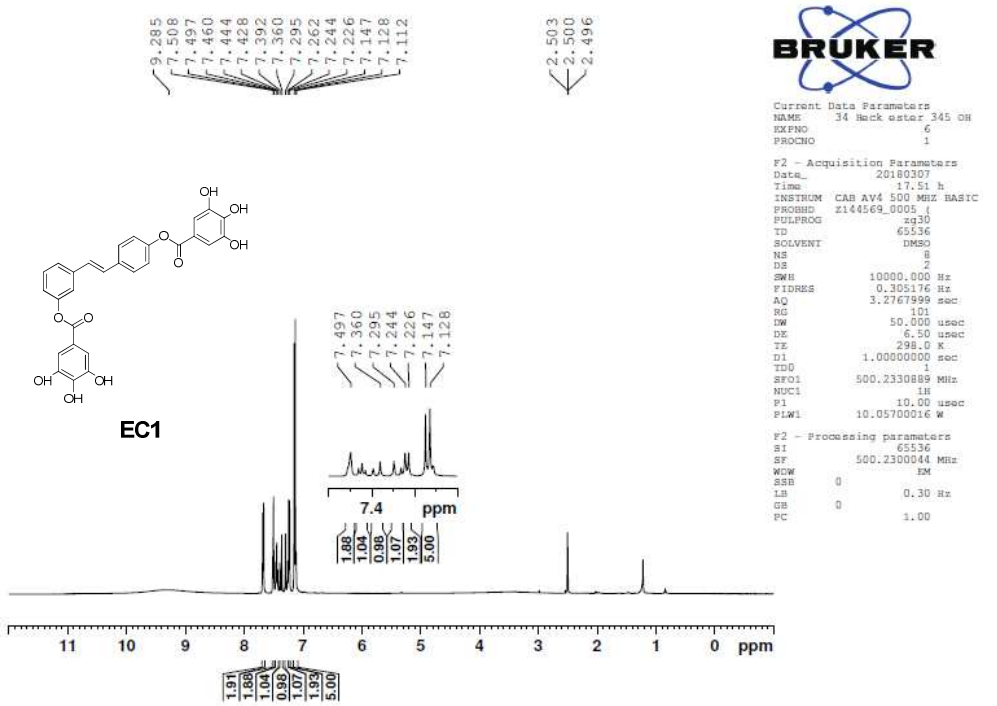

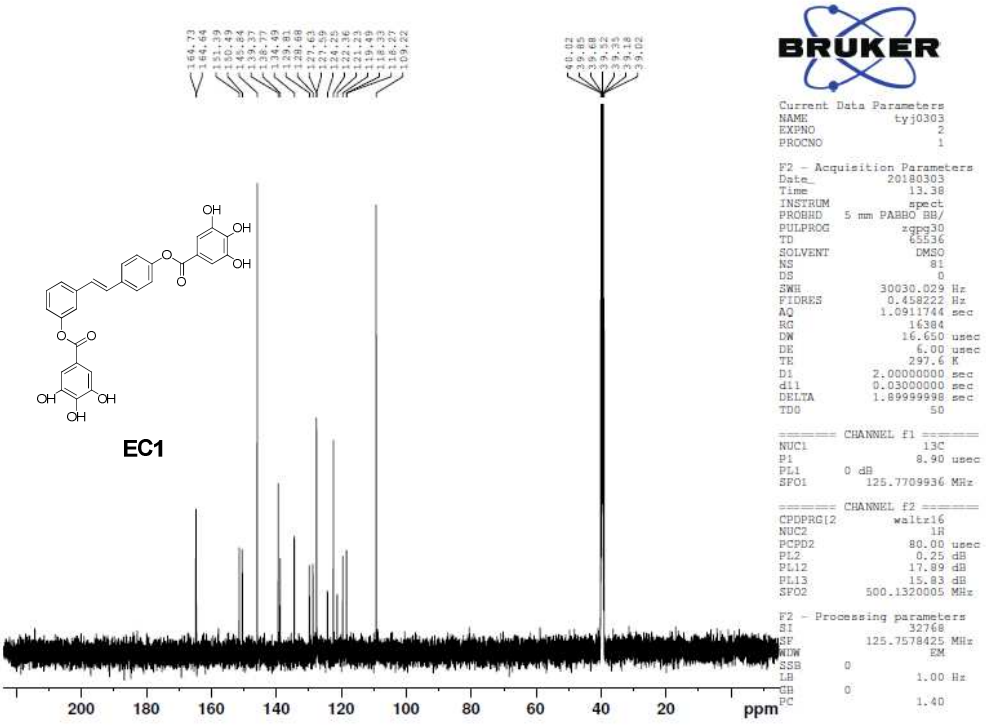

(*E*)-3-(4-((3,4-Dihydroxybenzoyl)oxy)styryl)phenyl 3,4-dihydroxybenzoate (**EC2**)

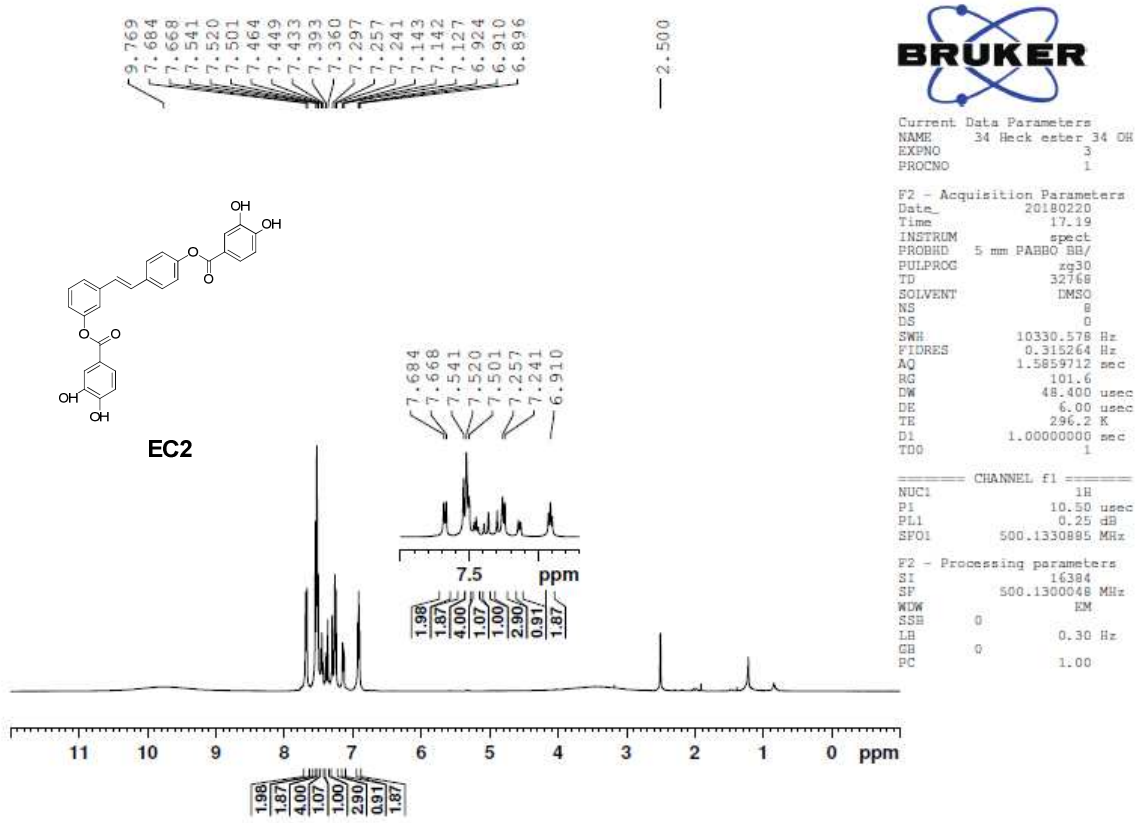

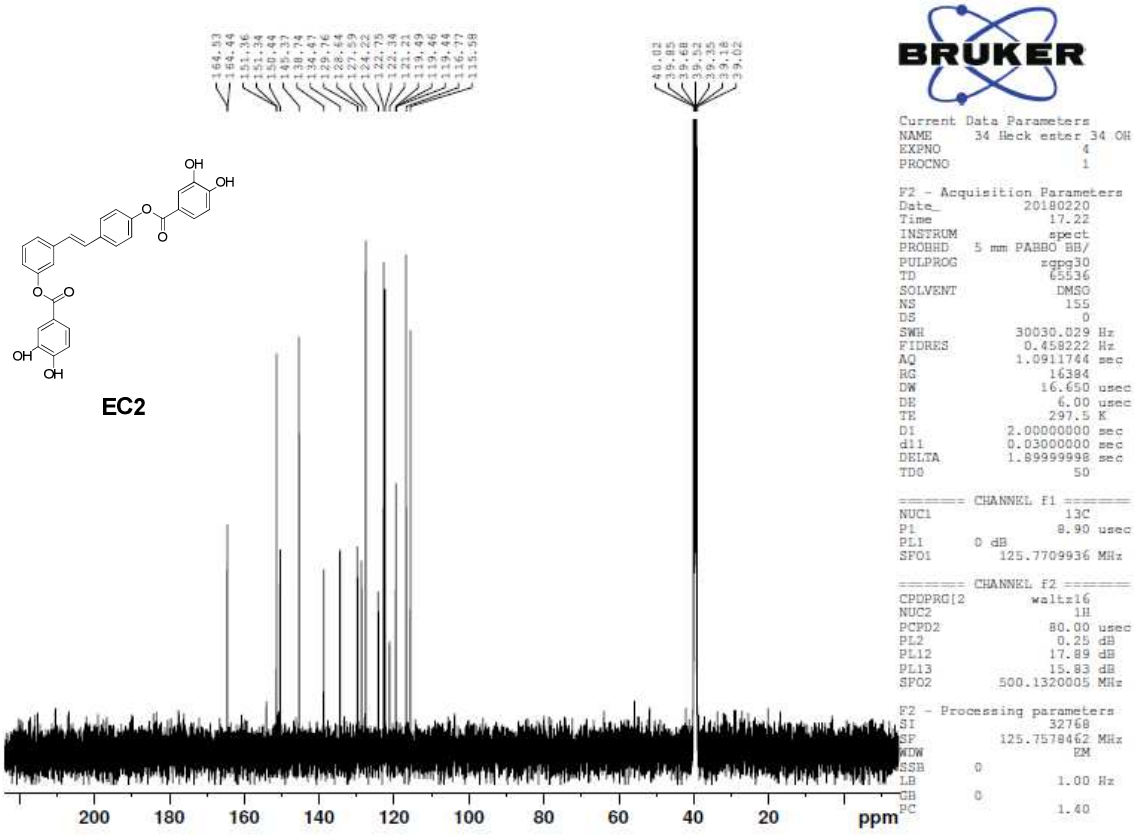

(*E*)-3-(4-((4-Hydroxybenzoyl)oxy)styryl)phenyl 4-hydroxybenzoate (**EC3**)

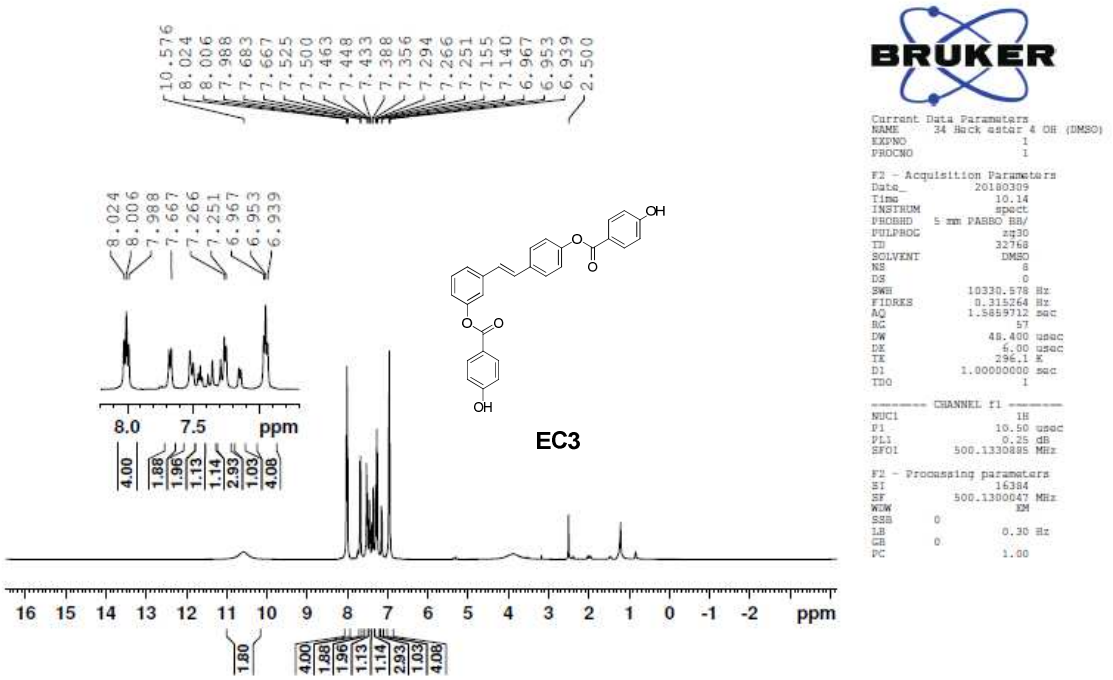

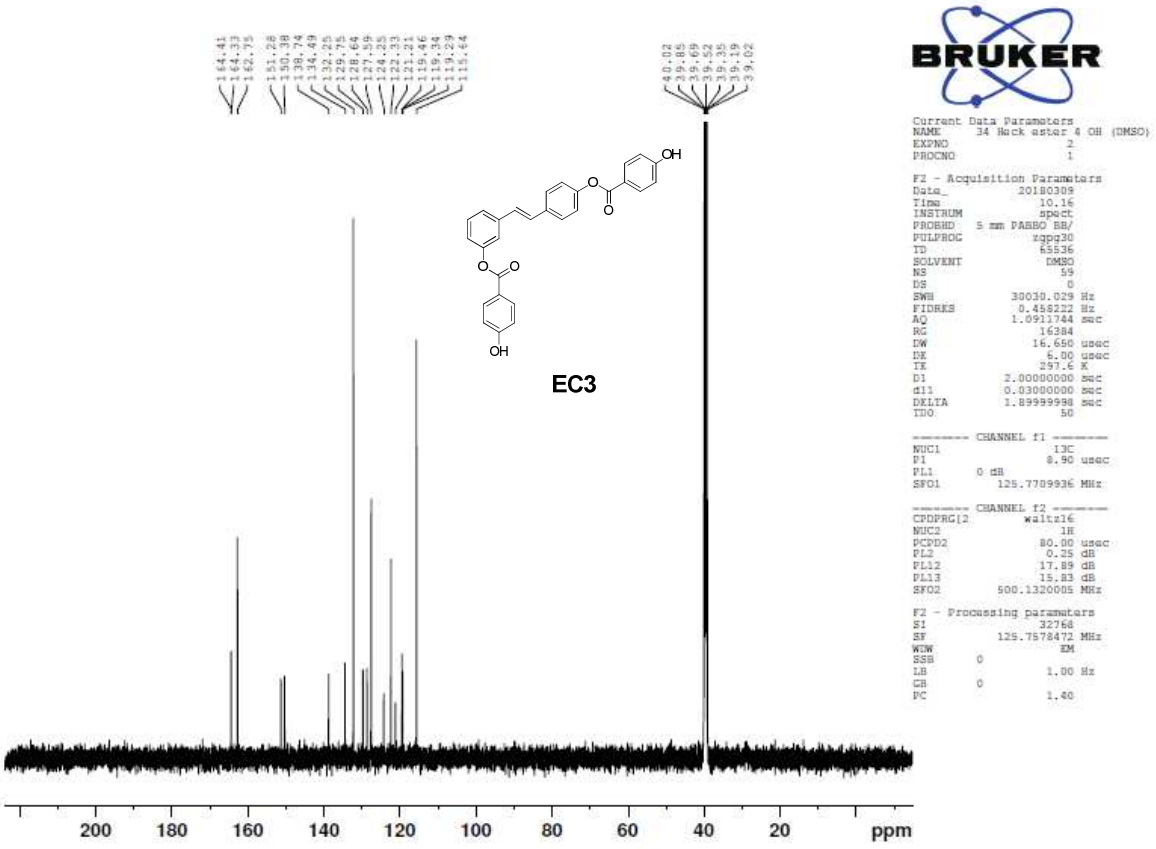

(*E*)-3-(4-((3,4,5-Trimethoxybenzoyl)oxy)styryl)phenyl 3,4,5-trimethoxybenzoate (**EC4**)

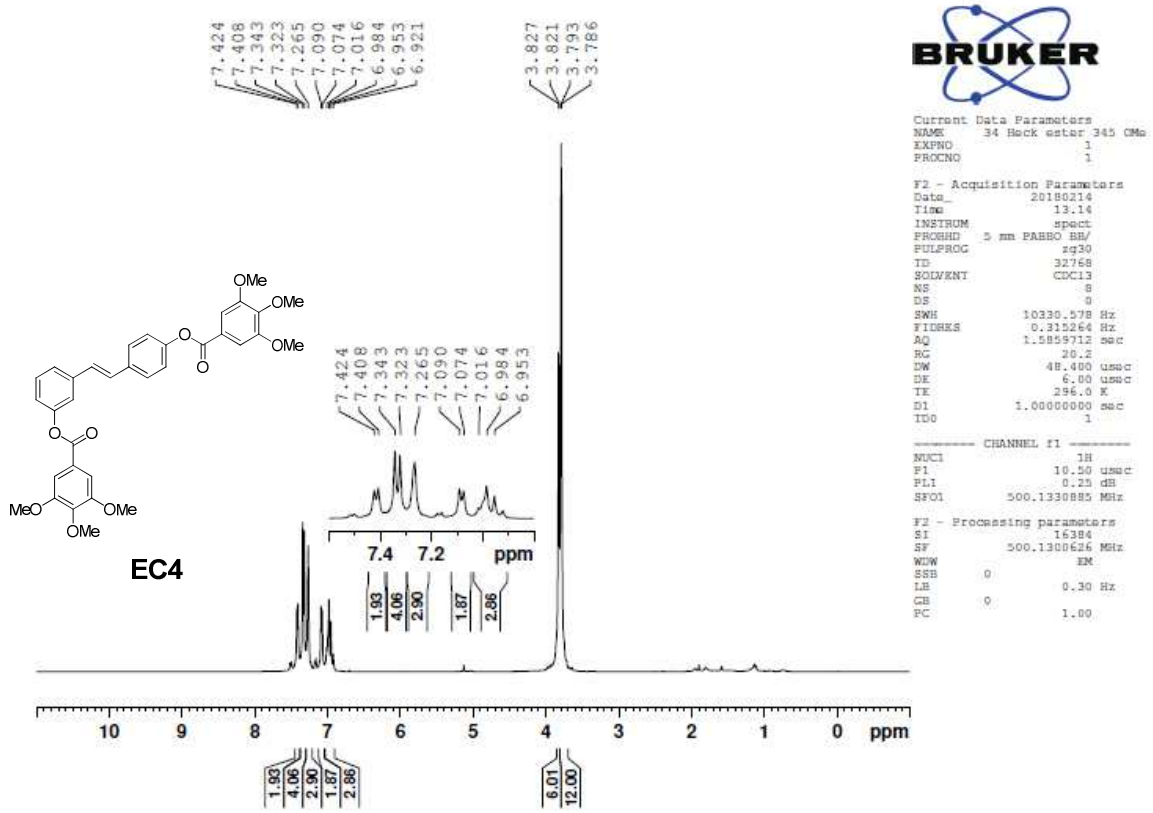

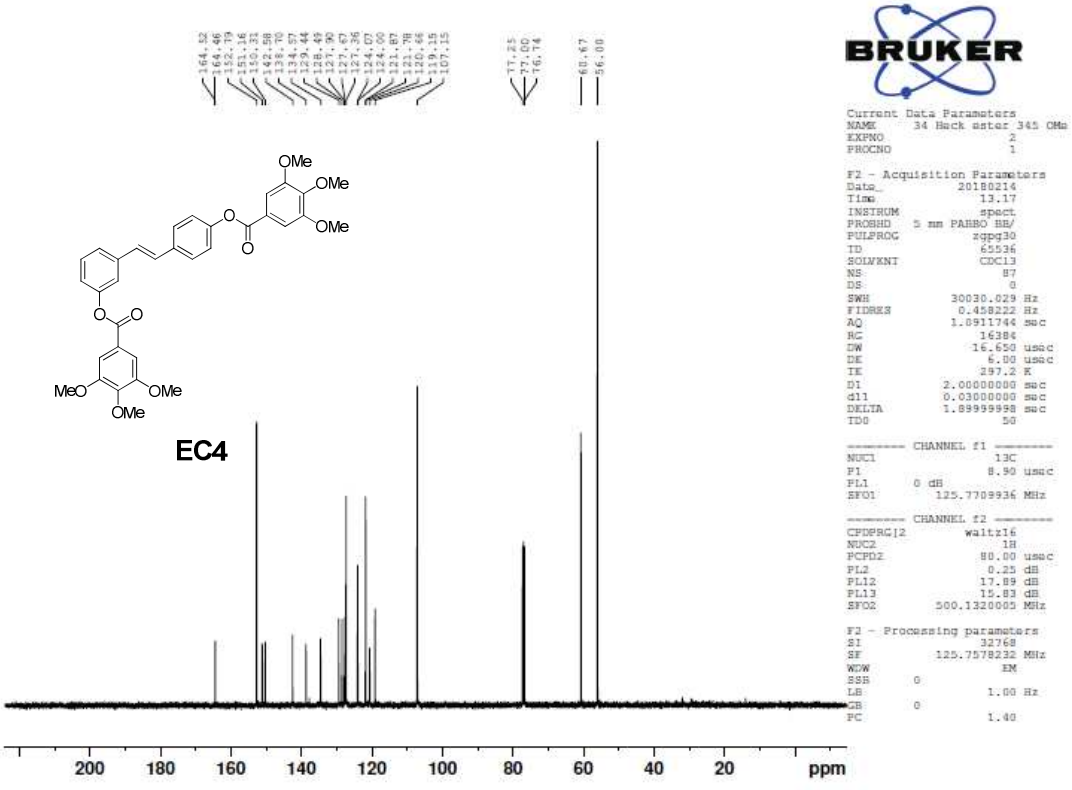

(*E*)-Ethene-1,2-diylbis(4,1-phenylene) bis(3,4,5-trihydroxybenzoate) (**EC5**)

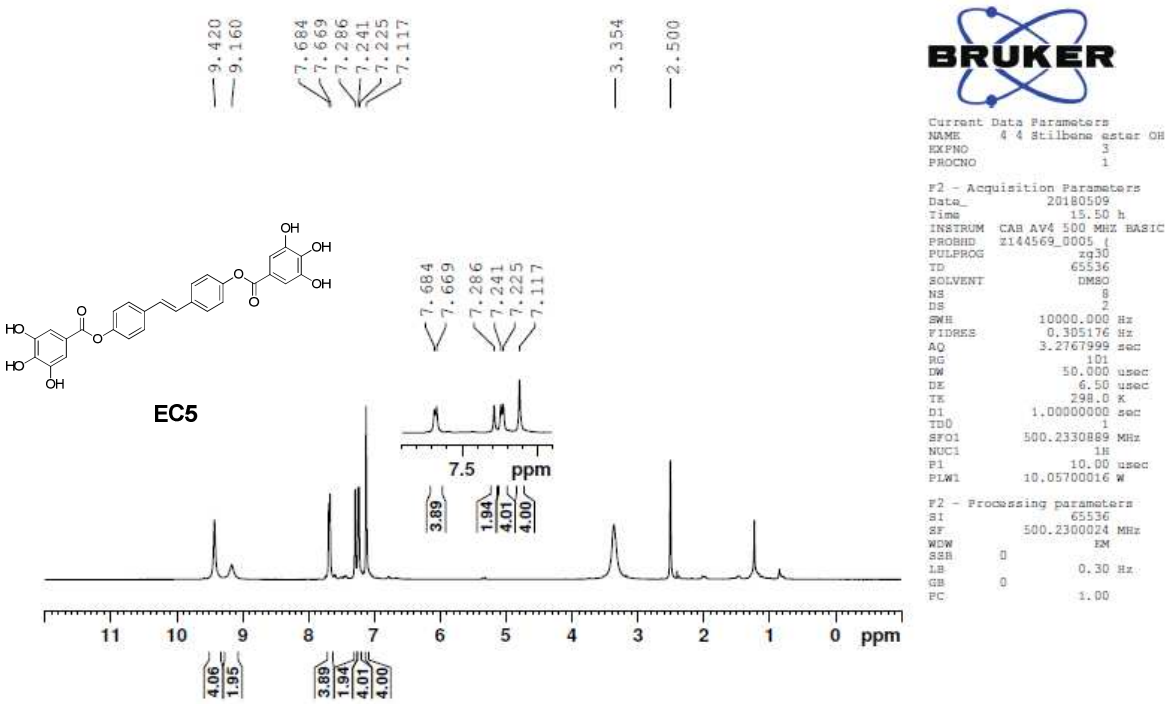

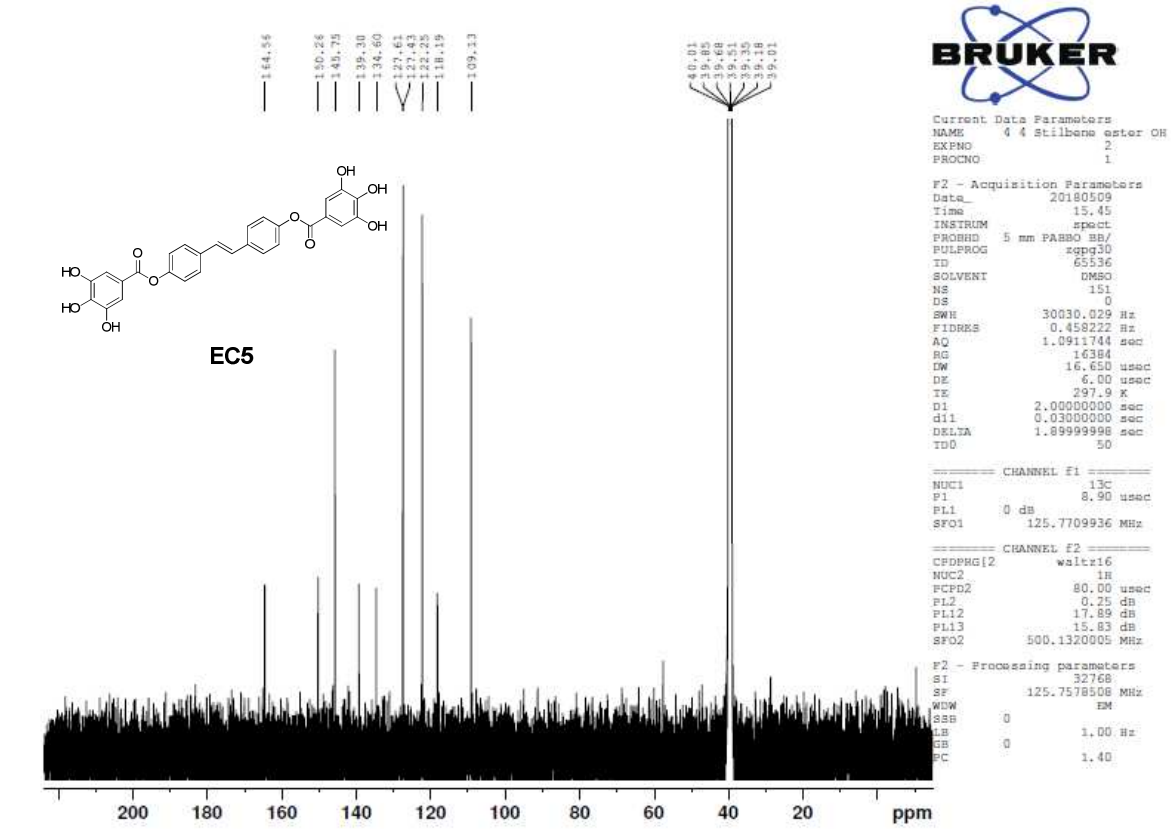

Methylenebis(4,1-phenylene) bis(3,4,5-trihydroxybenzoate) (**EC6**)

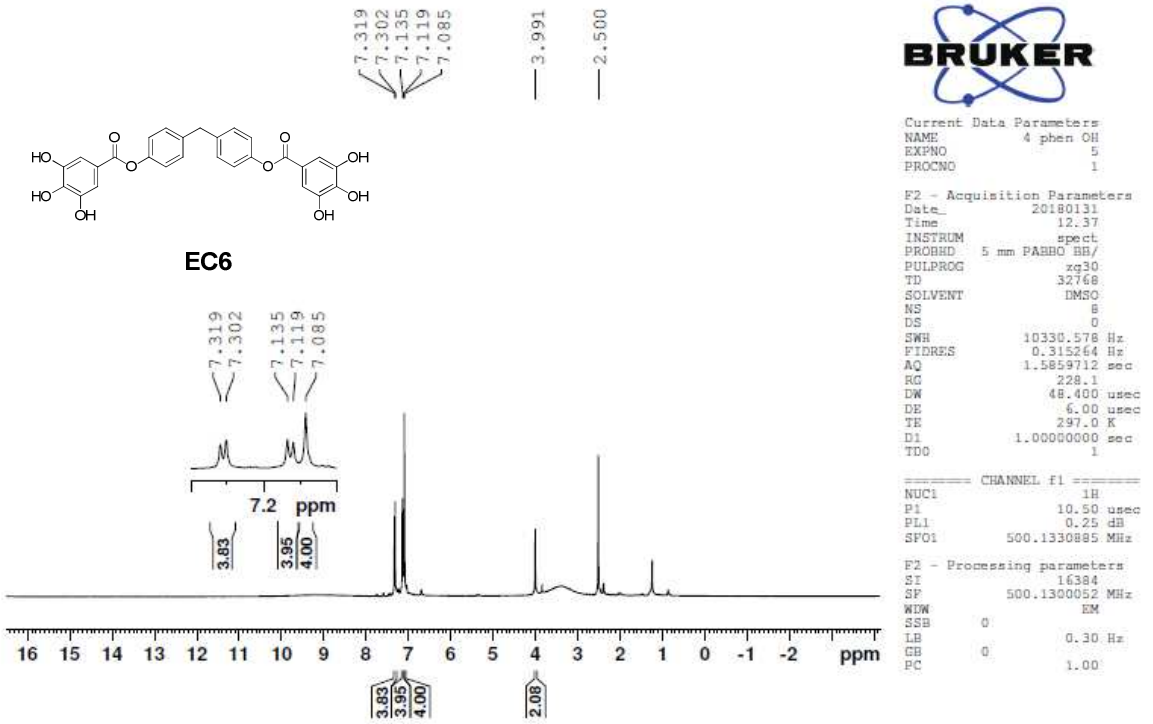

BRUKER

Current Data Parameters
NAME 4 phen OH
EXPNO 5
PROCNO 1

F2 - Acquisition Parameters
Date_ 20180131
Time 12.37
INSTRUM spect
PROBHD 5 mm PABBO BB/
PULPROG zg30
TD 32768
SOLVENT DMSO
NS 8
DS 0
SWH 10330.578 Hz
FIDRES 0.315264 Hz
AQ 1.5859712 sec
RG 228.1
DW 48.400 usec
DE 6.00 usec
TE 297.0 K
D1 1.00000000 sec
TD0 1

======== CHANNEL f1 ========
NUC1 1H
P1 10.50 usec
PL1 0.25 dB
SFO1 500.1330885 MHz

F2 - Processing parameters
SI 16384
SF 500.1300052 MHz
WDW EM
SSB 0
LB 0.30 Hz
GB 0
PC 1.00

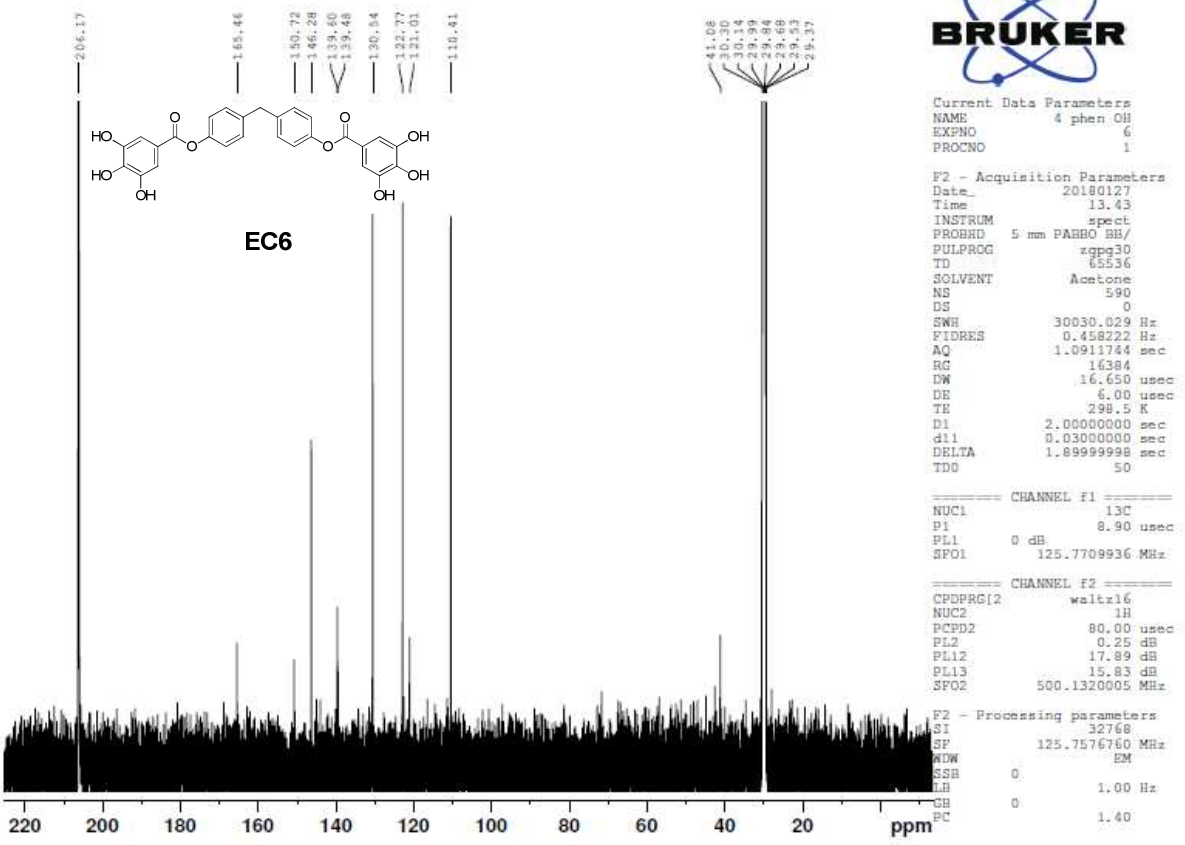

BRUKER

Current Data Parameters
NAME 4 phen OH
EXPNO 6
PROCNO 1

F2 - Acquisition Parameters
Date_ 20180127
Time 13.43
INSTRUM spect
PROBHD 5 mm PABBO BB/
PULPROG zgpg30
TD 65536
SOLVENT Acetone
NS 590
DS 0
SWH 30030.029 Hz
FIDRES 0.458222 Hz
AQ 1.0911744 sec
RG 16384
DW 16.650 usec
DE 6.00 usec
TE 298.5 K
D1 2.00000000 sec
d11 0.03000000 sec
DELTA 1.89999998 sec
TD0 50

======== CHANNEL f1 ========
NUC1 13C
P1 8.90 usec
PL1 0 dB
SFO1 125.7709936 MHz

======== CHANNEL f2 ========
CPDPRG[2 waltz16
NUC2 1H
PCPD2 80.00 usec
PL2 0.25 dB
PL12 17.89 dB
PL13 15.83 dB
SFO2 500.1320005 MHz

F2 - Processing parameters
SI 32768
SF 125.7576760 MHz
WDW EM
SSB 0
LB 1.00 Hz
GB 0
PC 1.40

Methylenebis(4,1-phenylene) bis(3,4,5-trimethoxybenzoate) (**EC7**)

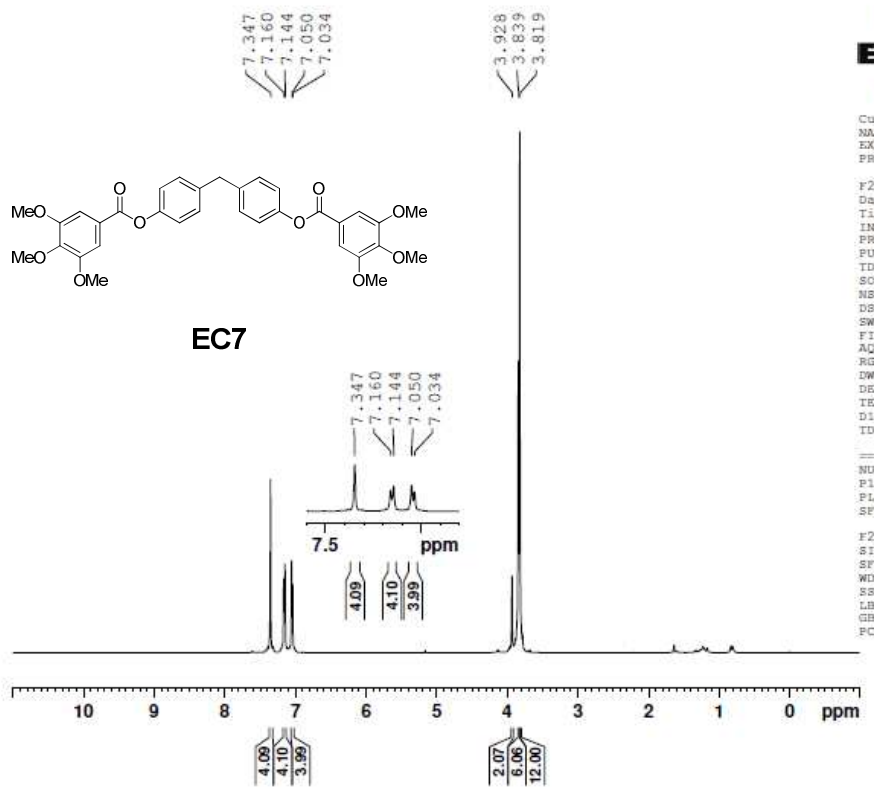


```
Current Data Parameters
NAME          4 phen OMe
EXPNO                  5
PROCNO                 1

F2 - Acquisition Parameters
Date_          20180119
Time              19.33
INSTRUM           spect
PROBHD   5 mm PABBO BB/
PULPROG           zg30
TD               32768
SOLVENT          CDCl3
NS                   8
DS                   0
SWH          10330.578 Hz
FIDRES        0.315264 Hz
AQ           1.5859712 sec
RG                28.5
DW               48.400 usec
DE                6.00 usec
TE               304.4 K
D1           1.00000000 sec
TD0                  1

======== CHANNEL f1 ========
NUC1                 1H
P1                10.50 usec
PL1                0.25 dB
SFO1        500.1330885 MHz

F2 - Processing parameters
SI                16384
SF        500.1300614 MHz
WDW                  EM
SSB                  0
LB                0.30 Hz
GB                   0
PC                1.00
```

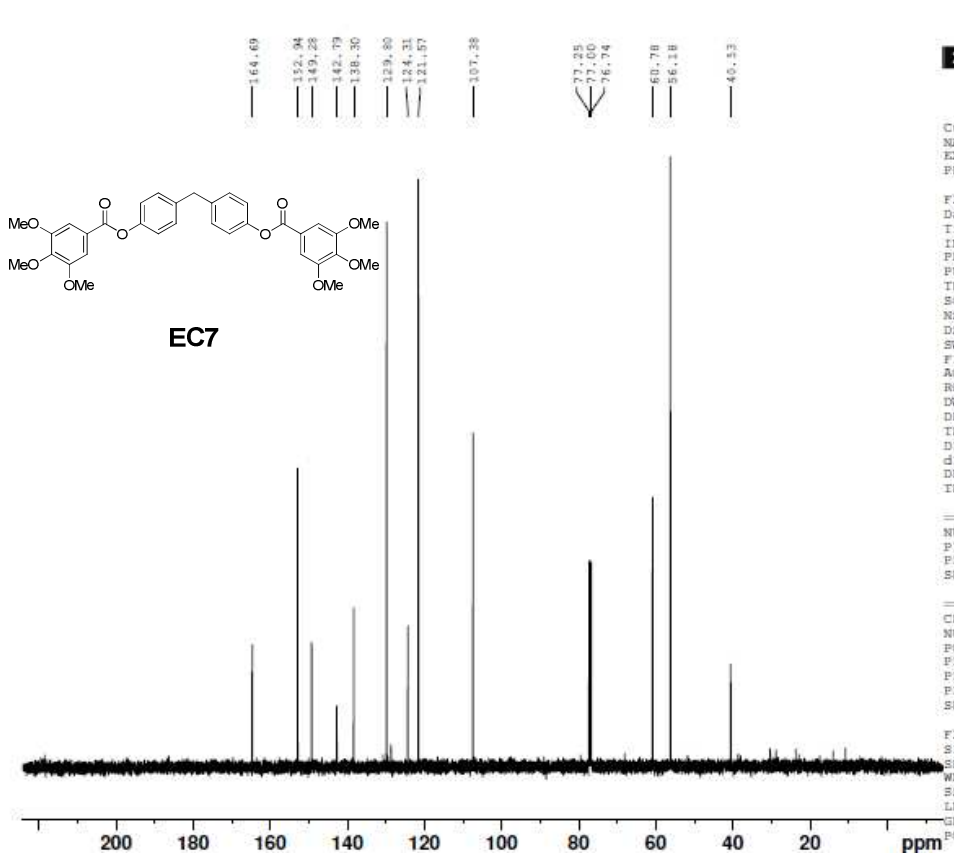


```
Current Data Parameters
NAME          4 phen OMe
EXPNO                  7
PROCNO                 1

F2 - Acquisition Parameters
Date_          20180119
Time              19.45
INSTRUM           spect
PROBHD   5 mm PABBO BB/
PULPROG         zgpg30
TD               65536
SOLVENT          CDCl3
NS                  22
DS                   0
SWH          30030.029 Hz
FIDRES        0.458222 Hz
AQ           1.0911744 sec
RG               16384
DW               16.650 usec
DE                6.00 usec
TE               305.1 K
D1           2.00000000 sec
d11          0.03000000 sec
DELTA        1.89999998 sec
TD0                 50

======== CHANNEL f1 ========
NUC1                13C
P1                8.90 usec
PL1              0 dB
SFO1        125.7709936 MHz

======== CHANNEL f2 ========
CPDPRG[2        waltz16
NUC2                 1H
PCPD2             80.00 usec
PL2                0.25 dB
PL12              17.89 dB
PL13              15.83 dB
SFO2        500.1320005 MHz

F2 - Processing parameters
SI                32768
SF        125.7578085 MHz
WDW                  EM
SSB                  0
LB                1.00 Hz
GB                   0
PC                1.40
```

Methylenebis(2,1-phenylene) bis(3,4,5-trihydroxybenzoate) (**EC8**)

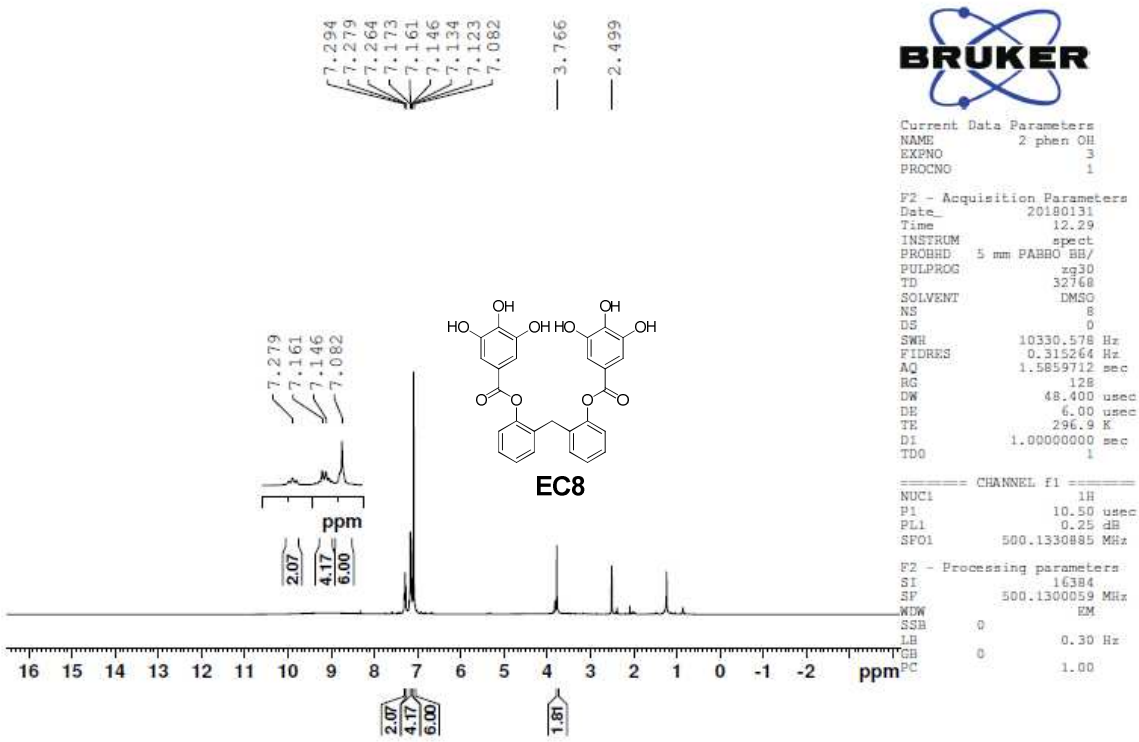

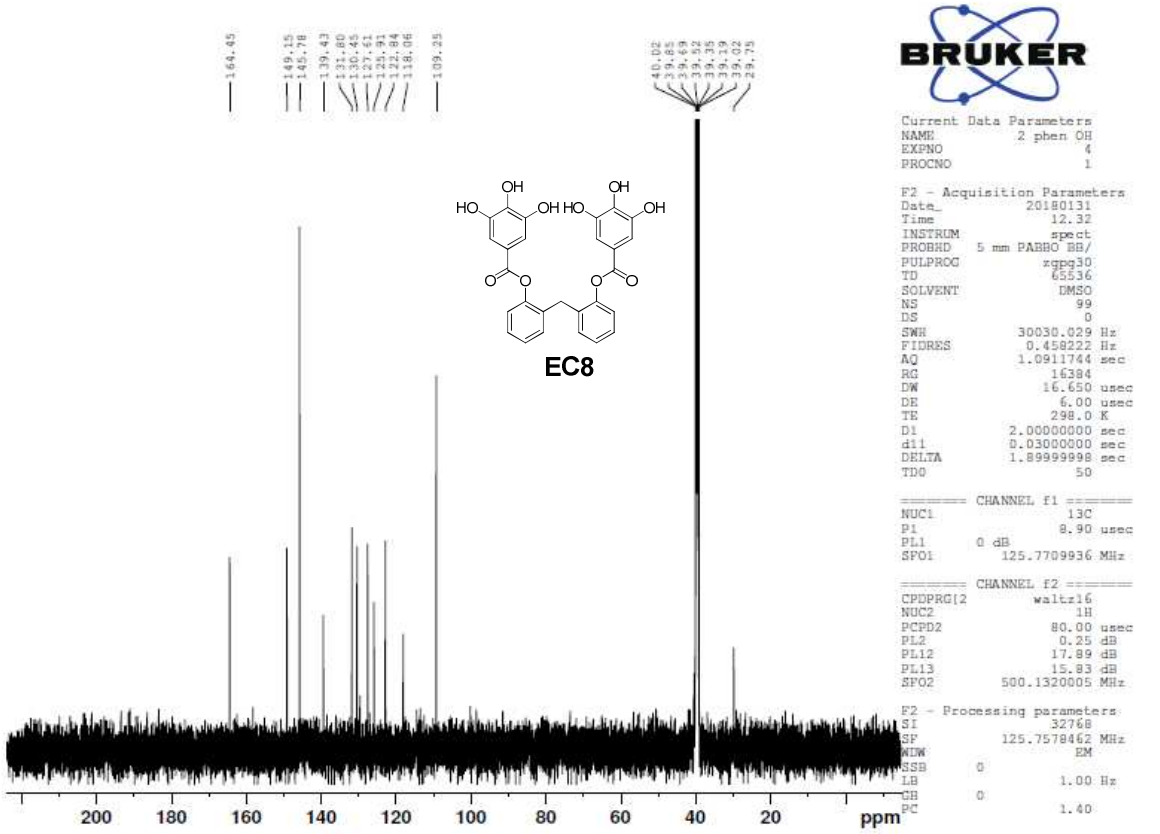

1,2,3,4-Tetrahydronaphthalene-1,5-diyl bis(3,4,5-trihydroxybenzoate) (**EC9**)

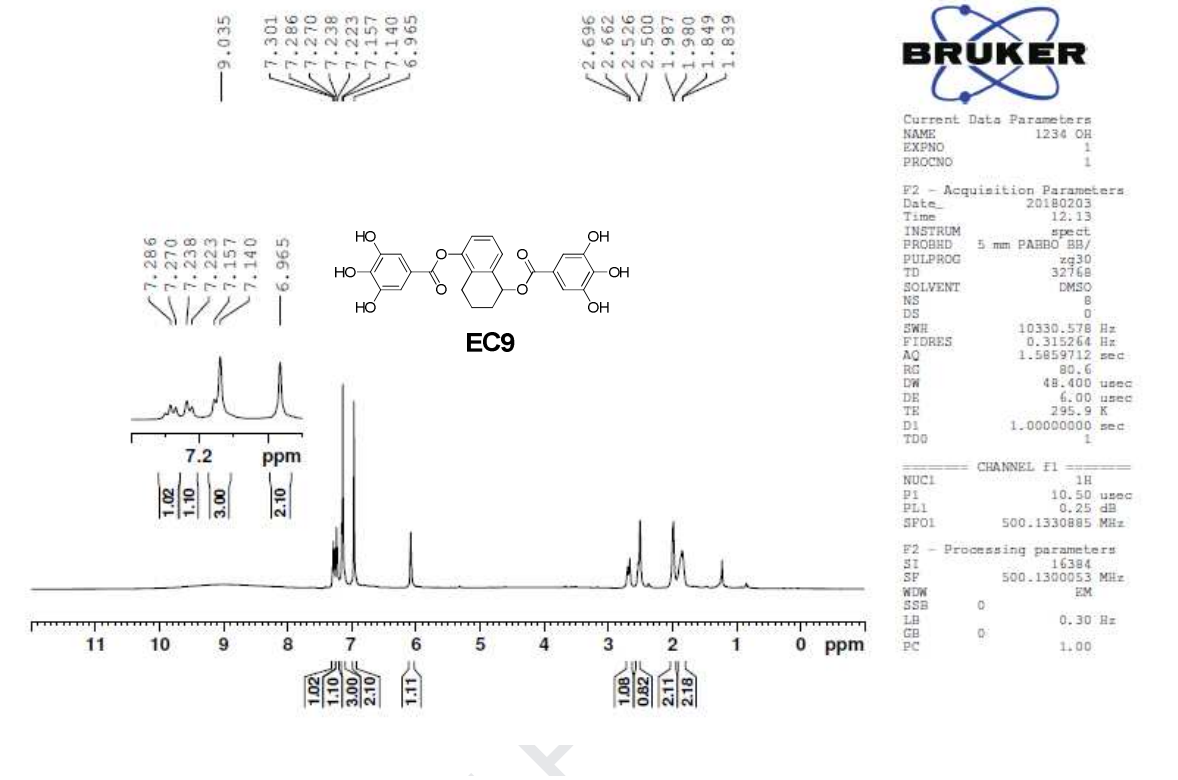

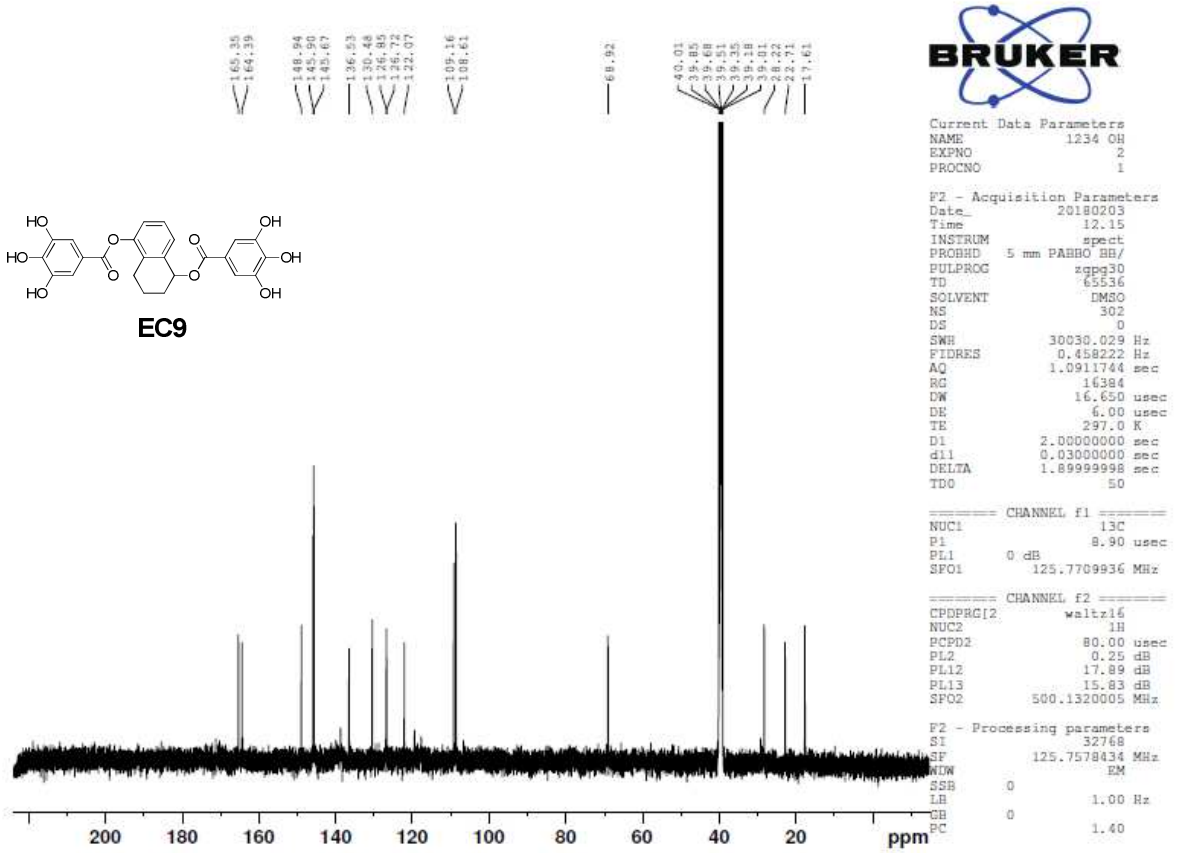

(*E*)-3-Styrylphenyl 3,4,5-trihydroxybenzoate (**EC10**)

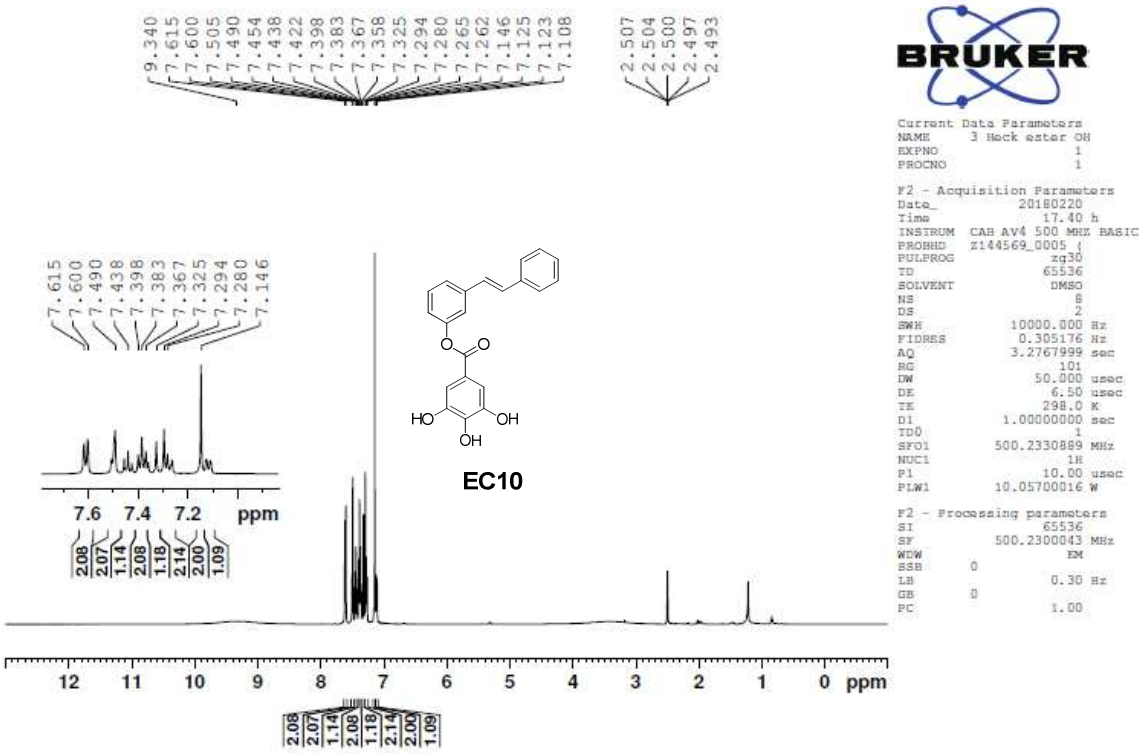

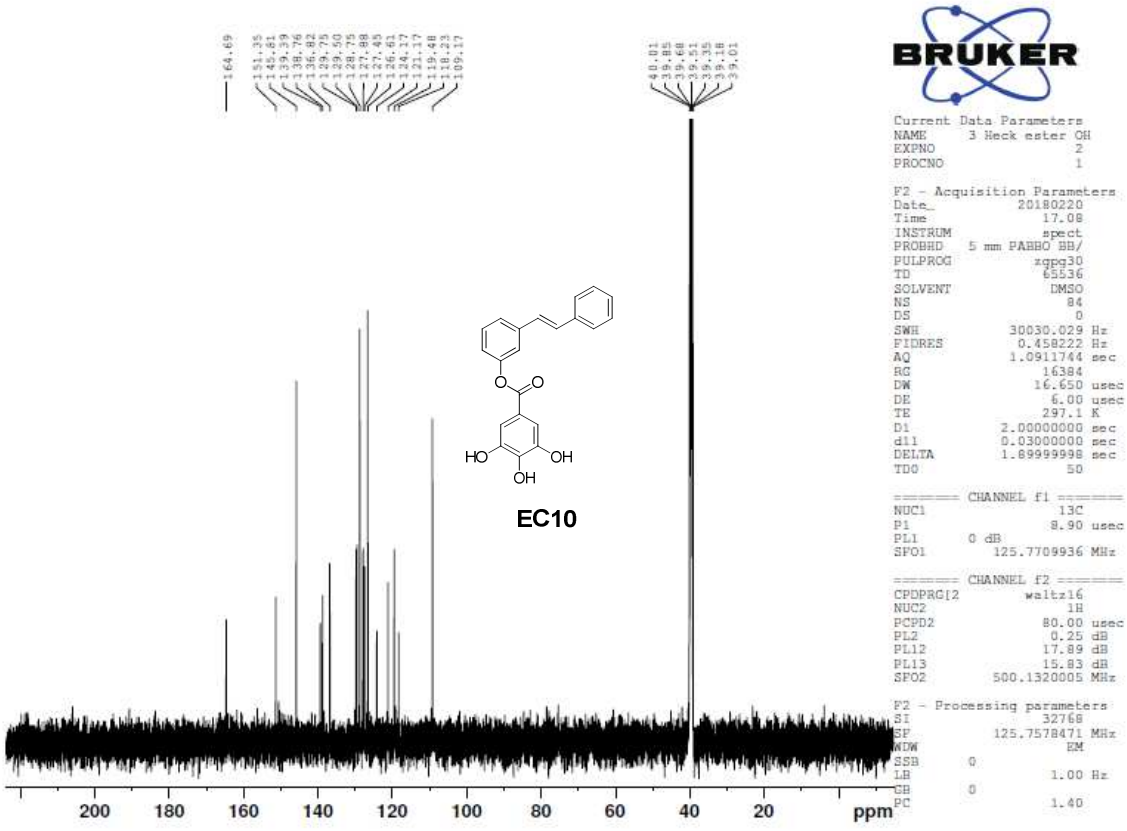

(*E*)-4-Styrylphenyl 3,4,5-trihydroxybenzoate (**EC11**)

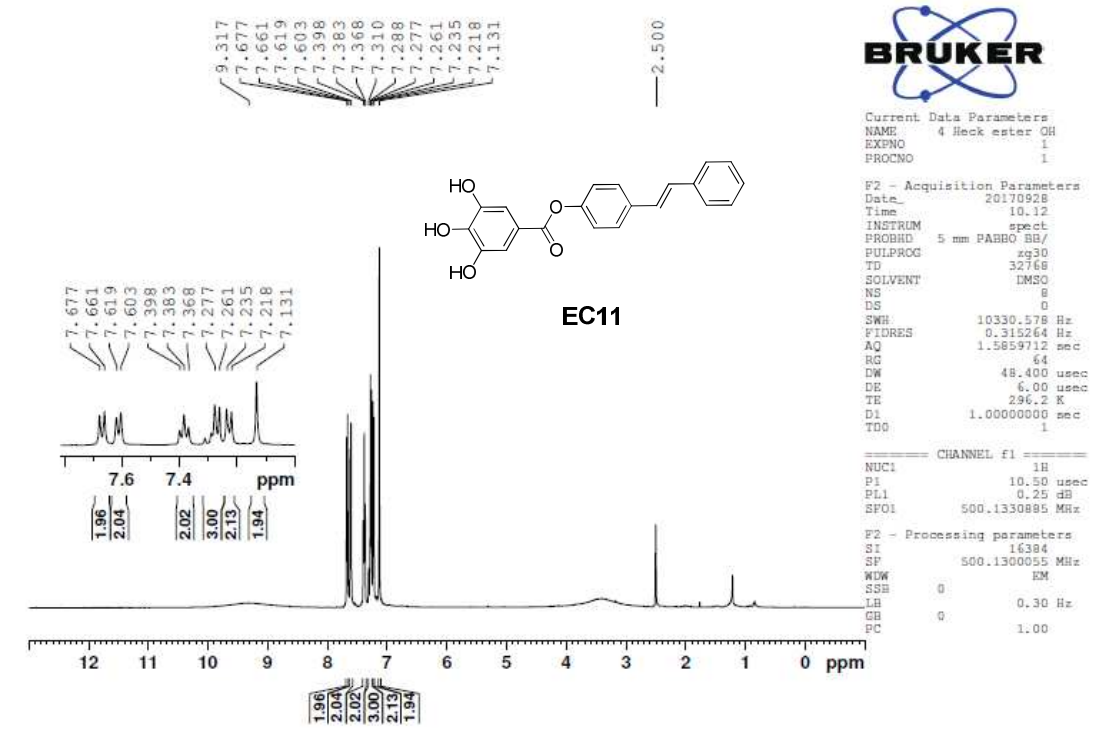

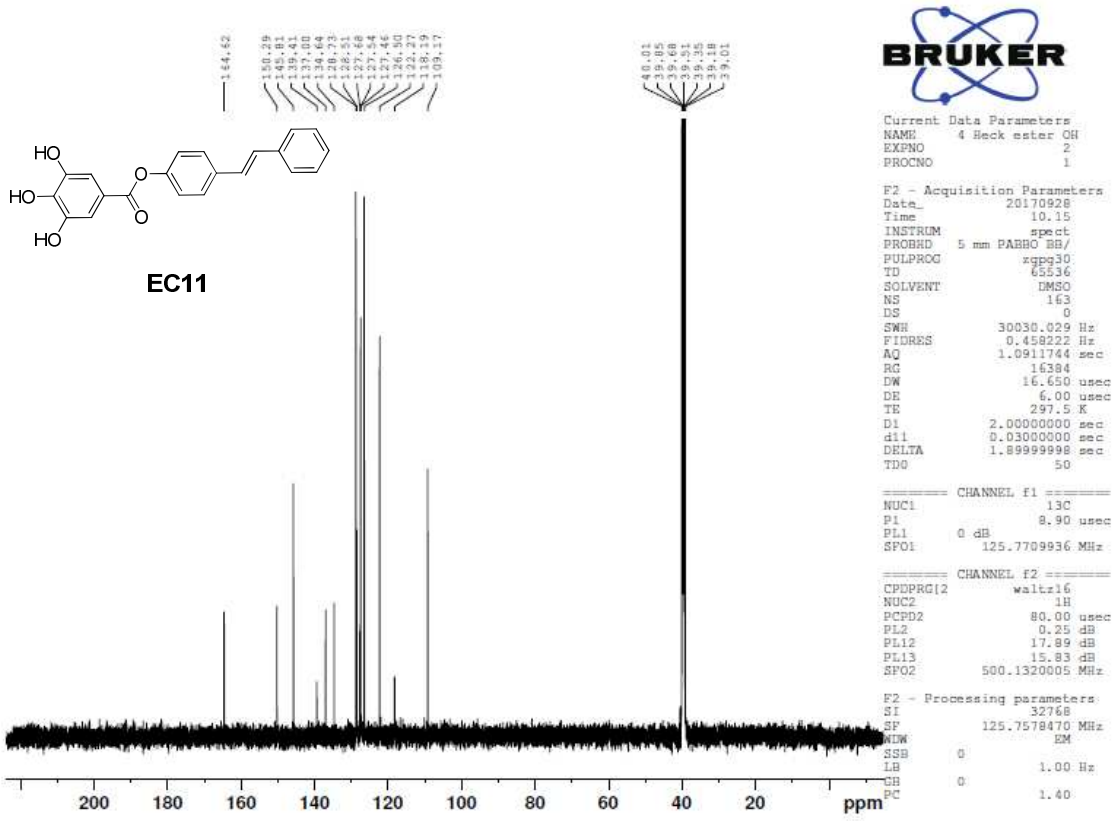

(*E*)-4-Styrylphenyl 3,4,5-trimethoxybenzoate (**EC12**)

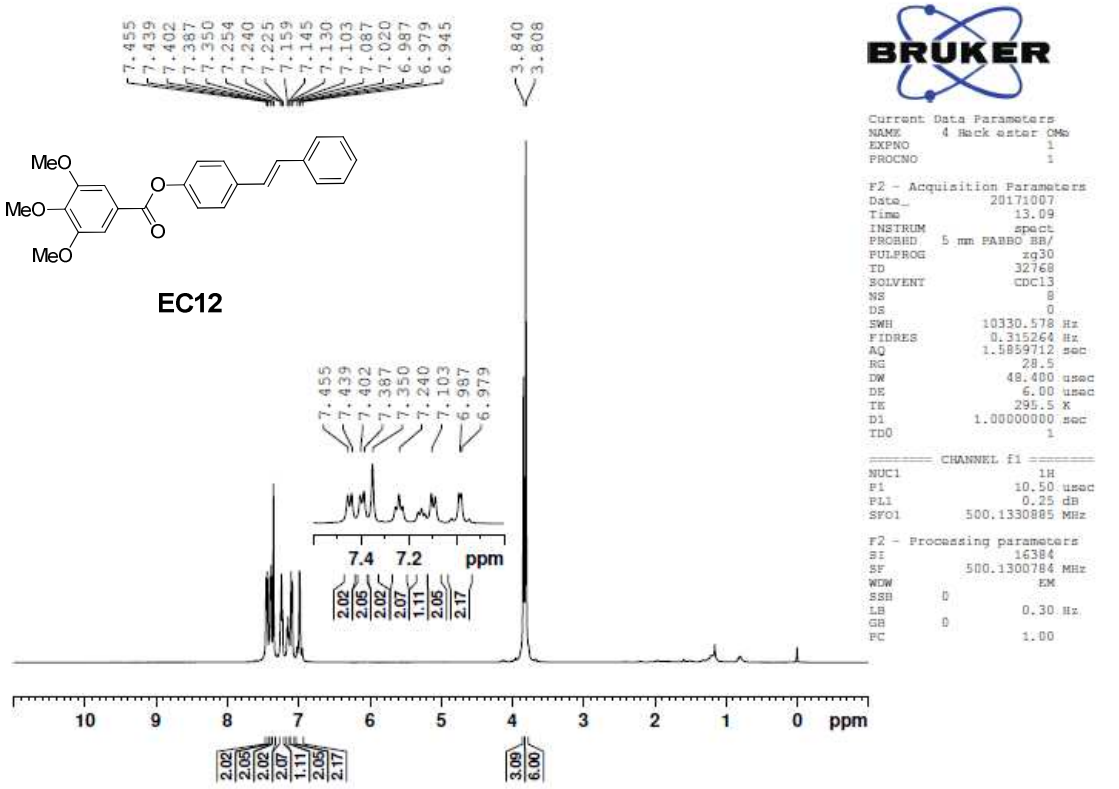

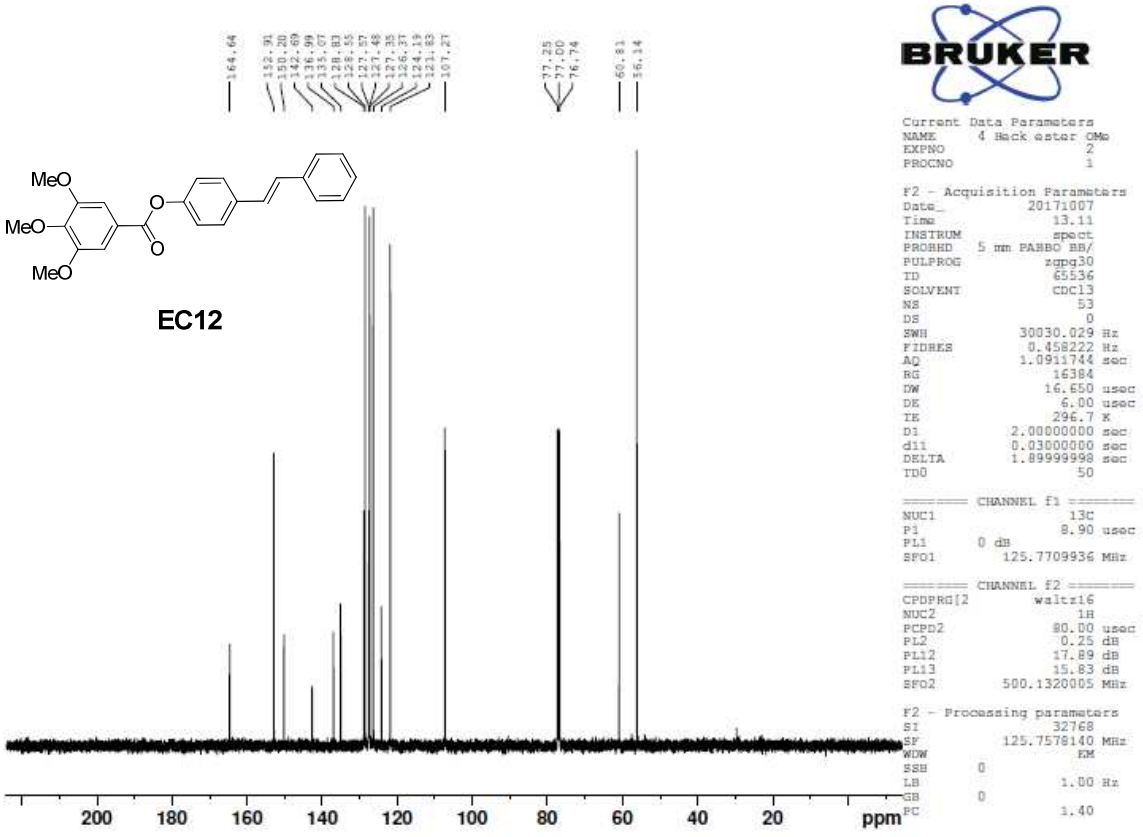

4-(Naphthalen-1-yl)phenyl 3,4,5-trihydroxybenzoate (**EC13**)